8. Luminescence Mechanisms

Contents

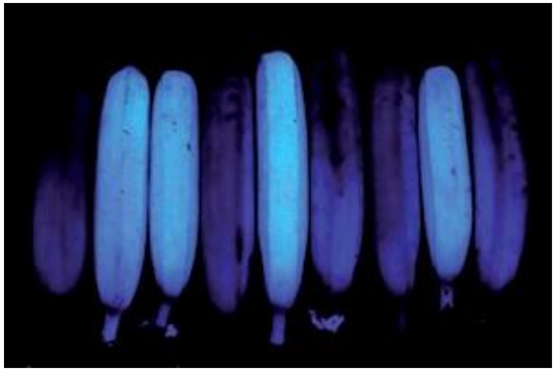

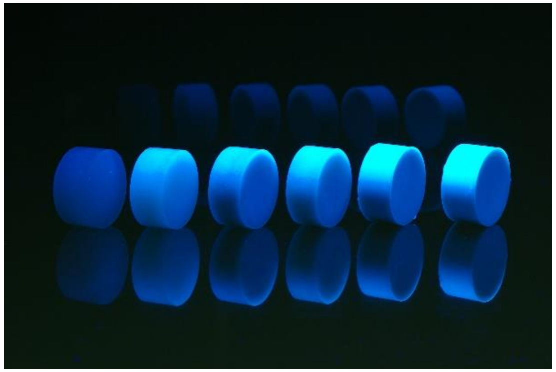

8.1 Luminescence - Definition

Luminescence is a process that corresponds to emission of electromagnetic radiation beyond thermal equilibrium (→ not Planck radiation)

Inorganic materials: Radiative recombination involving impurity levels within the band gap!
(a) Conduction-band–acceptor-state transition
(b) Donor-state–valence-band transition
(c) Donor-acceptor recombination
(d) Bound-exciton recombination

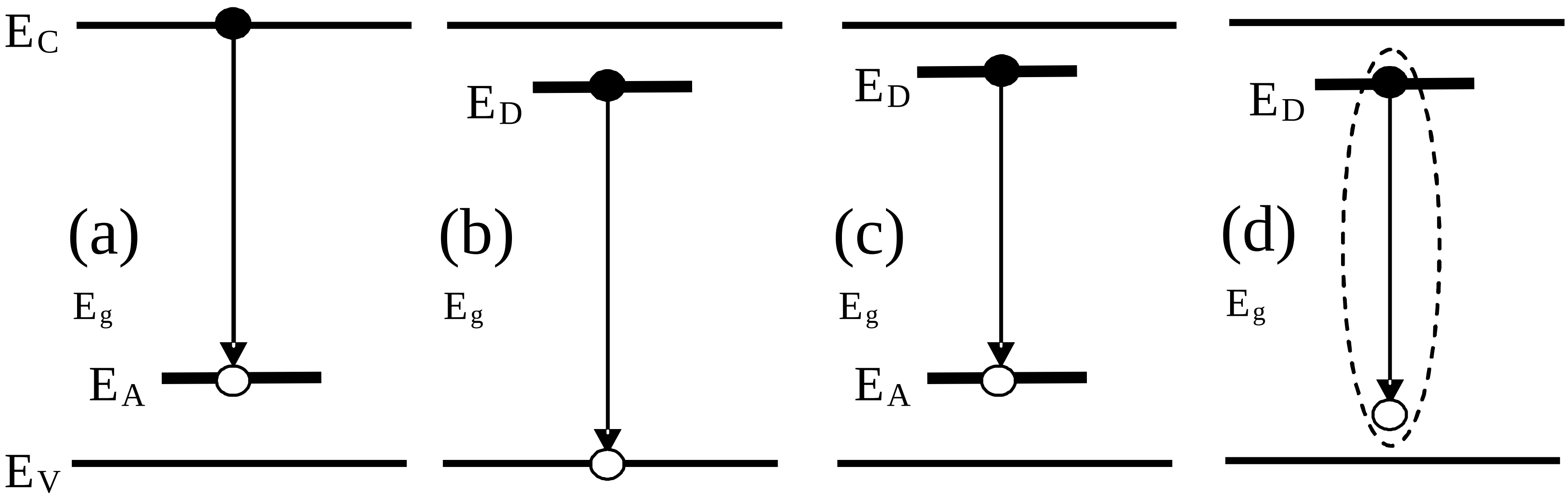

Thus: Luminescence requires localisation of absorbed energy by discrete states! No metals!

8.1 Luminescence - Definition

Thermal and non-thermal radiators

Thermal radiators emit a radiation spectrum that equals black body radiation at a corresponding temperature
→ Planck radiation

Examples: Cosmic background radiation, celestial objects, halogen and incandescent lamps

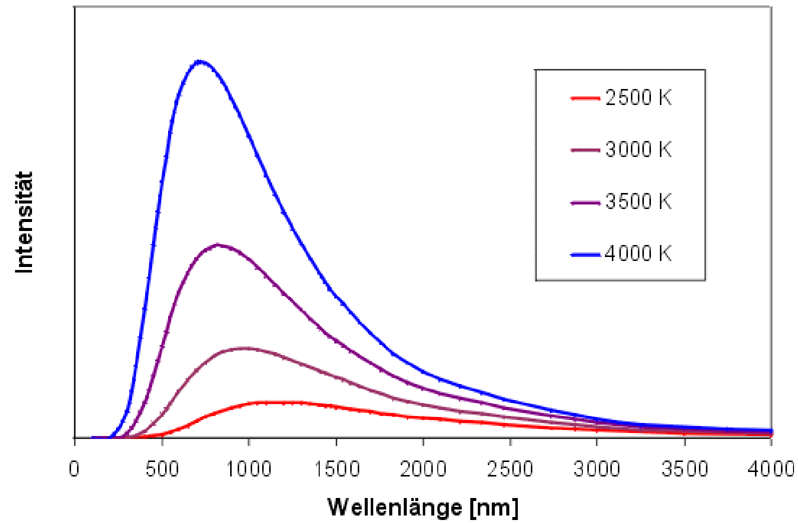

Non-thermal radiators emit a radiation spectrum originating from electronic transitions between discrete electronic energy levels
→ Luminescence

Examples: Luminescent materials, (O)LEDs, Lasers

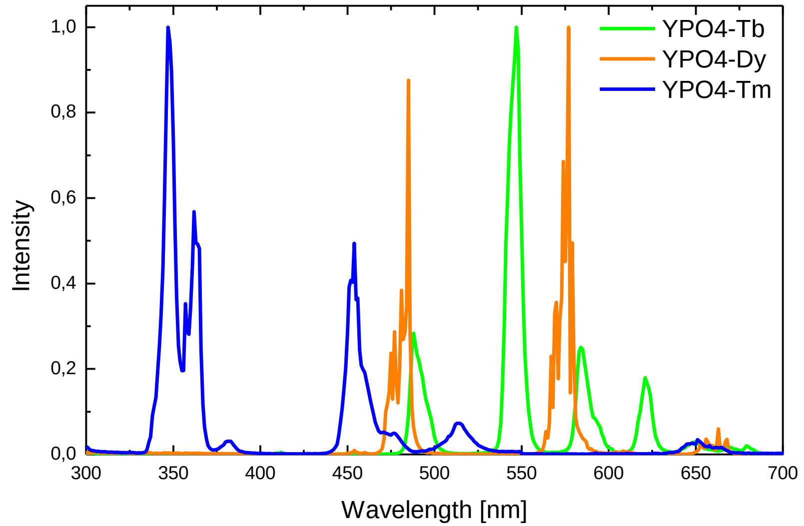

8.1 Luminescence – Materials

Inorganic luminescent materials: Some requirements for high quantum efficiency

Strong absorption, efficient energy transfer, and high internal quantum yield:

- Highly crystalline particles, low defect density
- High purity (99.99% or higher)
- Redox stable optical centres
- Homogeneous distribution of optical centres
- Low phonon frequencies
- Inert surfaces (core-shell approach)

Absorption process related to
optical centres (impurities)

- activators (A)
- sensitizers (S)
- defects (D)
- host lattice (band edge)

Energy transfer often occurs prior to emission processes!

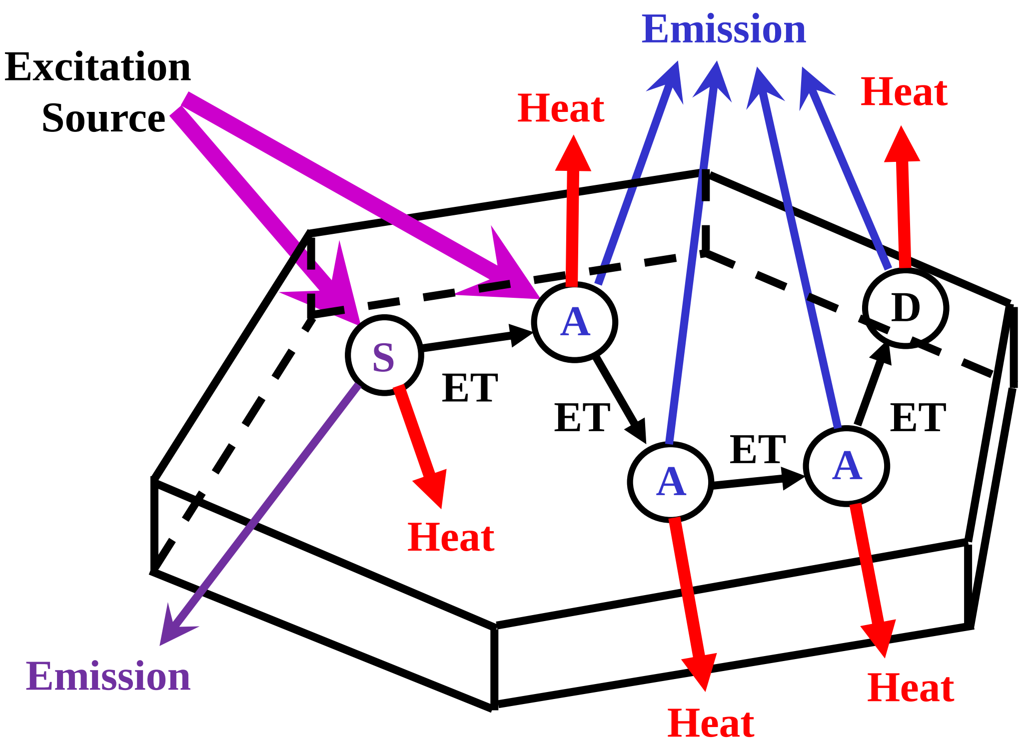

8.1 Luminescence – Materials

Inorganic luminescent materials – The role of the host lattice (Example YBO_3)

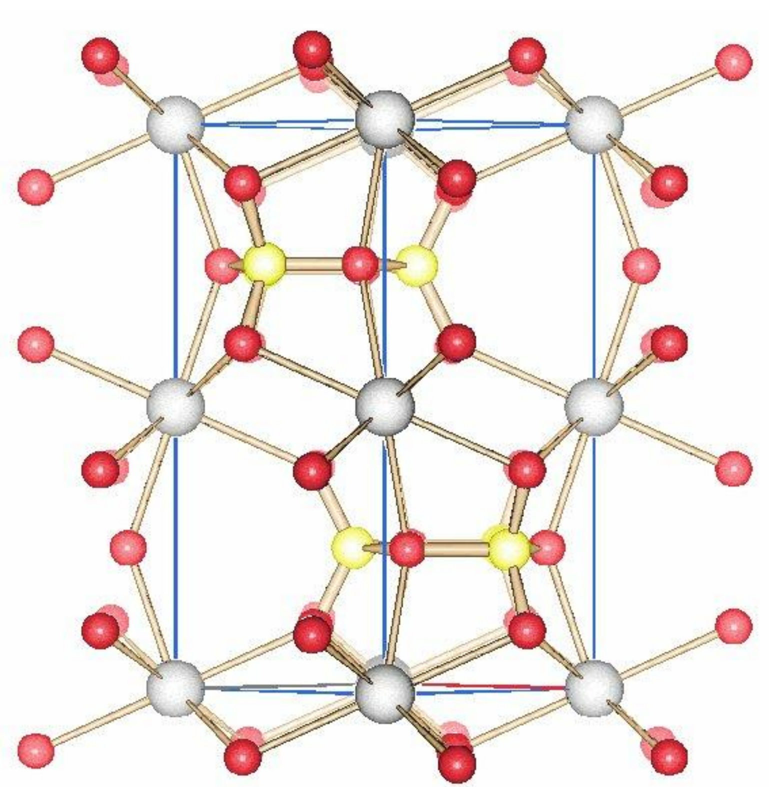

YBO_3 (Vaterite)

Band gap E_g = 6.5 eV

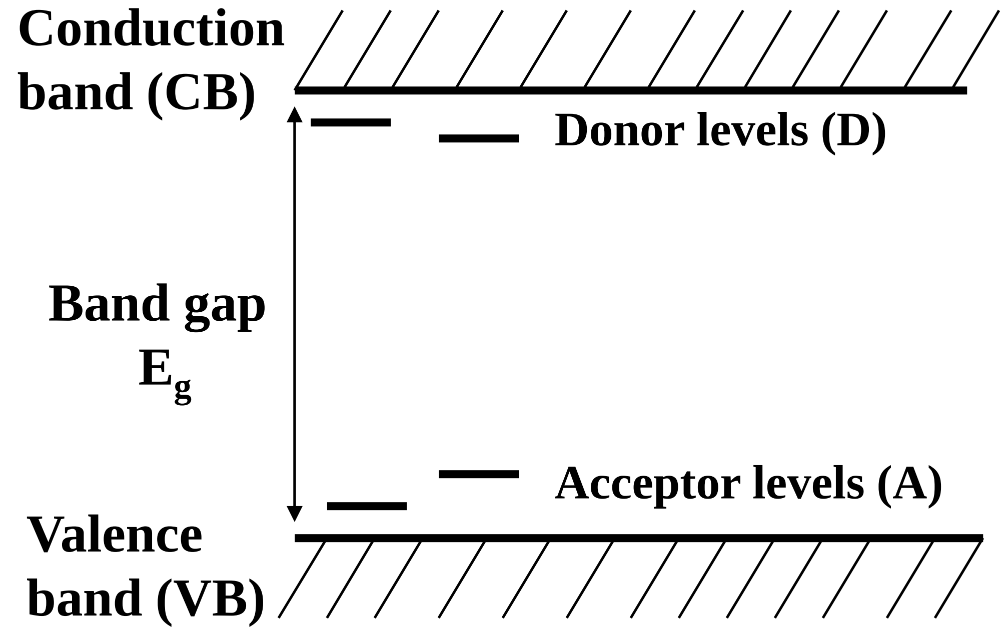

Absorption via

- Host lattice
  → Charge-Transfer or VB to CB
- Defects (colour centers)
  → Donor and acceptor levels (Urbach tailing)

8.1 Luminescence – Materials

Inorganic luminescent materials – The role of the host lattice

Reflection spectrum of YBO_3

Emission spectrum of YBO_3 upon 160 nm excitation

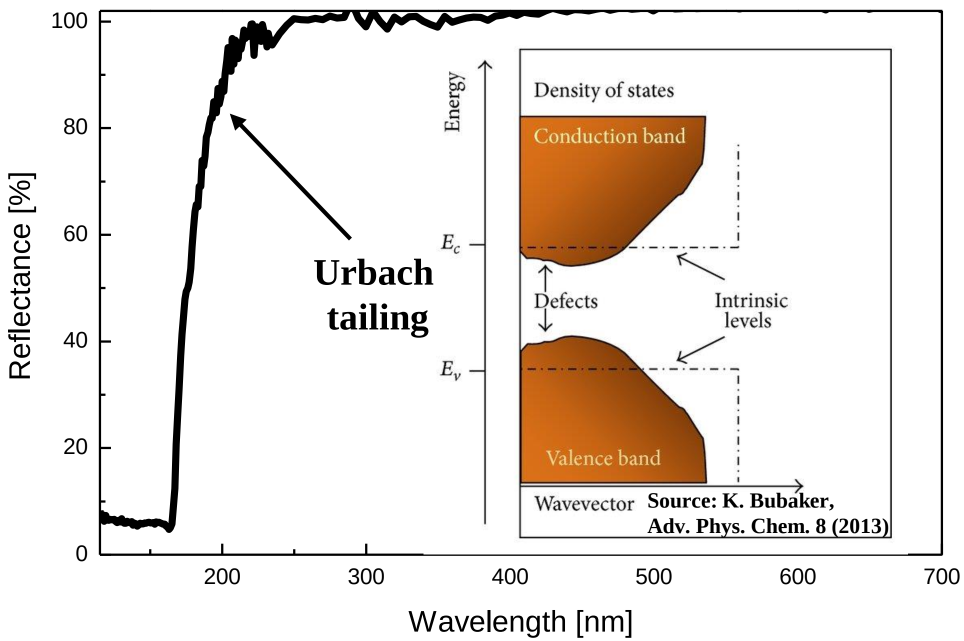

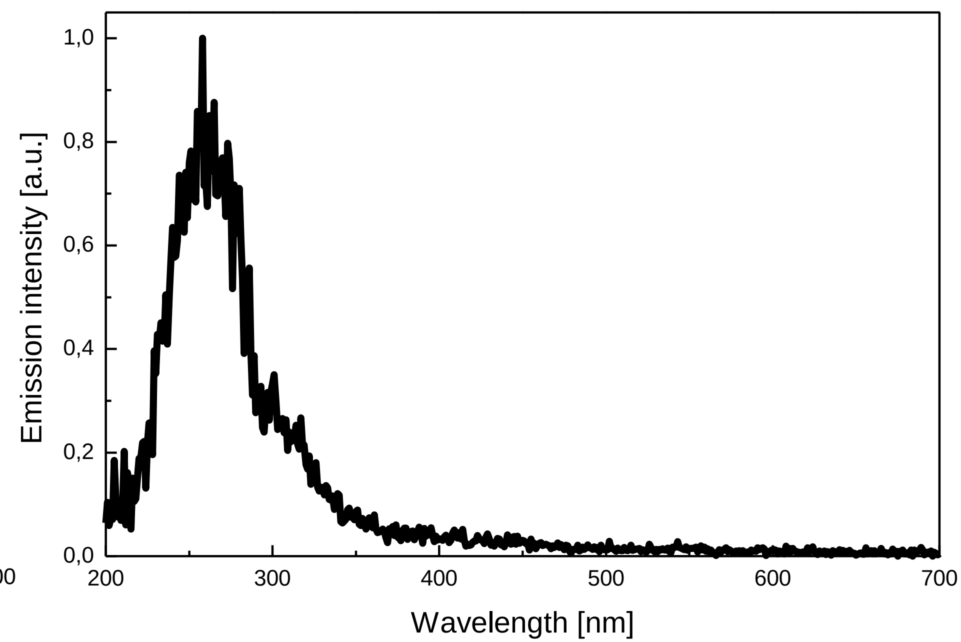

Band gap absorption at 170 nm

Exciton luminescence at 260 nm

Inorganic luminescent materials – The role of the dopants

YVO_4 (tetragonal), E_g = 4.2 eV

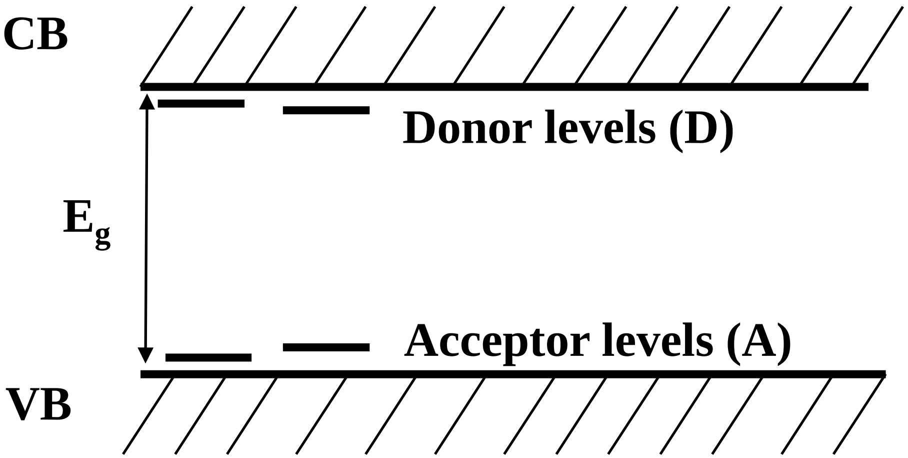

YPO_4:V,Eu (tetragonal), E_g = 8.2 eV

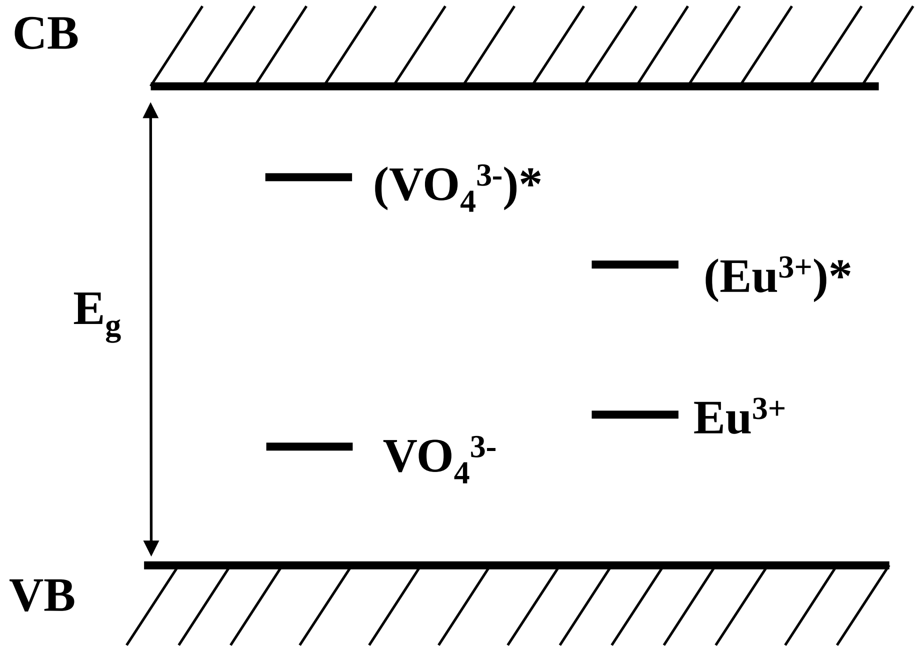

Absorption via

- Host lattice → Charge-Transfer or VB to CB
- Defects (colour centers) → Donor and acceptor levels
- Dopants (impurities) → Activators and sensitizers

8.1 Luminescence - Processes

The overall picture

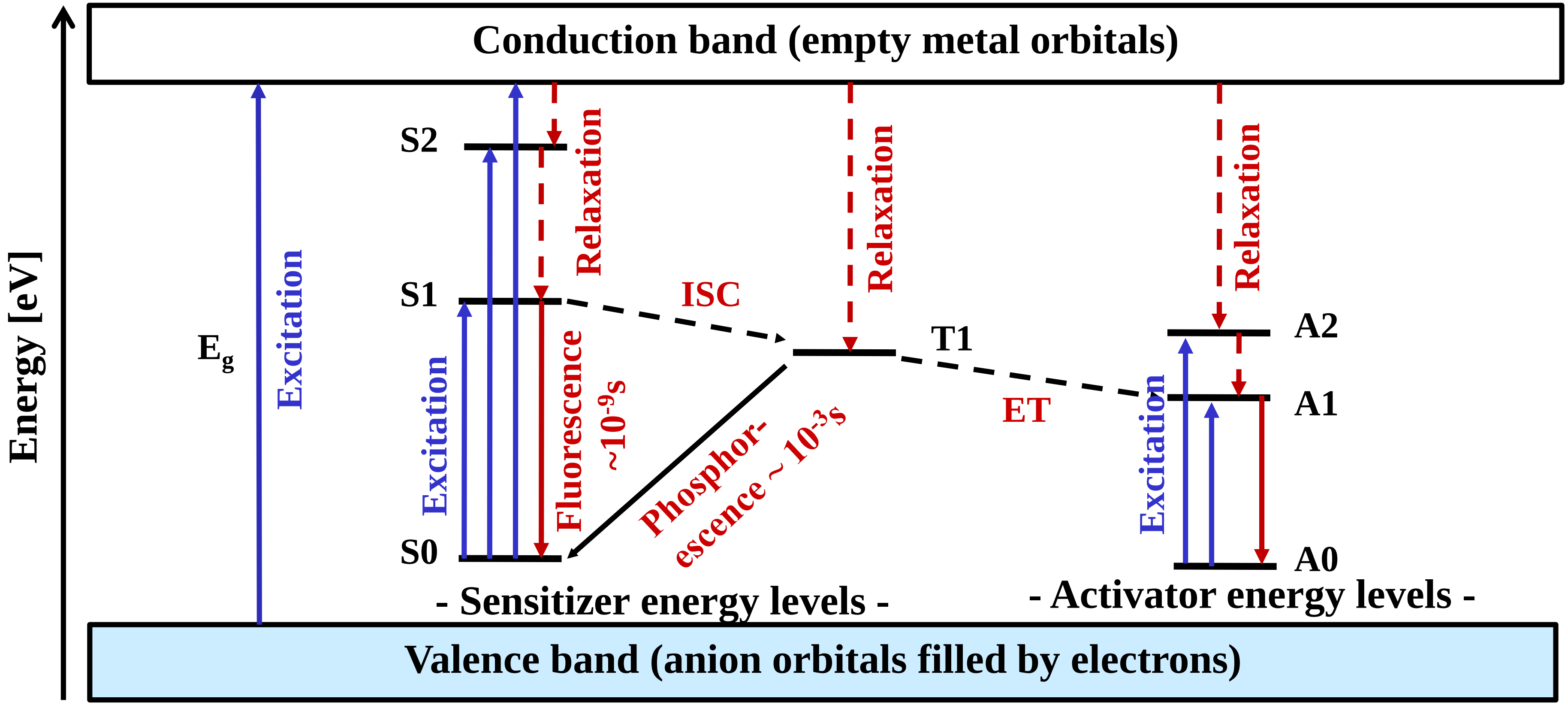

S0, S1, S2, T1, A0, A1 = Energy levels of activator and sensitizer ions

ISC = Intersystem Crossing "spin-forbidden singulett-triplett transition"

ET = Energy transfer

8.1 Luminescence - Processes

Photonic or thermal stimulated luminescence (PSL or TSL)

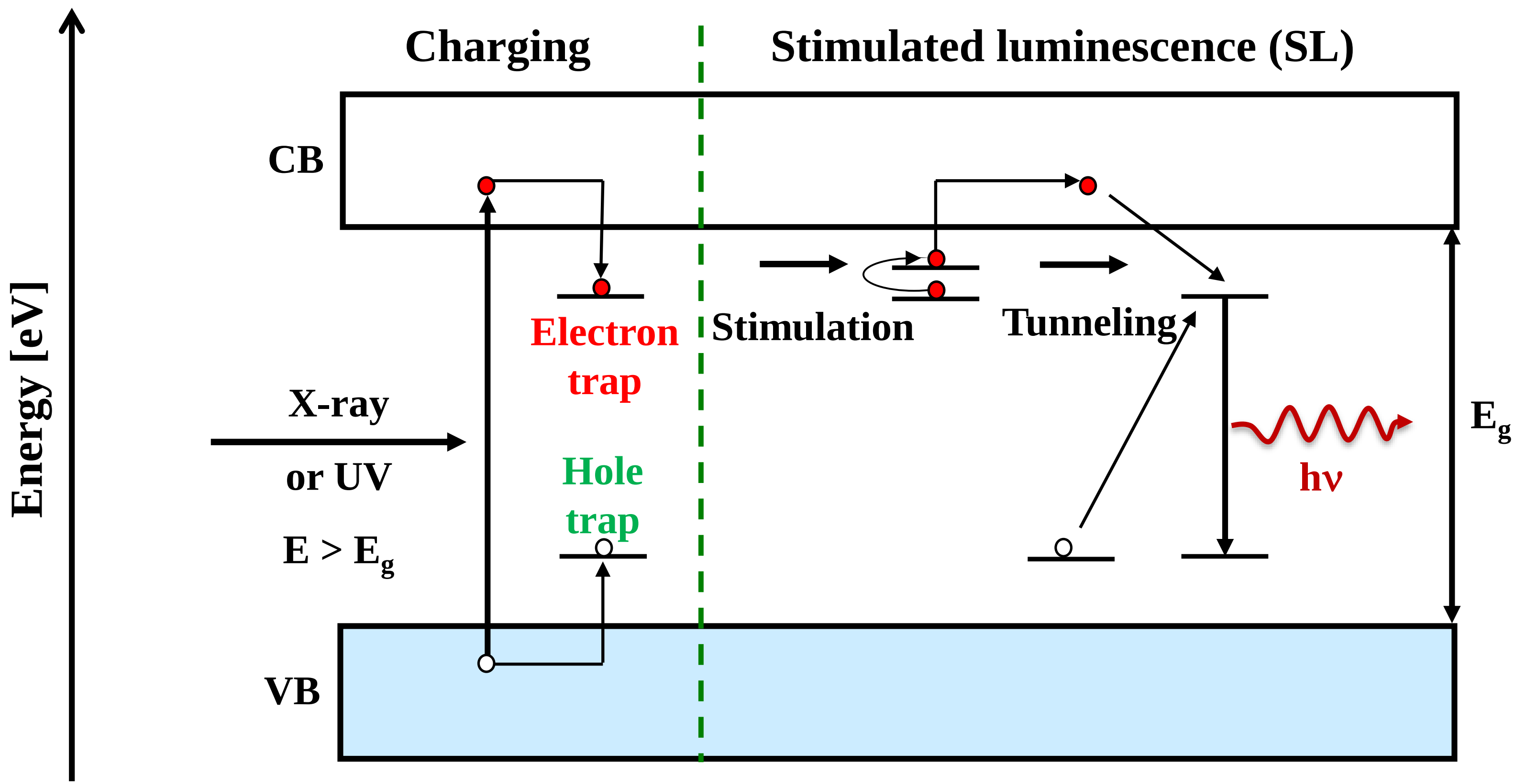

8.1 Luminescence - Processes

Electronic Ground States of Atoms and Ions (Dopants)

The electronic energy levels are defined by the spin and orbital momentum of the electrons and by the coupling of these to the total spin and total (orbital) momentum

Atom/Ion	Electron configuration	Spectroscopic term $^{2S+1}L_J$
Li^0	$1s^2\ 2s^1$	$^2S_{1/2}$
Li^+	$1s^2$	$^1S_0$
Na^0	$[Ne]3s^1$	$^2S_{1/2}$
Ti^{3+}	$[Ar]3d^1$	$^2D_{3/2}$
Cr^{3+}/Mn^{4+}	$[Ar]3d^3$	$^4F_{3/2}$
Mn^{2+}/Fe^{3+}	$[Ar]3d^5$	$^6S_{5/2}$
Zn^{2+}/Cu^+	$[Ar]3d^{10}$	$^1S_0$
Ce^{3+}	$[Xe]4f^1$	$^2F_{5/2}$
Eu^{3+}	$[Xe]4f^6$	$^7F_0$
$Eu^{2+}/Gd^{3+}/Tb^{4+}$	$[Xe]4f^7$	$^8S_{7/2}$
Tb^{3+}	$[Xe]4f^8$	$^7F_6$
Lu^{3+}	$[Xe]4f^{14}$	$^1S_0$

8.1 Luminescence - Processes

Selection rules for electric dipole radiation (transitions)

Overall requirement: Conservation of momentum of the system "atom/ion + photon"

1.	Spin selection rule	$\Delta S = 0$
2.	Angular momentum (single electron)	$\Delta l = \pm 1$
3.	Angular momentum (multi electron)	$\Delta J = 0, \pm 1$ (but not $J = 0 \rightarrow J = 0$) $\Delta L = 0, \pm 1$ (but not $L = 0 \rightarrow L = 0$)
4.	Laporte selection rule	$g \rightarrow u$ or $u \rightarrow g$ not $g \rightarrow g$ or $u \rightarrow u$

Spectroscopic terms

$^{2S+1}L_J$

Examples:				
	Ce^{3+}	$[Xe]4f^1\,(^2F_{5/2}) \rightarrow [Xe]5d^1\,(^2D_{3/2})$	$\Rightarrow$ allowed	~ ns
	Eu^{3+}	$[Xe]4f^6\,(^7F_0) \rightarrow [Xe]4f^6\,(^5D_0)$	$\Rightarrow$ forbidden	~ ms

8.1 Luminescence - Processes

Type	Excitation by	Example
(roughly sorted top-down by decreasing energy of the excitation source)		
Scintillation	High energy particles	high-energy physics
	γ-rays	PET detectors
Radioluminescence	X-rays	X-ray amplifier, CT
Cathodoluminescence	Electrons (high voltage)	CRTs, oscilloscopes
Photoluminescence	UV/Vis photons	Fluorescent lamps
Electroluminescence	Electrical field (low voltage)	LEDs, EL displays
Chemiluminescence	Chemical reaction	Emergency signals
Bioluminescence	Biochemical reaction	Jelly fish, glow worms
Thermoluminescence	Heat	Afterglow phosphors
Sonoluminescence	Ultra sound	-
Mechanoluminescence (Elasto-, Fracto-, Plasto-, Tribo-)	Mechanical energy	Peeling scotch tape

Lit.: Nature 455 (2008) 1089, blue + UV + x-ray!

8.2 Absorption

Penetration depth R of photons into matter (Example H_2O)

Photon impingement
→ Lambert-Beer equation with T in [%]

$A(\lambda) = \varepsilon_\lambda \cdot c \cdot d = -\log_{10}T$

R ~ T at 0.135 or 13.5% ~ $1/e^2$

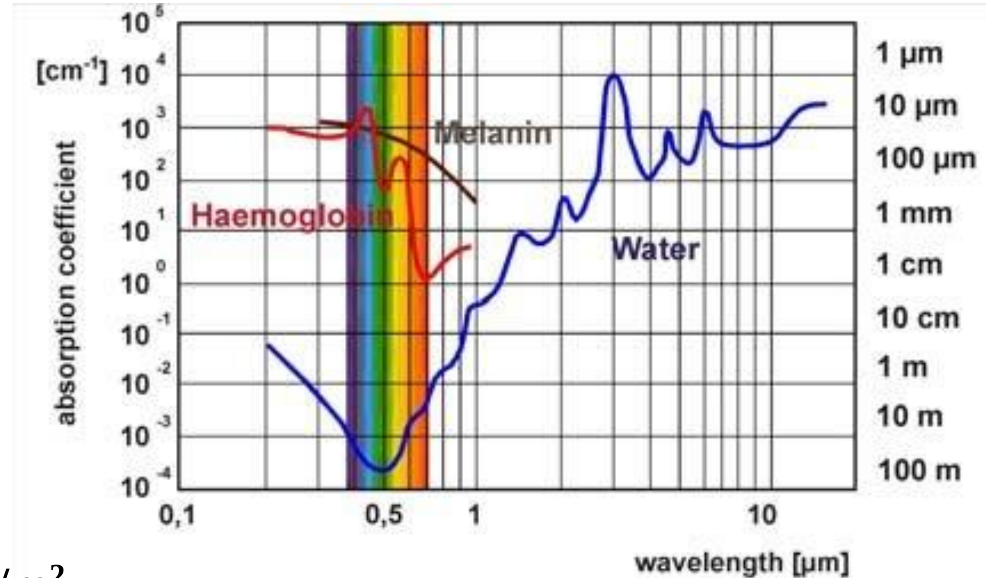

Solar irradiation at water surface	**1000 W/m²**
Photosynthesis limit	**~ 1 - 10 W/m²**
Full moon	**~ $5\cdot10^{-3}$ W/m²**
Phototaxis planctic Crustacea	**~ 10^{-7} - 10^{-8} W/m²**
B/W image vision human	**~ 10^{-7} W/m²**
Light perc. threshold deep sea fish	**~ 10^{-11} W/m²**
Light perc. threshold human	**~ 10^{-12} W/m²**
(~ star 6th magnitude)	**(~ 10^{-17} W/cm²)**

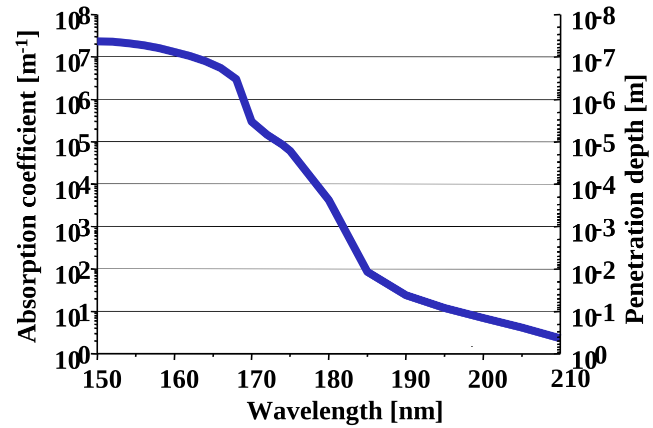

8.2 Absorption

Penetration depth R of photons and electrons into matter (Example Y_2O_3)

Photon impingement
→ Lambert-Beer equation with T in [%]

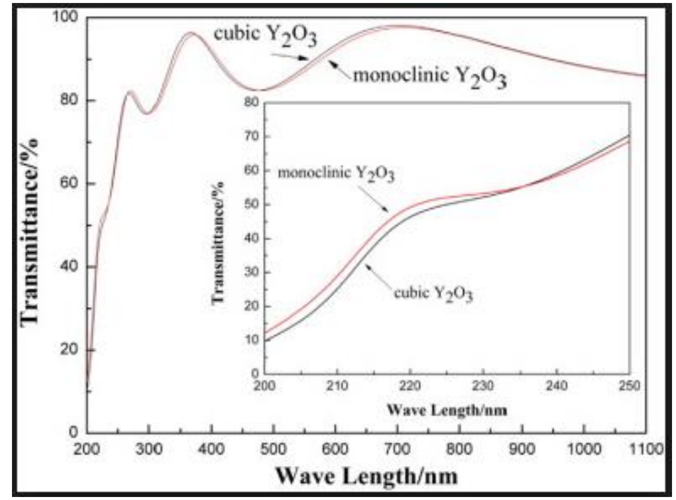

$$A(\lambda) = \varepsilon_\lambda \cdot c \cdot d = -\log_{10} T$$

R ~ T at 0.135 or 13.5% ~ 1/e²

1-10 µm

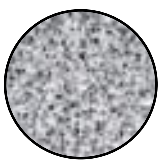

E = hν < E_g
e.g. 254 or 450 nm
Absorption by activator or sensitizer
Whole particle excitation

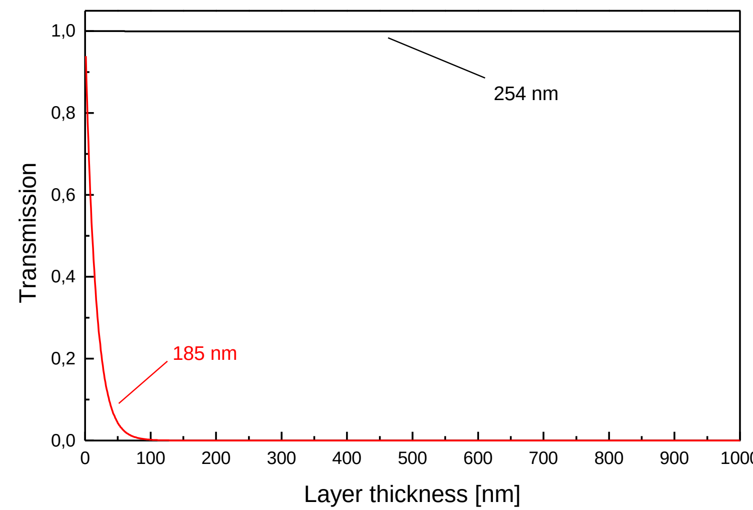

< 1 µm

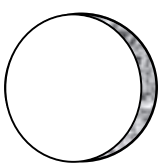

E = hν > E_g
e.g. 172 or 185 nm
Absorption by host material
Surface excitation

8.2 Absorption

Penetration depth R of photons and electrons into matter

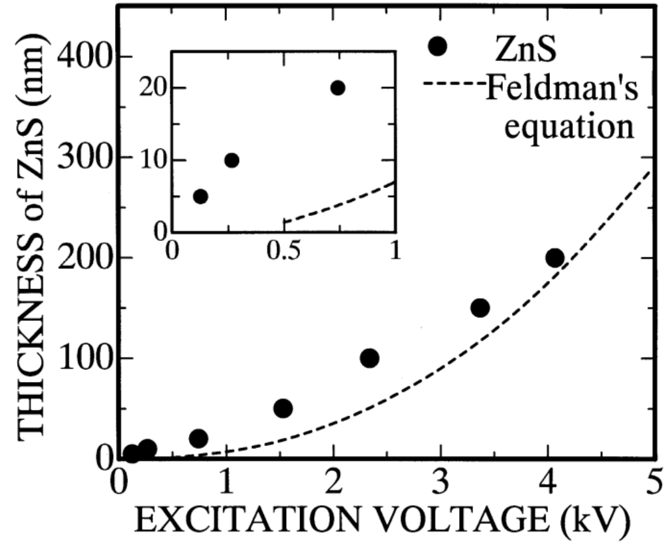

Electron impingement

→ Feldman equation with R in [Å]

$R = 250\ A/(\rho Z^{n/2})U^n$ with $n = 1.2/(1.0-0.29\log_{10}Z)$

Simplified equation: $R \sim 0.046 \cdot U^{5/3}/\rho$ [µm]

Example Y_2O_3 → $\rho = 5.0$ g/cm³

10 kV electrons R ~ 400 nm

2 kV electrons R ~ 30 nm

Example: 5.7 keV electrons	Density [g/cm³]	R [Å]	R [nm]
SiO_2	2.20	6171	617.8
Al_2O_3	3.97	3476	347.6
$Mg_3(PO_4)_2$	2.56	5345	534.4
ZnS	4.04	4248	424.8
MgO	3.59	3799	379.8
MgF_2	3.15	4464	446.4
MgS	2.68	5603	560.4

8.3 Excitation Mechanisms

High energy particles, γ- ray, x-ray, and high voltage electron excitation

1. Excitation of highly energetic core states
2. Thermalization and generation of electron-hole pairs with band gap energy
3. Energy transfer to activator ions or centers
4. (Center) Luminescence

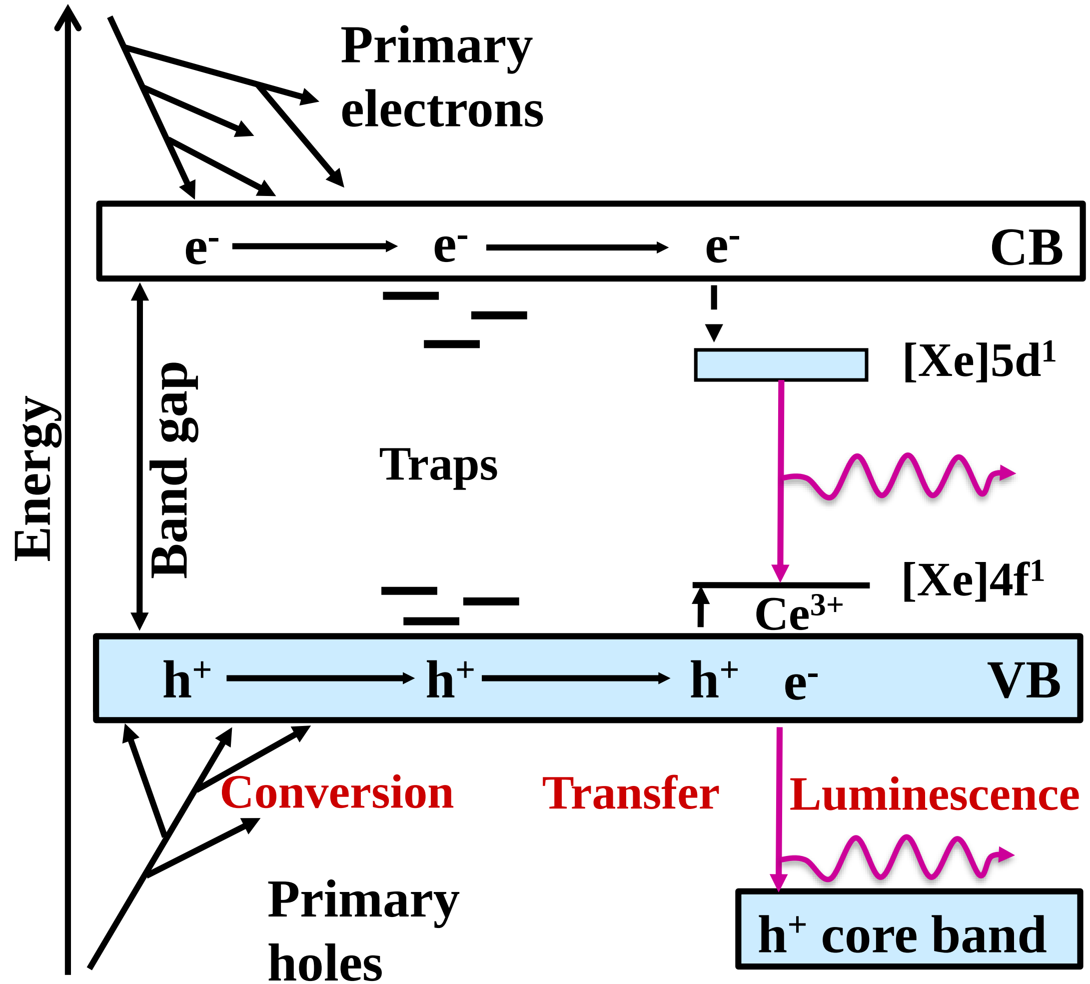

Efficiency and electron-hole pair generation well understood, but with two different models:

1. D.J. Robbins (J. Electrochem. Soc. 127 (1980) 2694)
2. R.H. Bartram, Lempicki (J. Luminescence 68 (1996) 225)

8.3 Excitation Mechanisms

Photons with energy > band gap of host matrix: Ne, Xe, or Xe/Ne excimer discharges

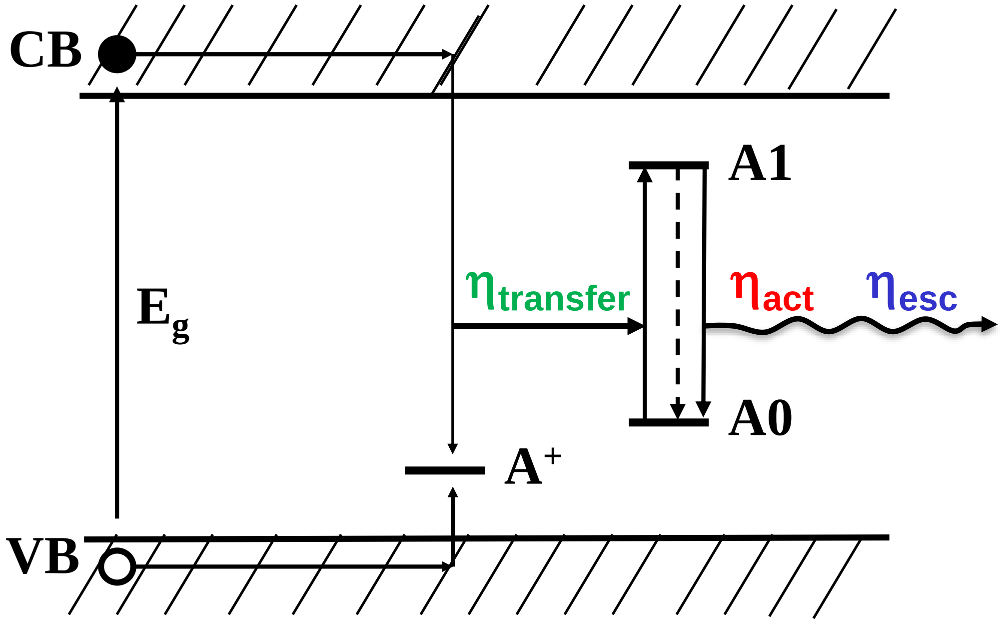

Host lattice	Band gap E_g [eV]
MgF_2	12.2
Al_2O_3	8.0
Y_2O_3	5.6
ZnS	3.9
ZnSe	2.8
ZnTe	2.4
CdS	2.6
CdSe	1.74
CdTe	1.6

Internal quantum efficiency: $IQE = \eta_r/(\eta_r + \eta_{nr}) = \eta_{act}$

External quantum efficiency: $EQE = \eta_{act} * \eta_{transfer} * \eta_{esc}$

8.3 Excitation Mechanisms

Photons with energy < band gap of host matrix : Hg discharges, (Al,In,Ga)N chips

Activator excitation

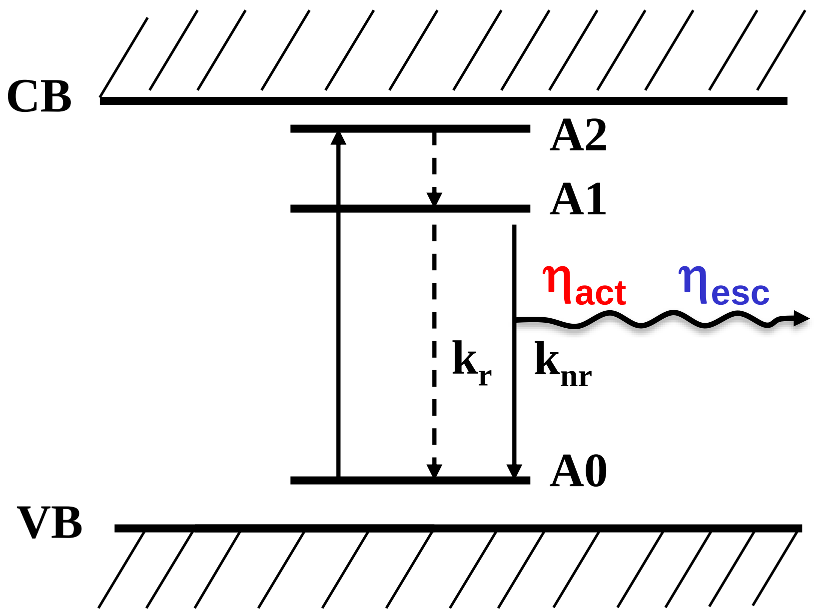

IQE = $\eta_{act} = k_r/(k_r + k_{nr}) = \tau/\tau_0$

with $k_r + k_{nr} = 1/\tau$ **and** $k_r = 1/\tau_0$

Sensitizer excitation

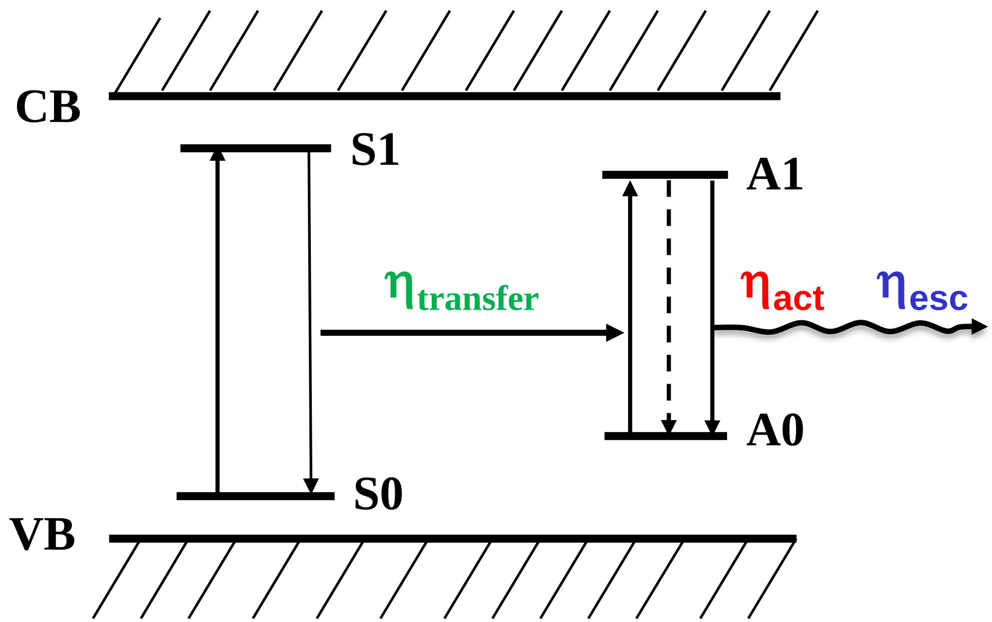

EQE = $\eta_{act} * \eta_{transfer} * \eta_{esc}$

8.3 Excitation Mechanisms

Example: $BaMgAl_{10}O_{17}$ doped by 10% Eu^{2+} (4f-5d transition)

Reflection spectra

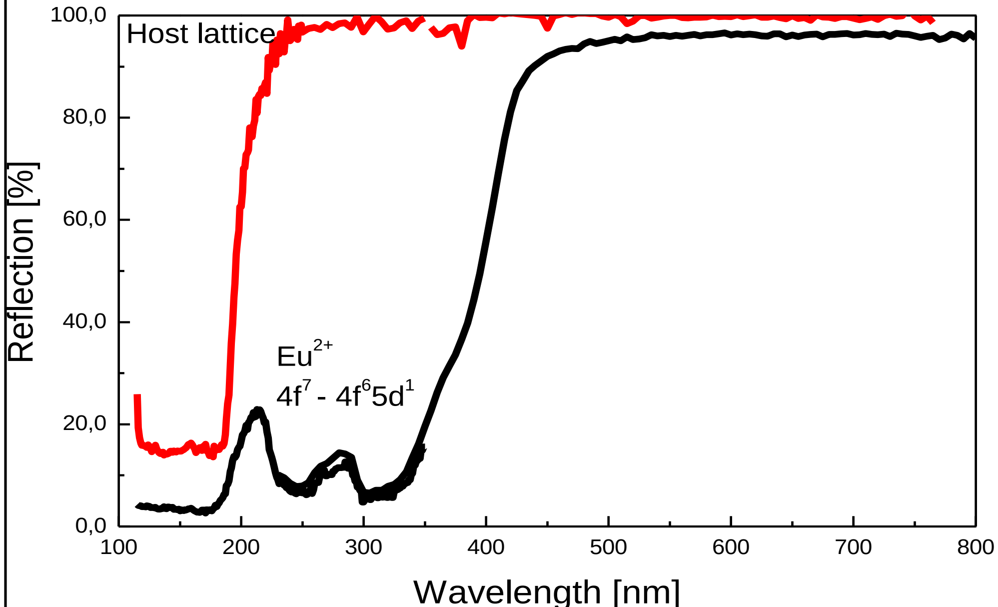

Emission and excitation spectra

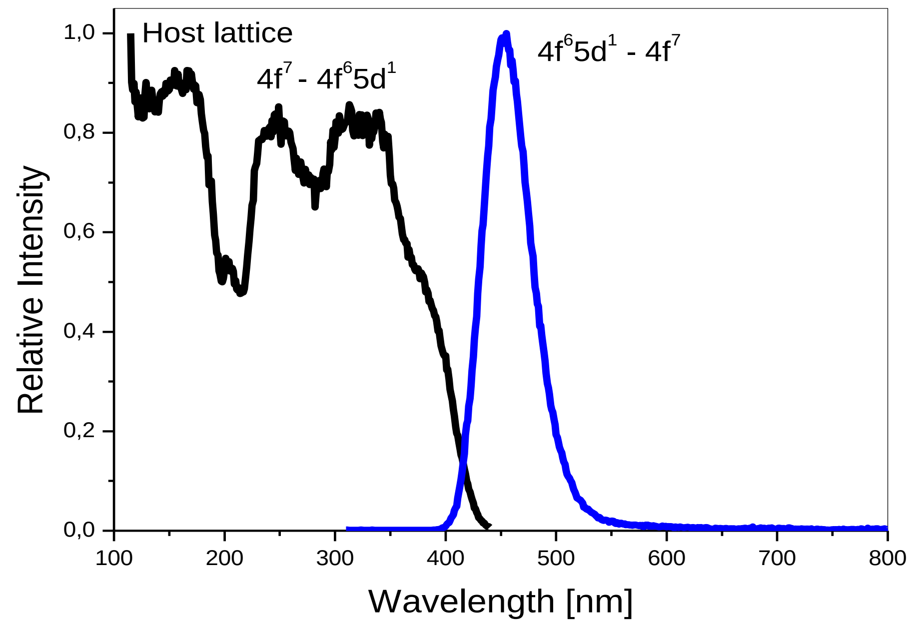

- **Host material VB → CB 180 nm (7.0 eV)**
- **Eu^{2+} $[Xe]4f^7 \rightarrow [Xe]4f^65d^1$ 250 nm (5.0 eV) and 310 nm (4.0 eV)**
- **Allowed transition ⇒ Intense absorption bands and fast decay (τ ~ 1 µs)**

8.3 Excitation Mechanisms

Example: $BaMgAl_{10}O_{17}$ doped by 5% Mn^{2+} (3d-3d transition)

Reflection spectra

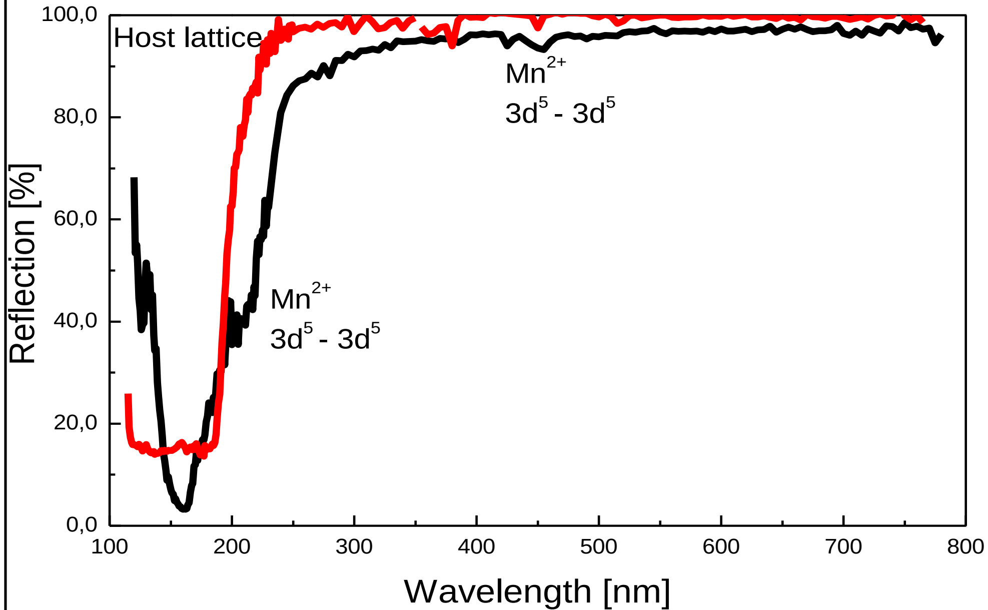

Emission and excitation spectra

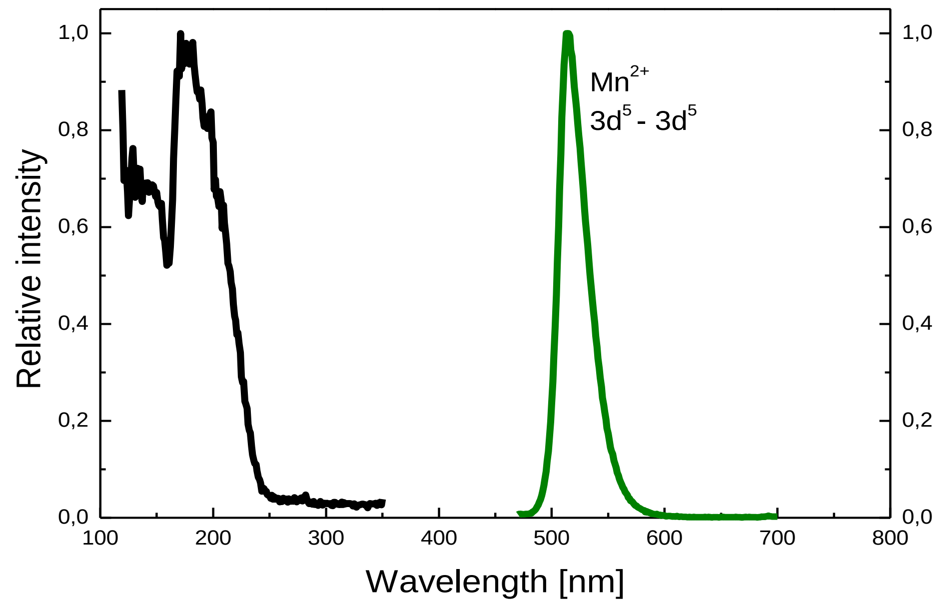

- **Host material VB → CB 180 nm (7.0 eV)**
- **Mn^{2+} [Ar]$3d^5$ → [Ar]$3d^5$ 200 nm (6.2 eV) and 450 nm (2.8 eV)**
- **Forbidden transition ⇒ Weak absorption bands and slow decay (τ ~ 10 ms)**

8.3 Excitation Mechanisms

Example: $LaPO_4$ doped by 20% Ce^{3+} (4f-5d transition)

Reflection spectra

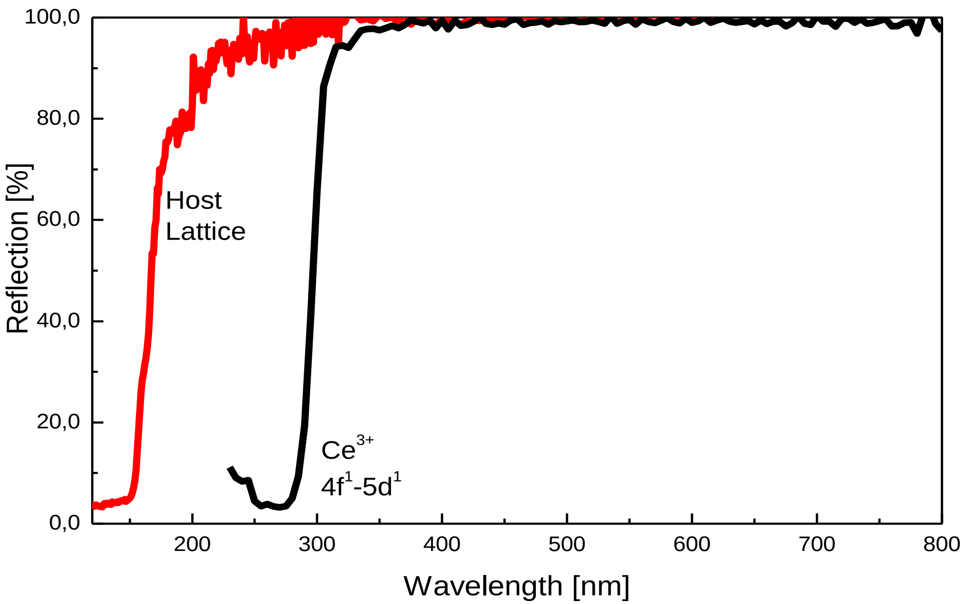

Emission and excitation spectra

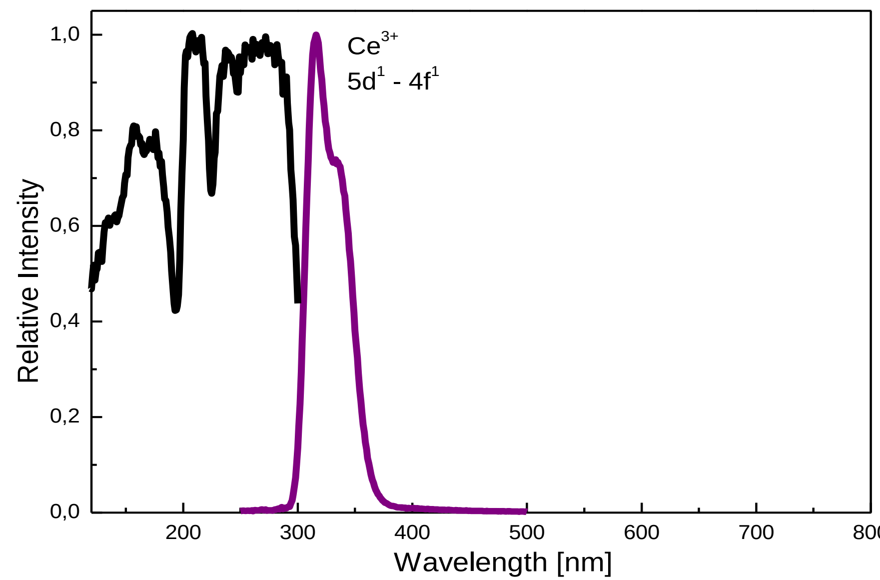

- **Host material VB → CB** **150 nm (8.2 eV)**
- **Ce^{3+} $[Xe]4f^1 \rightarrow [Xe]5d^1$** **200 nm (6.2 eV) and 450 nm (2.8 eV)**
- **Allowed transition ⇒ Intense absorption bands and fast decay (τ ~ 30 ns)**

8.3 Excitation Mechanisms

Example: Y_2O_3 doped by 5% Eu^{3+} (4f-4f transition)

Reflection spectra

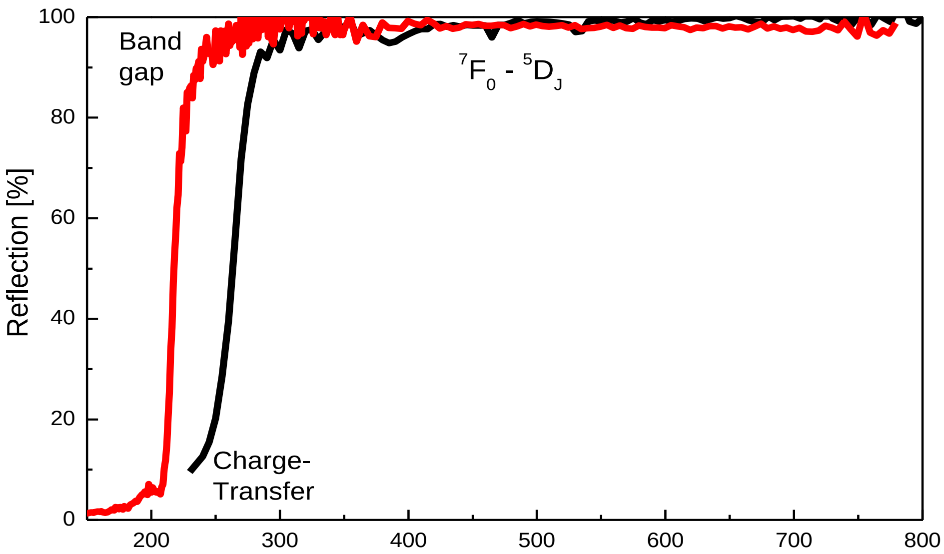

Emission and excitation spectra

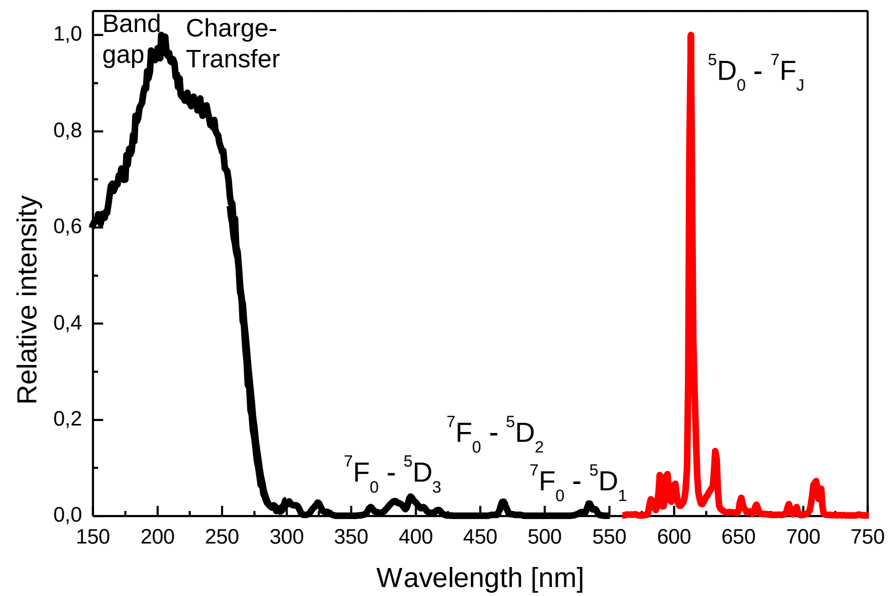

• Host material	VB → CB	210 nm (5.9 eV)
• Eu^{3+}	Charge-Transfer	230 nm (5.4 eV)
	$[Xe]4f^6 \rightarrow [Xe]4f^6$	395 nm (3.1 eV) and 465 nm (2.2 eV)

- Forbidden transitions ⇒ Weak absorption bands and slow decay (τ ~ 3 ms)

8.3 Excitation Mechanisms

Sensitisation to enhance absorption strength

→ $3d^n$ - $3d^n$ and $4f^n$ - $4f^n$ transitions are forbidden / weak

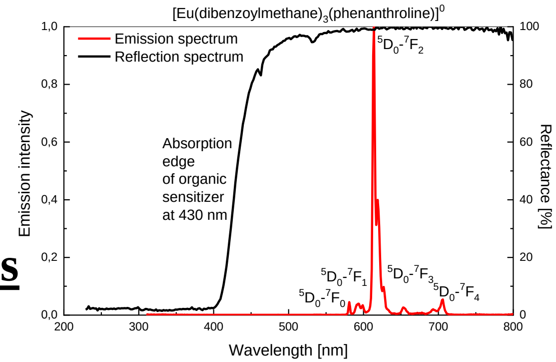

<u>Ways to enhance absorption strength of RE or TM doped materials</u>

- Taking advantage of allowed transitions
  - Charge-Transfer (CT) states → Eu^{3+}, Yb^{3+}
  - Low-lying energy levels of the $[Xe]4f^{n-1}5d^1$ configuration → Tb^{3+}, Eu^{2+}, Ce^{3+}, Pr^{3+}
- Sensitisation (via energy transfer)
  - Ce^{3+} (→ Gd^{3+}) → Tb^{3+}
  - Pr^{3+} → Tb^{3+}
  - Nd^{3+} → Gd^{3+}
  - Pr^{3+} → Gd^{3+}
  - Bi^{3+} → Eu^{3+}
  - $[UO_2]^{2+}$ → Eu^{3+}
  - Sb^{3+} → Mn^{2+}
  - Ce^{3+} → Mn^{2+}
  - Eu^{2+} → Mn^{2+}
  - Aromatic ligands (→ π-π* transitions) → Eu^{3+} or Tb^{3+}, e.g. $[Eu(dbm)_3(phen)]^0$

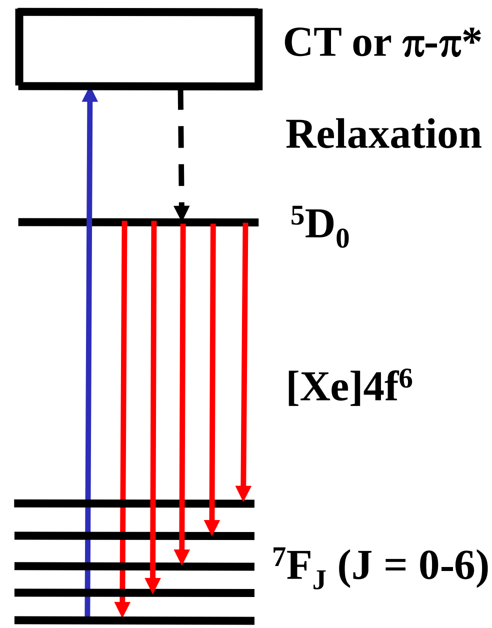

Simplified energy diagram of Eu^{3+}

8.4 Energy Transfer

Requirements for ET ($S^* + A \rightarrow S + A^*$)

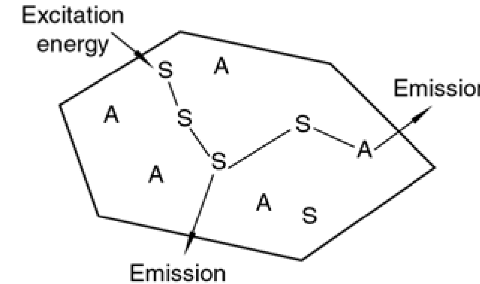

(a) Sensitizer S and activator A interact with each other by

– **Multipolar or Coulomb interaction via space**

Dipole-Dipole:	$P_{SA} = (1/\tau_S)(r_0/r_{SA})^6$	Ce^{3+} - Eu^{2+}
Dipole-Quadrupole:	$P_{SA} = (1/\tau_S)(r_0/r_{SA})^8$	Ce^{3+} - Tb^{3+}
Quadrupole-Quadrupole:	$P_{SA} = (1/\tau_S)(r_0/r_{SA})^{10}$	unknown

– **Exchange interaction via orbital overlap**

$P_{SA} \sim J \cdot \exp(-2\, r_{SA})$

for $r_{SA} < 5$ Å with J = coupling constant [cm^{-1}]

(b) Spectral overlap

→ energy conservation law

→ resonant transfer

→ ΔE bridged by phonons

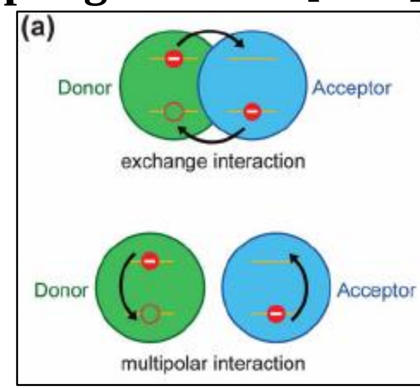

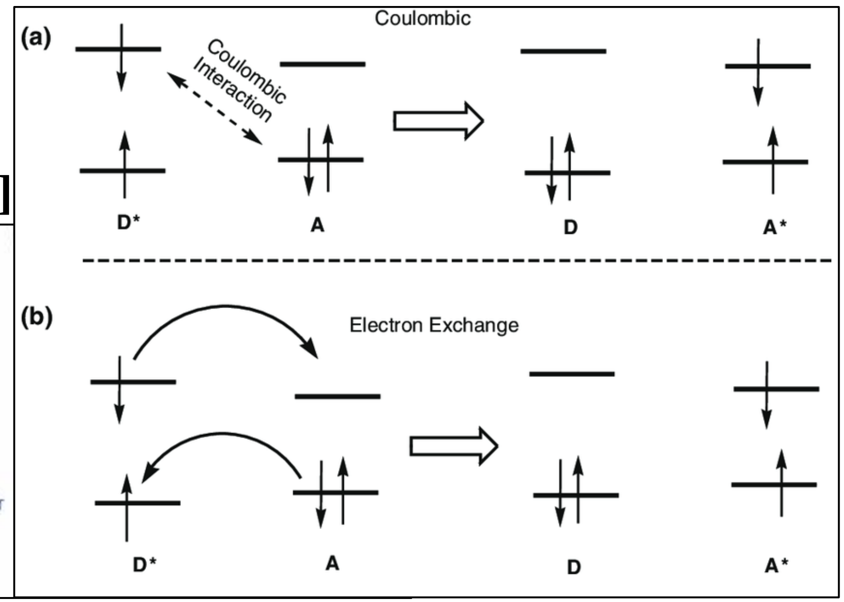

8.4 Energy Transfer

Probability P_{ET}

The probability P_{ET} for an energy transfer is given by the following term:

$$P_{ET} = (2\pi/\hbar)\cdot(\rho) < \varphi_i \,|\, H \,|\, \varphi_f >^2$$

φ_i: Wave function of the initial state

φ_f: Wave function of the final state

H: Operator coupling the states

ρ: Spectral overlap (energy conservation law)

Spectral overlap

$\rho = g_S(E)\cdot g_A(E)\cdot dE$

$g_S(E)$ and $g_A(E)$: Normalised optical line shape functions for sensitizer and activator ions

Energy Transfer

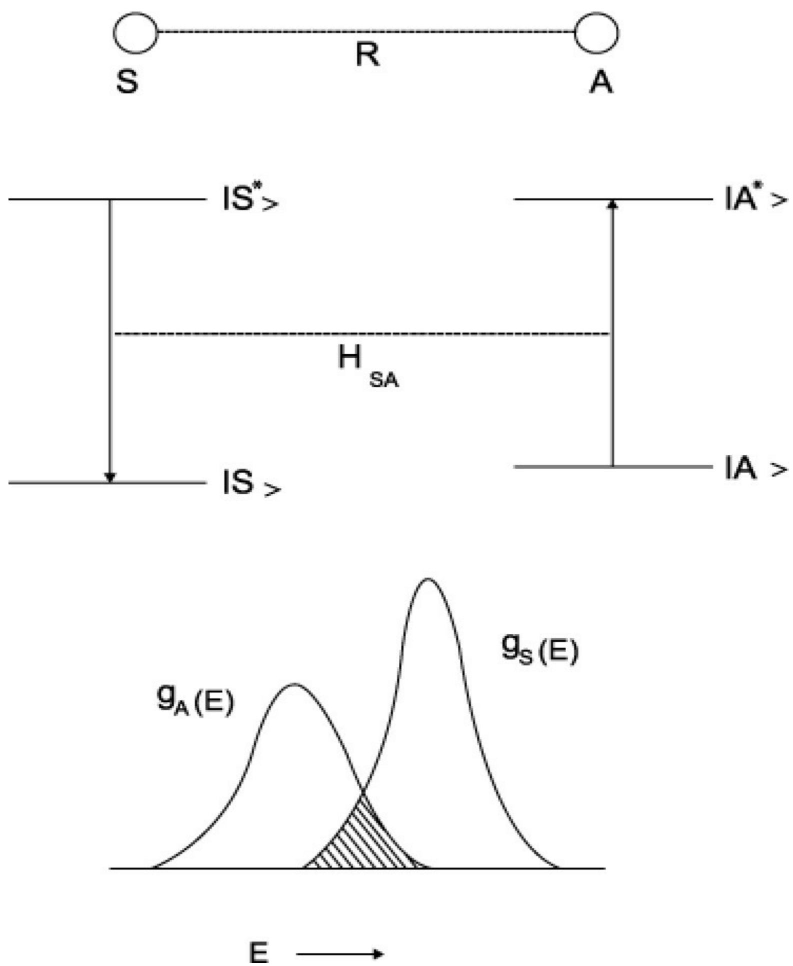

8.4 Energy Transfer

Consequences for luminescence processes

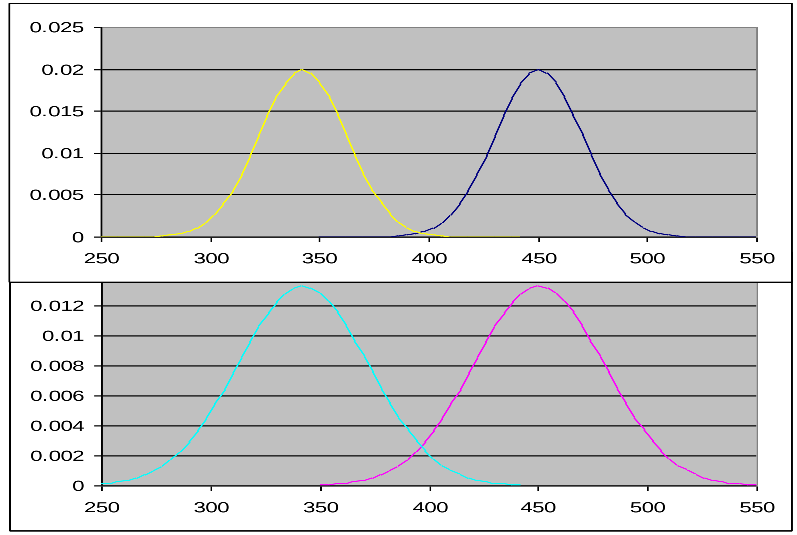

ET causes

- **Energy migration**
- **Concentration quenching**
- **Thermal quenching**
- **Cross-relaxation**
- **Possibility of sensitization**

Some rules

- **ET efficiency correlates to spectral overlap ρ**
- **ET from a broad band emitter to a line emitter only possible for nearest neighbors in the host lattice (Ce^{3+} - Tb^{3+})**
- **ET from a line emitter to a band absorber proceeds over long distances (Gd^{3+} - Ce^{3+})**
- **ET strongly depends on average distance and thus concentration of luminescent centers (Eu^{3+} - Eu^{3+})**
- **ET strongly depends on average lifetime of luminescent centers**

8.4 Energy Transfer

Example: ET in $LaPO_4:Ce^{3+},Tb^{3+}$

$LaPO_4:Ce^{3+}$

$Ce^{3+} \rightarrow (Ce^{3+})^*$	Excitation 4f - 5d
$(Ce^{3+})^* \rightarrow Ce^{3+}$	Emission 5d - 4f

$LaPO_4:Tb^{3+}$

$Tb^{3+} \rightarrow (Tb^{3+})^{**}$	Excitation 4f - 5d
$(Tb^{3+})^{**} \rightarrow (Tb^{3+})^*$	Relaxation
$(Tb^{3+})^* \rightarrow Tb^{3+}$	Emission 4f - 4f

$LaPO_4:Ce^{3+},Tb^{3+}$

$Ce^{3+} \rightarrow (Ce^{3+})^*$	Excitation 4f - 5d
$(Ce^{3+})^* + Tb^{3+} \rightarrow Ce^{3+} + (Tb^{3+})^*$	ET from Ce^{3+} to Tb^{3+}
$(Tb^{3+})^* \rightarrow Tb^{3+}$	Emission 4f - 4f

Fluorescent lamps $\Rightarrow$ Excitation at 254 nm (& 185 nm)

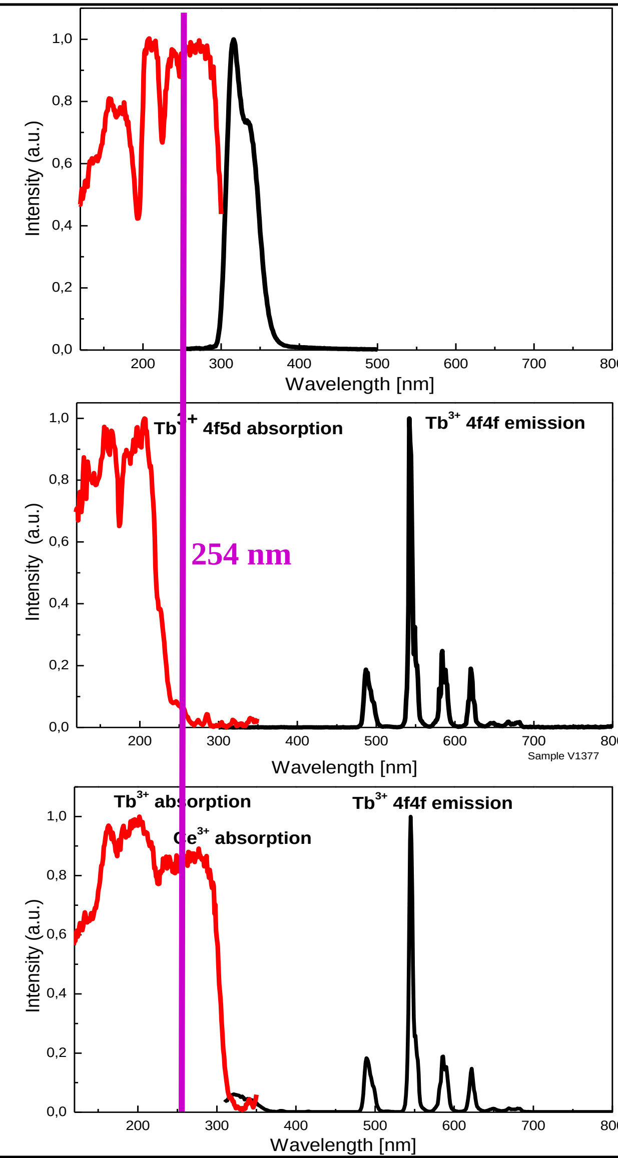

8.4 Energy Transfer

Example: ET in $BaMgAl_{10}O_{17}:Eu^{2+}$ co-doped by transition metal ions

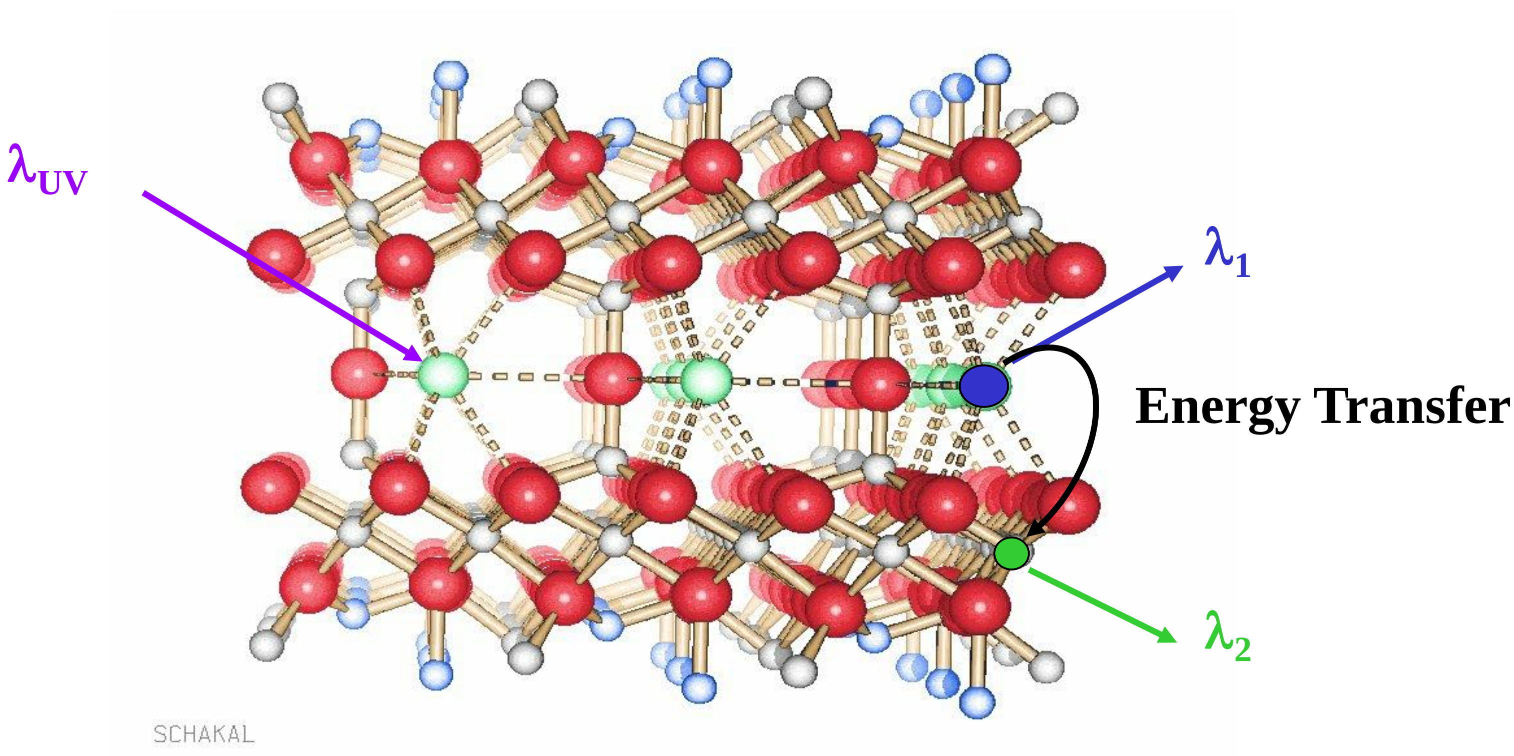

Divalent RE ions	**Ba^{2+} sites in the conduction layer**	**Eu^{2+}, Yb^{2+}**
Divalent TM ions	**tetrahedral gaps in the spinel blocks**	**Mn^{2+}, Co^{2+}**
Trivalent TM ions	**octahedral gaps in the spinel blocks**	**Cr^{3+}, Ti^{3+}**

8.4 Energy Transfer

Example: ET in $BaMgAl_{10}O_{17}:Eu^{2+}$ co-doped by TM ions

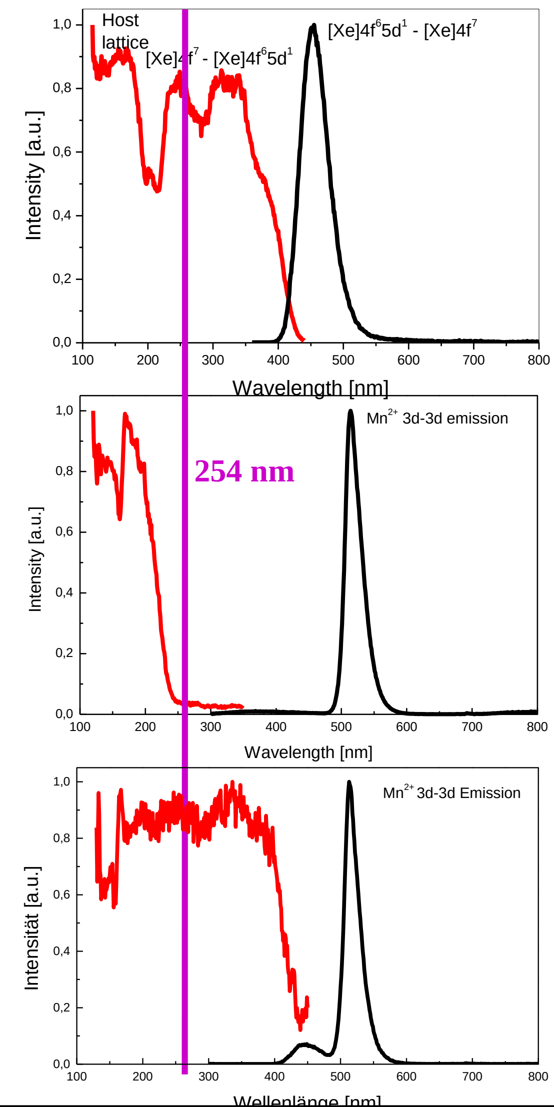

<u>$BaMgAl_{10}O_{17}:Eu^{2+}$</u>

$Eu^{2+} \rightarrow (Eu^{2+})^*$	Absorption 4f - 5d
$(Eu^{2+})^* \rightarrow Eu^{2+}$	Emission 5d - 4f

<u>$BaMgAl_{10}O_{17}:Mn^{2+}$</u>

$Mn^{2+} \rightarrow (Mn^{2+})^*$	Absorption 3d - 3d
$(Mn^{2+})^* \rightarrow Mn^{2+}$	Emission 3d – 3d

<u>$BaMgAl_{10}O_{17}:Eu^{2+},Mn^{2+}$</u>

$Eu^{2+} \rightarrow (Eu^{2+})^*$	Absorption 4f - 5d
$(Eu^{2+})^* + Mn^{2+} \rightarrow Eu^{2+} + (Mn^{2+})^*$	ET from Eu to Mn
$(Mn^{2+})^* \rightarrow Mn^{2+}$	Emission 3d – 3d

$BaMgAl_{10}O_{17}$:Eu(Mn) can be excited at 172 nm, 254 and 370 nm
$\Rightarrow$ Application in PDPs, FLs (and near UV emitting LEDs)

8.4 Energy Transfer

Energy pathways in $BaMgAl_{10}O_{17}$:$Eu^{2+}Mn^{2+}$

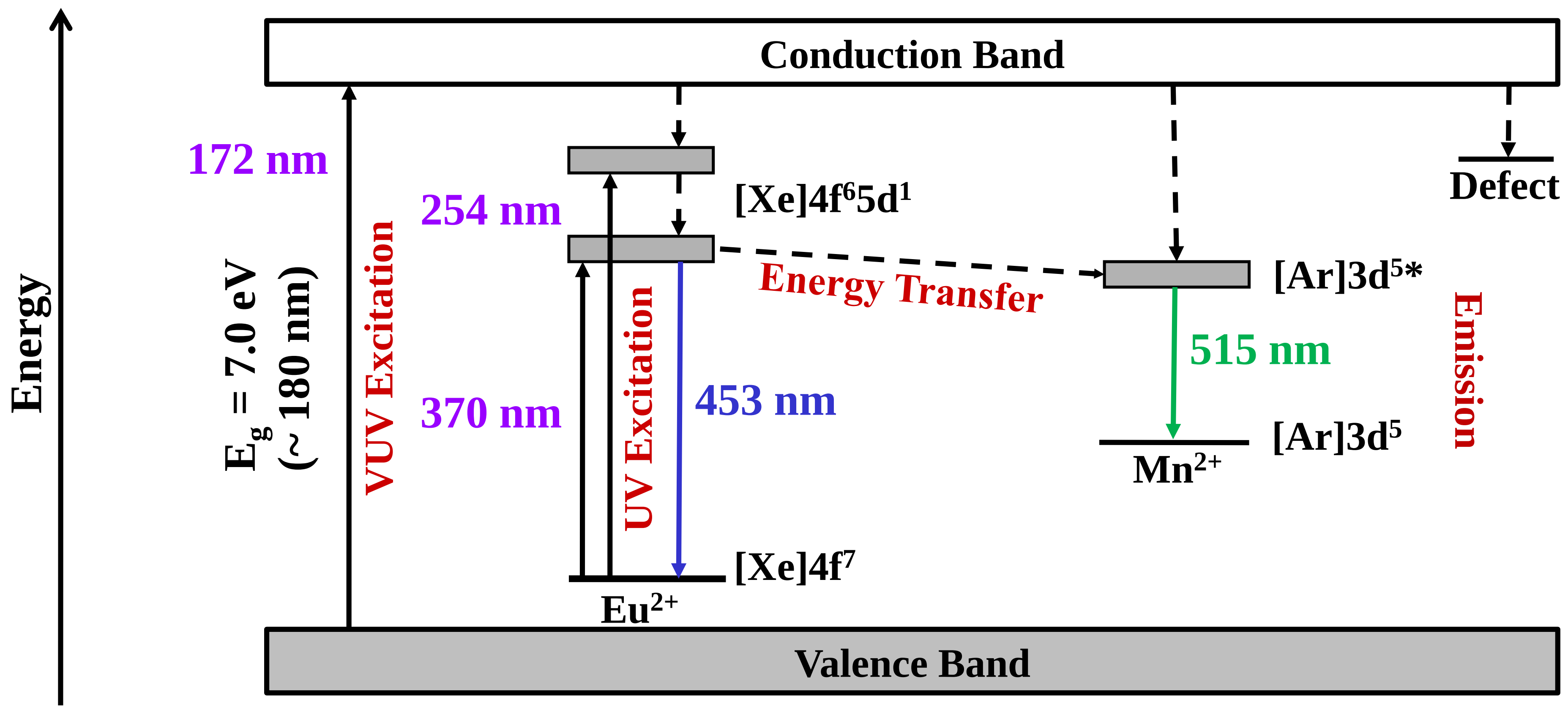

8.5 Loss Processes

Overview of the most relevant processes leading to luminescence quenching

1. **The absorbed energy does not reach the activator ion** ($\eta_{transfer}$)
   a) Competitive absorption
   b) ET to defects or non-luminescent impurity ions
   c) Excited state absorption (ESA)
   d) Auger processes

2. **The absorbed energy reaches the activator ion, but non-radiative channels dominate the radiative return to the ground state** (η_{act})
   a) Crossing of excited and ground state parabola
   b) Multi-phonon relaxation
   c) Cross-relaxation
   d) Photoionization
   e) Energy transfer to quenching sites = f(T)

$$W_{nr} = \frac{e^{-B \cdot p}}{A}$$

with A, B = fitting parameter
p = highest phonon frequency

3. **Emitted radiation is re-absorbed by the luminescent material** (η_{esc})
   a) Self-absorption due to spectral overlap between excitation and emission band
   b) Additional absorption bands due to degradation of the material, e.g. by colour centre formation

8.5 Loss Processes

Related to the host lattice and host lattice activator interaction

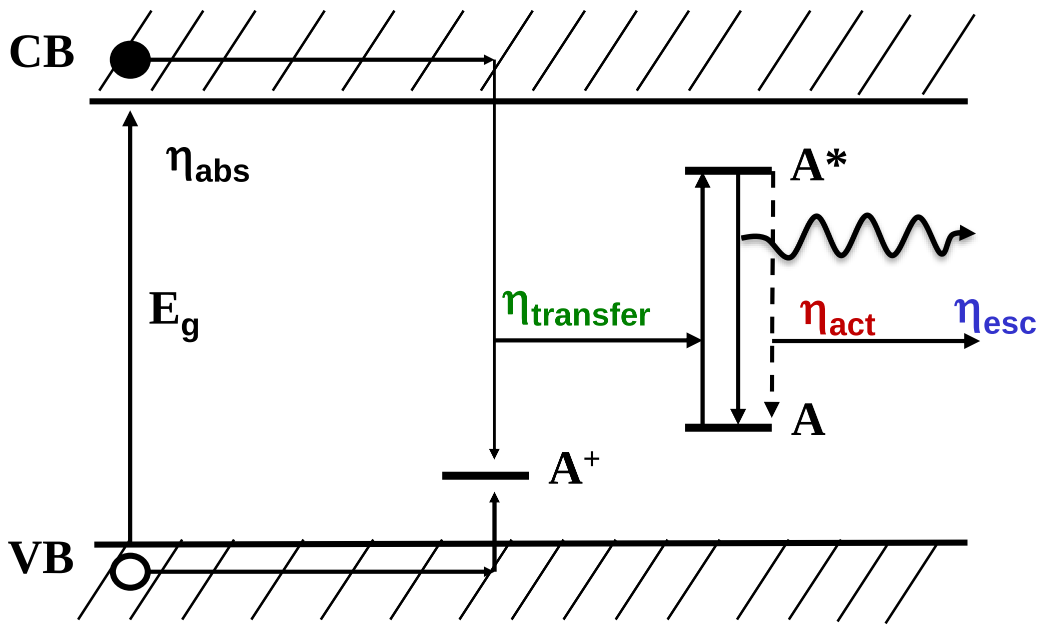

Internal Quantum Efficiency

IQE $= \eta_{act}$
$= \eta_r/(\eta_r + \eta_{nr})$
$= \tau/\tau_0$

(Anti proportional to decay time)

External Quantum Efficiency

EQE $= N_{h\nu(emitted)}/N_{h\nu(absorbed)}$
$= \eta_{transfer} * \eta_{act} * \eta_{esc}$

(No correlation to decay time!)

Light Yield

LY $= EQE * \eta_{abs} = EQE*(1-R)$

(No correlation to decay time!)

8.5 Loss Processes

Photoionization (PI) of the activator ion

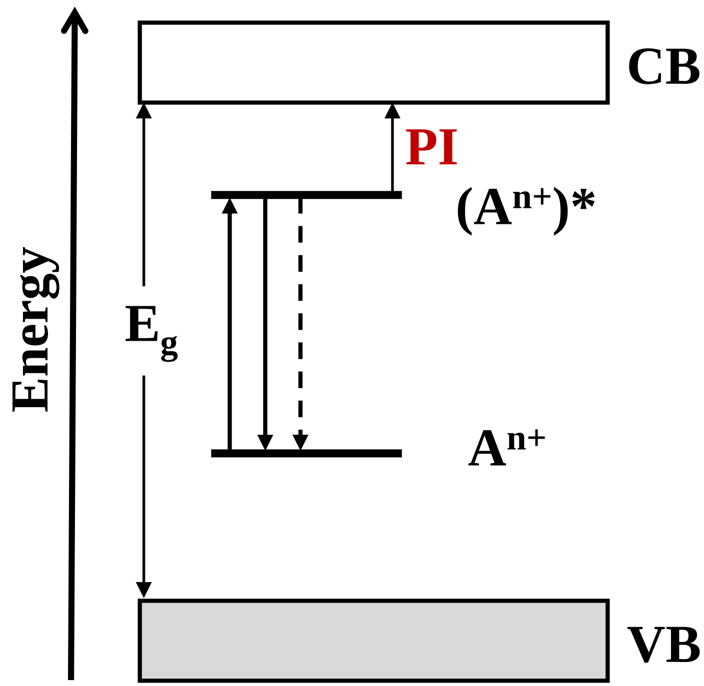

Process of Photionisation (PI)

- Excited A^{n+} ion gets ionised
  - $Ce^{3+} \rightarrow Ce^{4+}$
  - $Pr^{3+} \rightarrow Pr^{4+}$
  - $Sm^{2+} \rightarrow Sm^{3+}$
  - $Eu^{2+} \rightarrow Eu^{3+}$
  - $Tb^{3+} \rightarrow Tb^{4+}$
  - $Yb^{2+} \rightarrow Yb^{3+}$
- Released electron is re-trapped, e.g. by anion vacancies $\rightarrow$ reduced EQE
- Causes afterglow in
  - Scintillators
  - Displays phosphors
  - Persistent phosphors

8.6 Cross-Relaxation

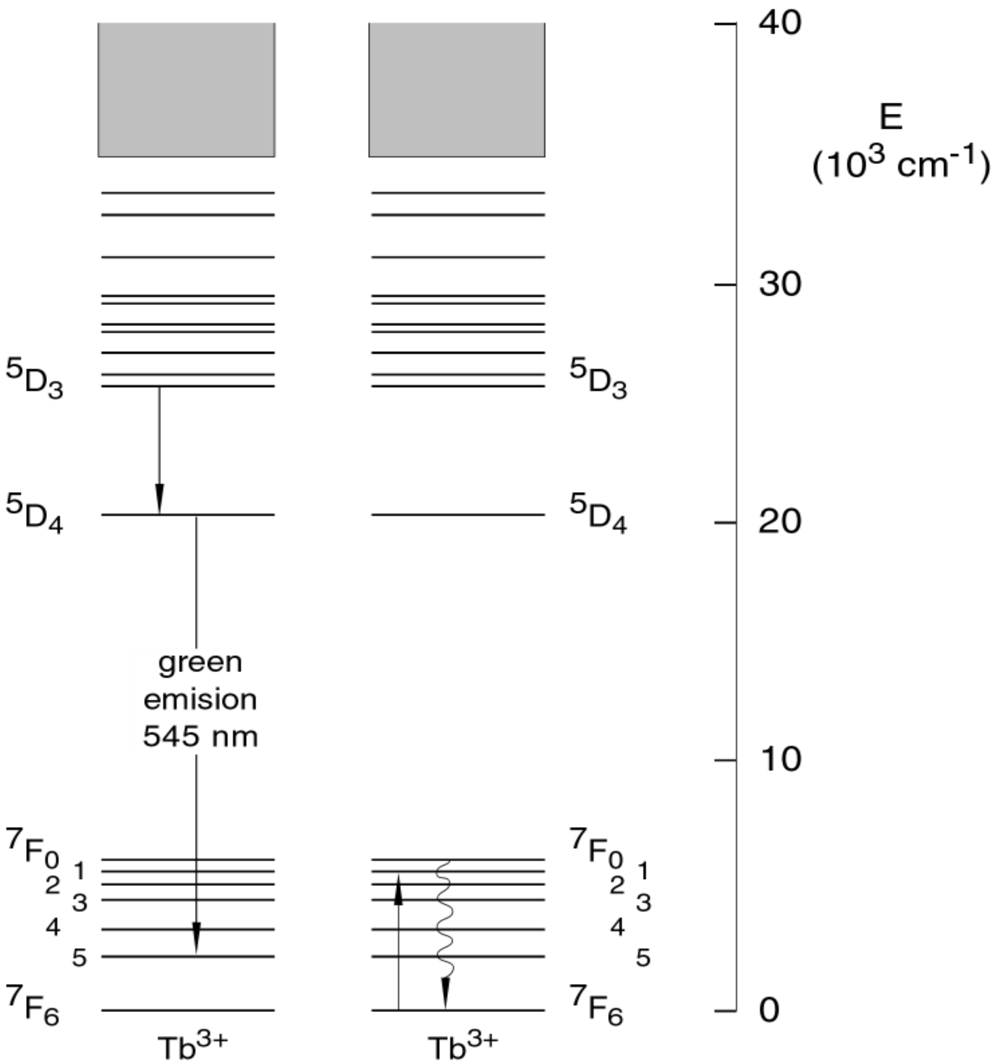

- Cross-relaxation processes are responsible for the quenching of luminescence of higher 4f levels of Tb^{3+} at a high Tb^{3+} concentration

Emission spectra of Tb^{3+} activated Yttrium oxysulphides

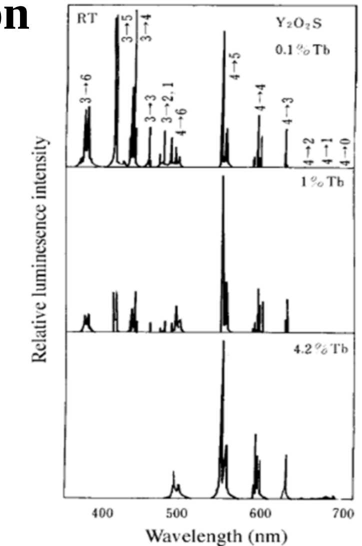

- Cross-relaxation also occurs in Eu^{3+}, Sm^{3+} , Pr^{3+}, and Dy^{3+} doped materials
- Concentration quenching for Sm^{3+} or Dy^{3+} activated materials by cross-relaxation and not by energy migration
- Relaxation to the first excited state can also be triggered by high energy photons

8.7 Configuration Coordinate Diagram

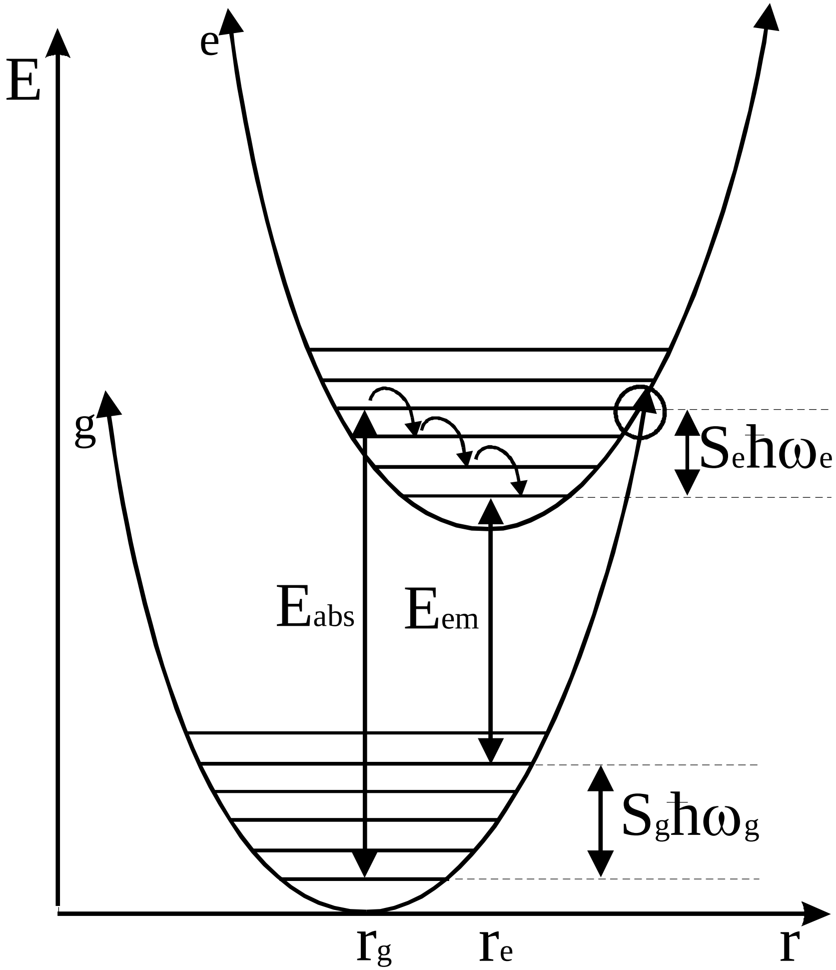

- **Stokes Shift**

  Energy gap between absorption and emission band

  $S = S_e h\omega_e + S_g h\omega_g$

- **Full width at half maximum of the emission band**

  FWHM ~ √S

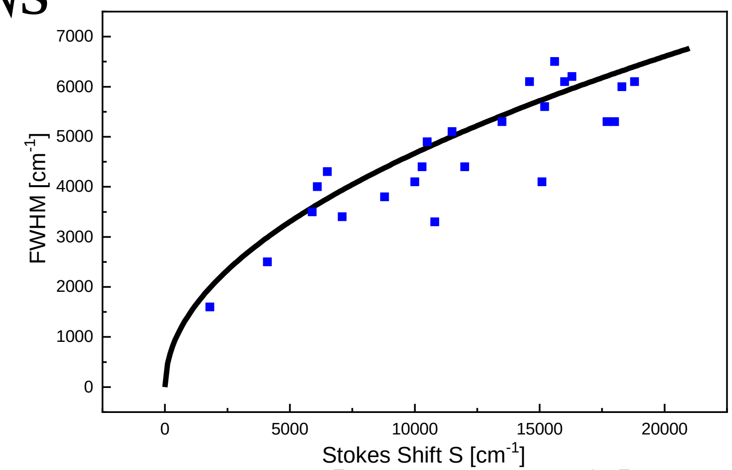

- **Quenching temperature decreases with increasing $\Delta R = r_e - r_g$**

8.7 Configuration Coordinate Diagram

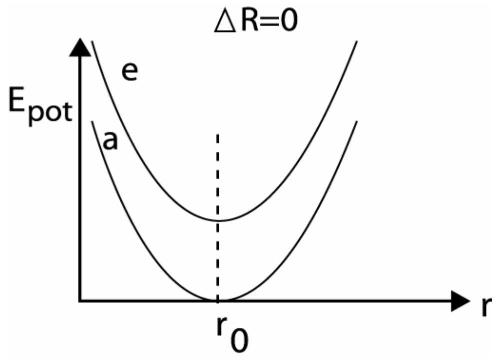

1. **Weak to no electron-phonon-coupling**

- **High IQE, EQE determined by ET processes**
- **Thermal quenching mainly due to photoionization**
- **4f → 4f transitions (shielded 4f-shell: small crystal field splitting [CFS])**
- **Lines** Eu^{3+}, Tb^{3+}, ….

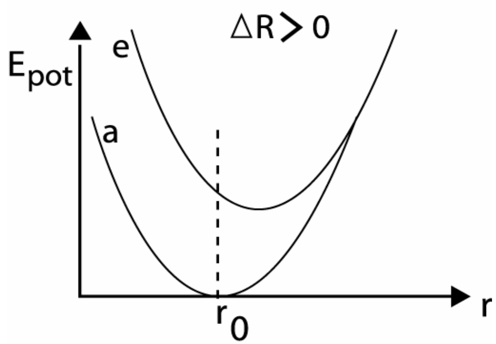

2. **Moderate electron-phonon-coupling**

- **High to moderate IQE**
- **Thermal quenching due to tunnelling or photoionization**
- **4f → 5d transitions (large CFS)**
- **Narrow bands** Eu^{2+}, Ce^{3+}, ….

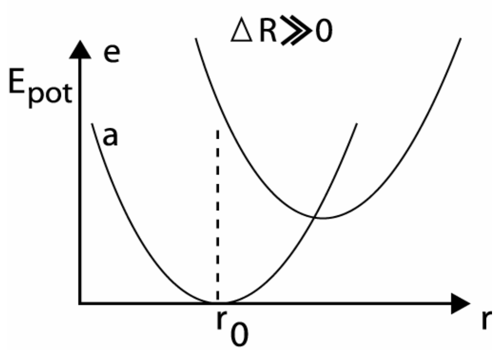

3. **Strong electron-phonon-coupling**

- **High to low IQE at RT, strong thermal quenching**
- **Thermal quenching mainly due to tunnelling**
- **ns^2 → ns^1np^1 or CT transitions**
- **Broad bands** Pb^{2+}, Bi^{3+}, ….

8.7 Configuration Coordinate Diagram

Width of the transitions can be explained by the model "harmonic oscillator"

$F = -k*(r - r_0)$: Integration

$\Rightarrow E = -1/2*k*(r - r_0)^2$

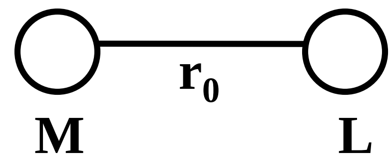

Quantum mechanics provides: $E_v = (v + 1/2)*h\nu$

Franck-Condon principle: Electrons motion is much faster than nuclear motion $\rightarrow$ "vertical transitions"

Transitions: $E_g(v_g = 0) \rightarrow E_e(v_e = x)$ for $v_e = 0$ "zero-phonon line"

$r_{0g} = r_{0e} \Rightarrow$ narrow bands or lines ($4f \rightarrow 4f$ absorption lines)

$r_{0g} < r_{0e} \Rightarrow$ broad bands ($4f^n \rightarrow 4f^{n+1}L^{-1}$, $4f^n \rightarrow 4f^{n-1}5d$, $6s^2 \rightarrow 6s6p$)

8.8 Thermal Quenching

Model based on a two-level system: Example $SrGa_2S_4:Eu^{2+}$

Emission spectrum

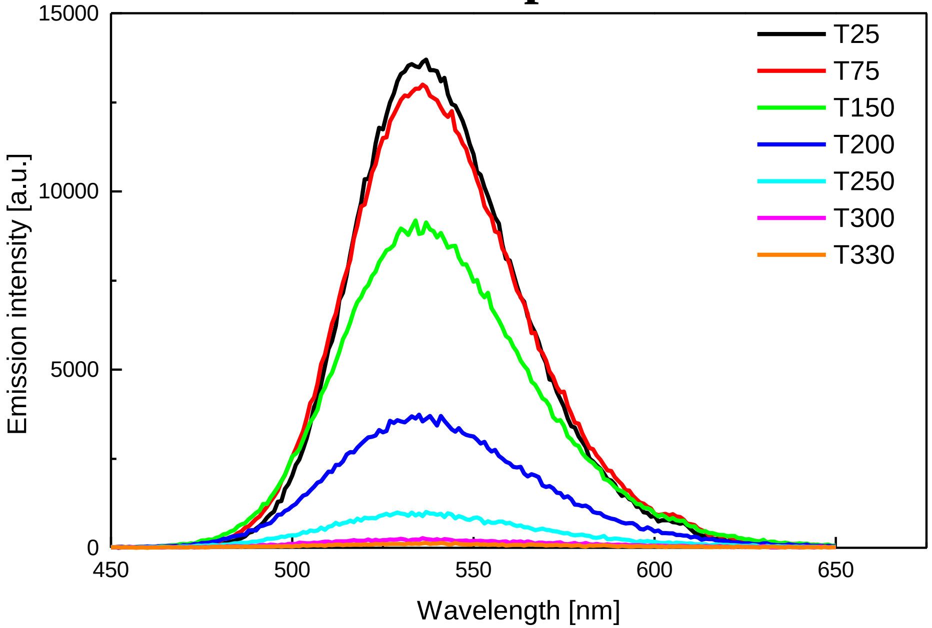

Peak intensity and integral

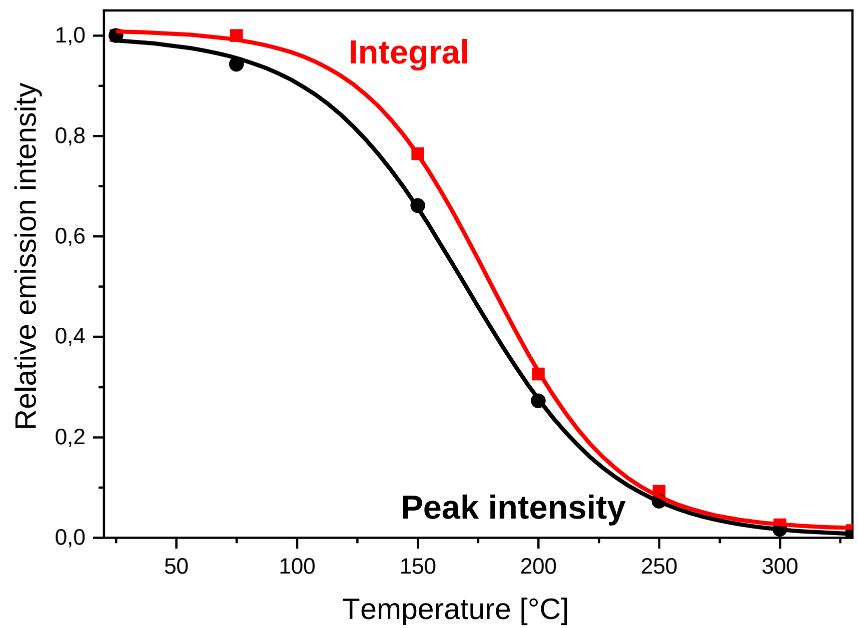

- **Mathematical fit: $I(T) = A_0 + I_0/(1 + B\cdot\exp(-\Delta E/k_BT))$ „Struck-Fonger-Model“**
- **$T_{1/2}$ = Temperature at which the phosphor loses 50% of its initial emission intensity (here ~ 170 °C) ~ activator-host lattice interaction**
- **In many industrially applied phosphors the quantum yield starts to decline between 100 and 150 °C**

8.8 Thermal Quenching

Eu^{2+} activated phosphors

Light yield as a function of the temperature

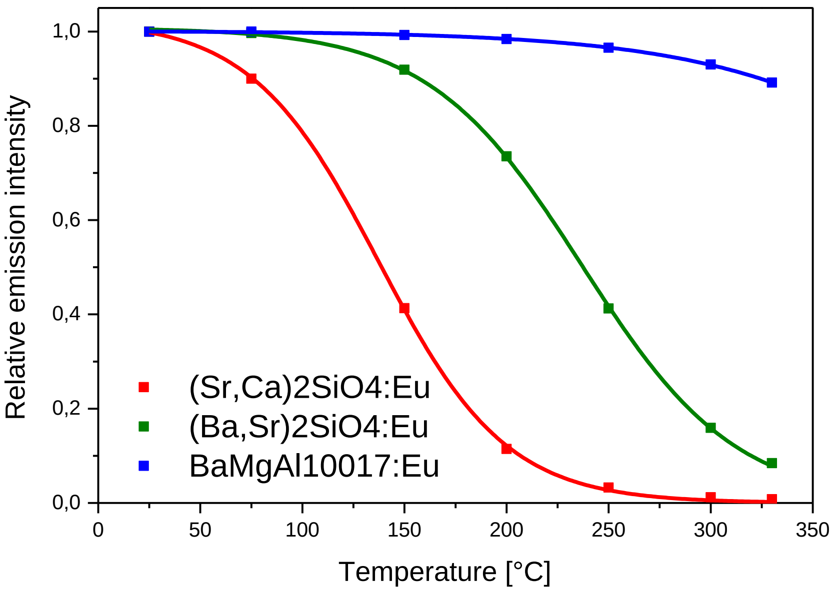

Spectral width of the emission band of $BaMgAl_{10}O_{17}$:Eu as a function of the temperature

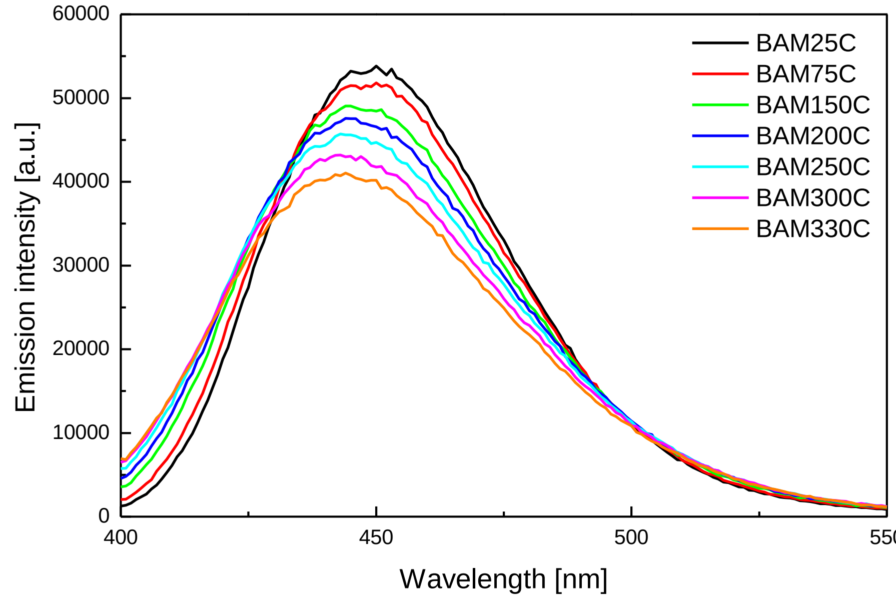

Stokes shift $BaMgAl_{10}O_{17}$:Eu < $(Ba,Sr)_2SiO_4$:Eu < $(Sr,Ca)_2SiO_4$:Eu

Thermal quenching $BaMgAl_{10}O_{17}$:Eu < $(Ba,Sr)_2SiO_4$:Eu < $(Sr,Ca)_2SiO_4$:Eu

Blue shift due to thermal expansion of the host and thus reduction in crystal field splitting!

8.8 Thermal Quenching

Some Rules

- **Decreases with increasing energy separation of the ground and excited state**

- **Increases with increasing phonon frequencies (thus most organic compounds exhibit luminescence only at low temperatures)**

- **Increases with $\Delta r = r_e - r_g$ and thus with Stokes Shift**

- **Thermal quenching due to photoionization concerns luminescent materials, where the excited state is located close to the conduction band**

8.9 Lifetime of the Excited State

Description equal to 1st order kinetics (no energy transfer!)

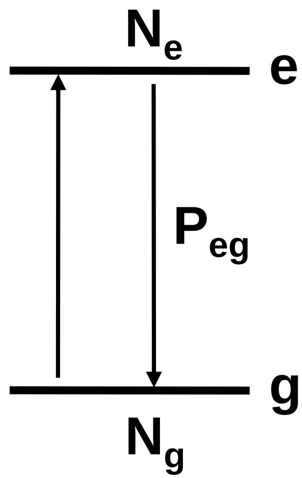

$dN_e/dt = - N_e * P_{eg}$

$\Rightarrow dN_e/N_e = -P_{eg} * dt$: Integration

$\Rightarrow \ln(dN_e(t)/N_e(0)) = -P_{eg} * t$

$\Rightarrow N_e(t) = N_e(0) * \exp(-P_{eg}/\tau)$ with $\tau = 1/P_{eg}$

Transition	Time scale	Oscillator strength	Activators
"allowed"	$\sim 10^{-9}$ s	$f \sim 0.1$	Eu^{2+}, Ce^{3+}
"weak"	$\sim 10^{-6}$ s	$f \sim 0.001$	Pr^{3+}, Nd^{3+}
"forbidden"	$\sim 10^{-3}$ s	$f \sim 10^{-5}$	Eu^{3+}, Mn^{2+}

8.9 Lifetime of the Excited State

Typical decay curves

$BaMgAl_{10}O_{17}:Eu^{2+}$ (τ = 1 µs)

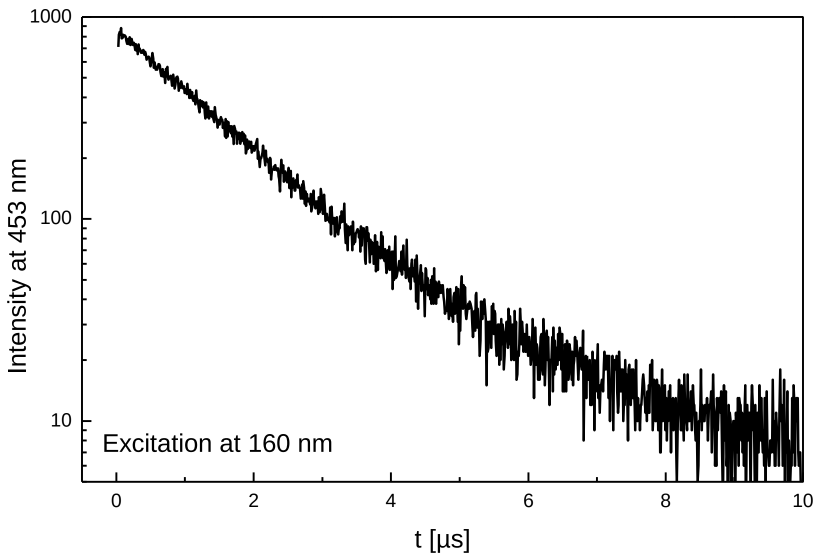

$(Y,Gd)BO_3:Eu^{3+}$ (τ = 3.5 ms)

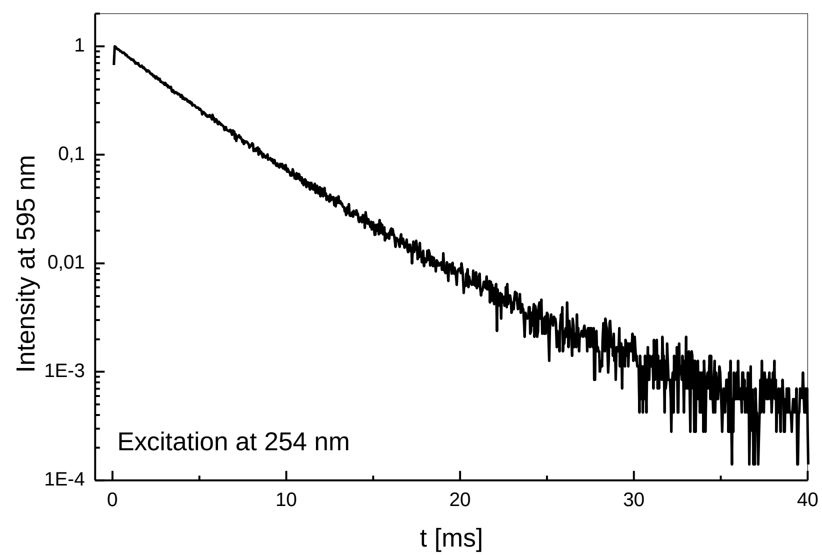

Mono-exponential decay ⇒ No energy transfer e.g. to impurities such as Fe^{3+} or Cr^{3+}

Deviation from mono-exponential decay ⇒ quenching, energy transfer to defects or impurity ions , afterglow and so on

8.10 Luminescence of Transition Metal Ions

Absorption processes of d^n-ions → Tanabe-Sugano diagrams

Energy level diagram of a d^1-ion (Ti^{3+}, V^{4+}, Cr^{5+}, Mn^{6+}): Russell-Saunders terms ⇒ $^2D_{3/2}$
Crystal-field terms (okt.) ⇒ $^2T_2$, ^2E

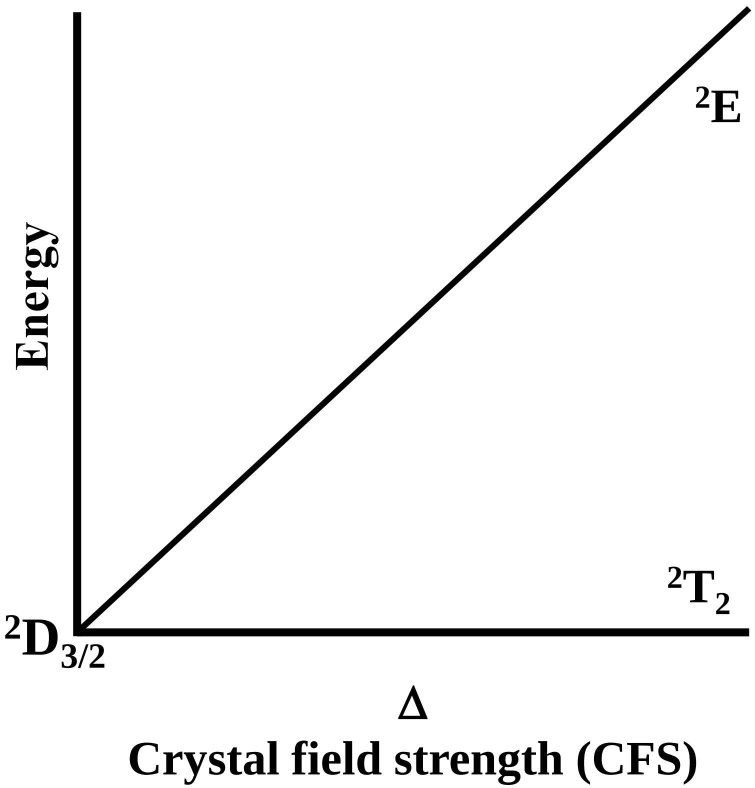

Ion	Configuration	Example
Ti^{3+}	$[Ar]3d^1$	Al_2O_3:Ti (Sapphire)
Cr^{3+}	$[Ar]3d^3$	Al_2O_3:Cr (Ruby)
Mn^{4+}	$[Ar]3d^3$	$Mg_4GeO_{5.5}F$:Mn
Mn^{2+}	$[Ar]3d^5$	Zn_2SiO_4:Mn (Willemite)
Fe^{3+}	$[Ar]3d^5$	$LiAlO_2$:Fe

d-d transitions are parity-forbidden
⇒ low absorption coefficient
⇒ high concentration needed

8.10 Luminescence of Transition Metal Ions

Absorption in glasses, laser crystals and phosphors

Ion	Configuration	Colour	Pigment	Structure type
Ti^{3+}	d^1	violet, brown	Al_2O_3:Ti	Corundum
V^{3+}	d^2	green		
V^{4+}	d^1	green, blue	$(Zr,V)SiO_4$	Zircon
Cr^{3+}	d^3	green, yellow	Cr_2O_3	Corundum
Mn^{2+}	d^5	light pink	MnO	NaCl
Mn^{3+}	d^4	violet	Mn_2O_3	Corundum
Mn^{4+}	d^3	red, brown	MnO_2	Rutile
Fe^{3+}	d^5	yellow to red	α-Fe_2O_3	Corundum
Fe^{2+}	d^6	blue, green	$Fe(C_2O_4)\cdot 2H_2O$	
Co^{2+}	d^7	blue, violet	$CoAl_2O_4$	Spinel
Ni^{2+}	d^8	green	NiO	NaCl
Cu^{2+}	d^9	blue, green	$CaCuSi_4O_{10}$	Cuprorivaite

8.10 Luminescence of Transition Metal Ions

Absorption processes of transition metal ions with d^0-configuration

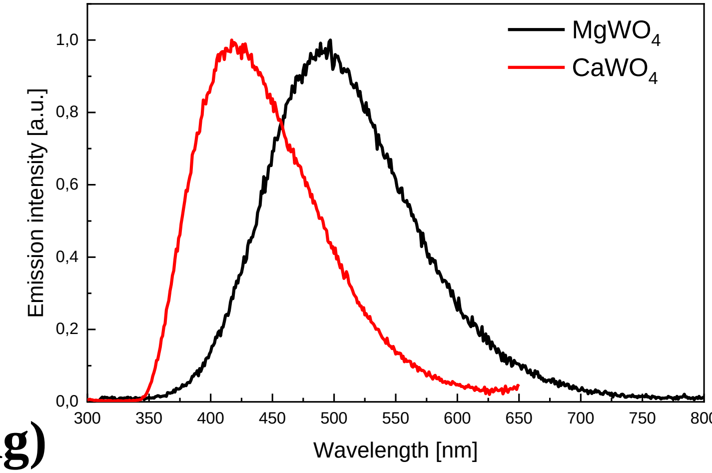

Ionic moieties (tetrahedral):

VO_4^{3-}, NbO_4^{3-}, TaO_4^{3-}, CrO_4^{2-}, MoO_4^{2-}, WO_4^{2-}, MnO_4^{-}

Process:

Ligand to Metal Charge-Transfer (LMCT)

$O^{2-} \rightarrow Me^{n+}$ or 2p(non-bonding) $\rightarrow$ d(e_g: anti-bonding)

Result: Bond is weakened $\Rightarrow \Delta R >> 0 \Rightarrow$ broad absorption band

Phosphor	Absorption [cm^{-1}]	CN	Polyhedron
$CaWO_4$	40000	4	Tetrahedron
Ca_3WO_6	35000	6	Octahedron

$\Rightarrow$ Position of the CT state decreases with increasing CN and effective charge of the metal center

8.10 Luminescence of Transition Metal Ions

Mn^{2+} and Mn^{4+} Luminescence

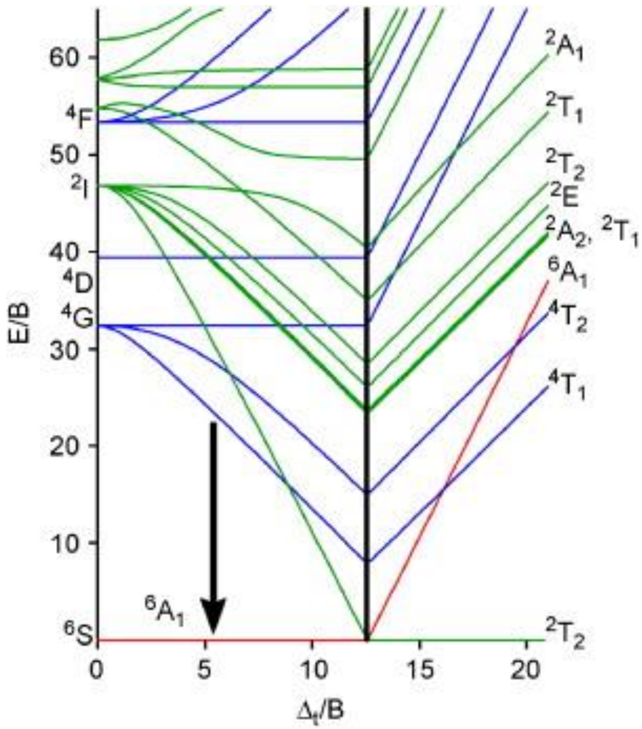

Mn^{2+} [Ar]$3d^5$ (h.s.)

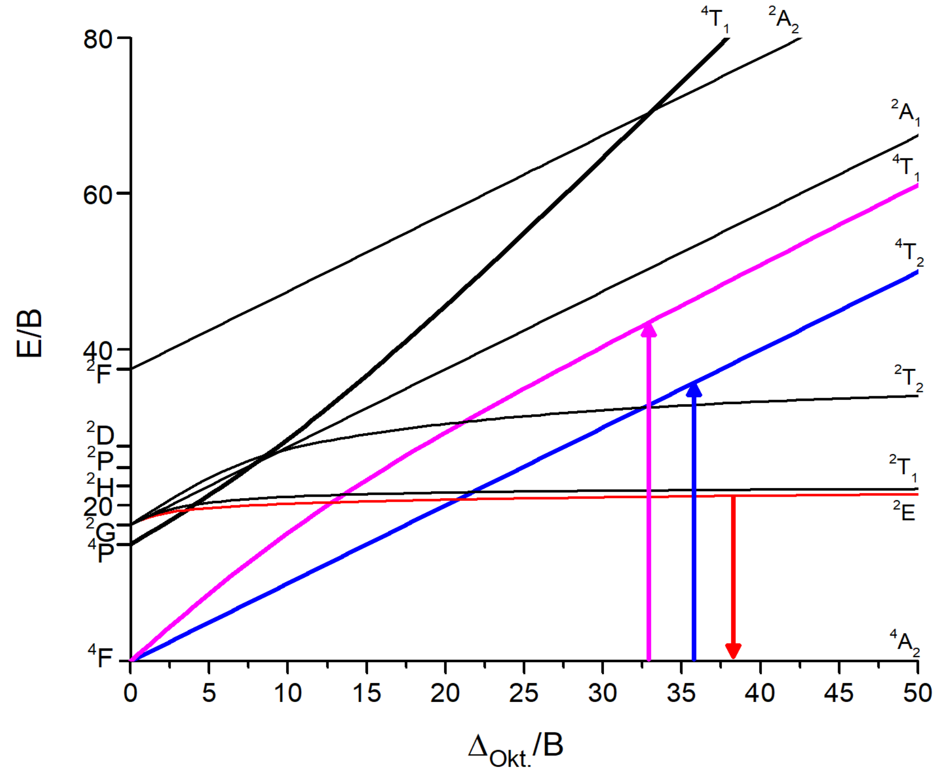

Mn^{4+} [Ar]$3d^3$

Δ < 10,000 cm^{-1}
$^4T_1(^4G) \rightarrow {}^6A_1(^6S)$
Band emission 500 – 750 nm = f(symmetry)

Δ ≈ 20,000 cm^{-1}
$^2E(^2G) \rightarrow {}^4A_2(^4F)$
Line emission ~ 620 – 730 nm = f(CFS, covalency)

8.10 Luminescence of Transition Metal Ions

Mn^{4+} Luminescence: Line Emission due to spin-forbidden $^2E(^2G) \rightarrow {}^4A_2(^4F)$ trans.

Optical properties of Mn^{4+} are governed by

- **Crystal field splitting Dq, usually 1.9 – 2.3 · 10^4 cm^{-1}**
- **Covalency can be parametrised**

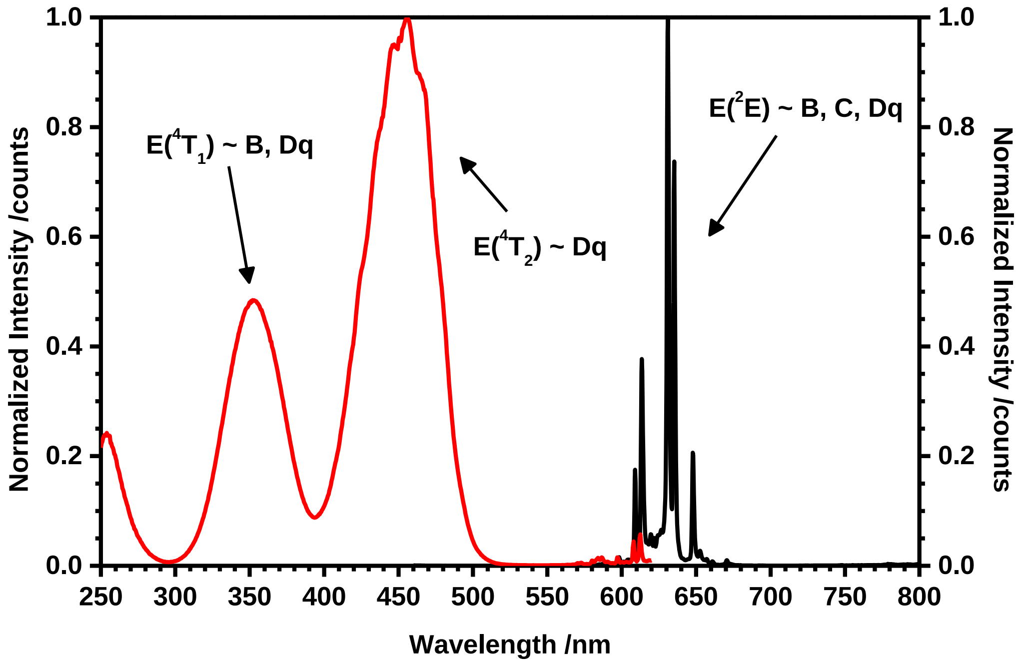

Racah Parameter A, B, and C

A = F0 − 49 F4

B = F2 – 5 F4

C = 35 F4

(with F0, F2, F4 = Slater integrals)

B: Usually 600 – 800 cm^{-1}

C: Usually 2800 – 3300 cm^{-1}

Determination of B and C →

$$\frac{B}{Dq} = \frac{\left(\frac{\Delta E}{Dq}\right)^2 - 10\frac{\Delta E}{Dq}}{15\left(\frac{\Delta E}{Dq} - 8\right)} \qquad C = \frac{E\left(^2E\right) - 7.9B + \frac{1.8B^2}{Dq}}{3.05}$$

8.11 Luminescence of Ions with s^2-Configuration

Examples: Ga^+, In^+, Tl^+, Ge^{2+}, Sn^{2+}, Pb^{2+}, As^{3+}, Sb^{3+}, Bi^{3+}

Electron configuration of s^2-ions

Ga^+, Ge^{2+} and As^{3+}:	$[Ar]3d^{10}4s^2$
In^+, Sn^{2+} and Sb^{3+}:	$[Kr]4d^{10}5s^2$
Tl^+, Pb^{2+} and Bi^{3+}:	$[Xe]4f^{14}5d^{10}6s^2$

Energy level diagram of s^2-ions

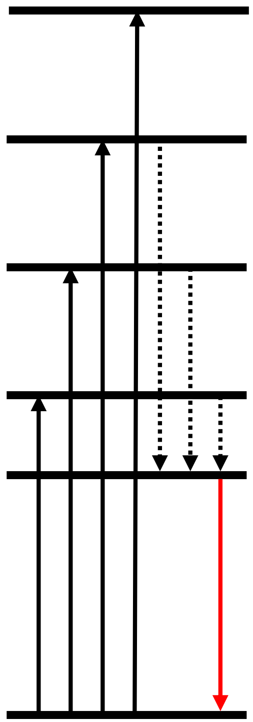

Proof of $SnCl_2$ by blue Sn^{2+} Emission

Excitation and emission spectra of $BaYB_9O_{16}:Sb^{3+}$

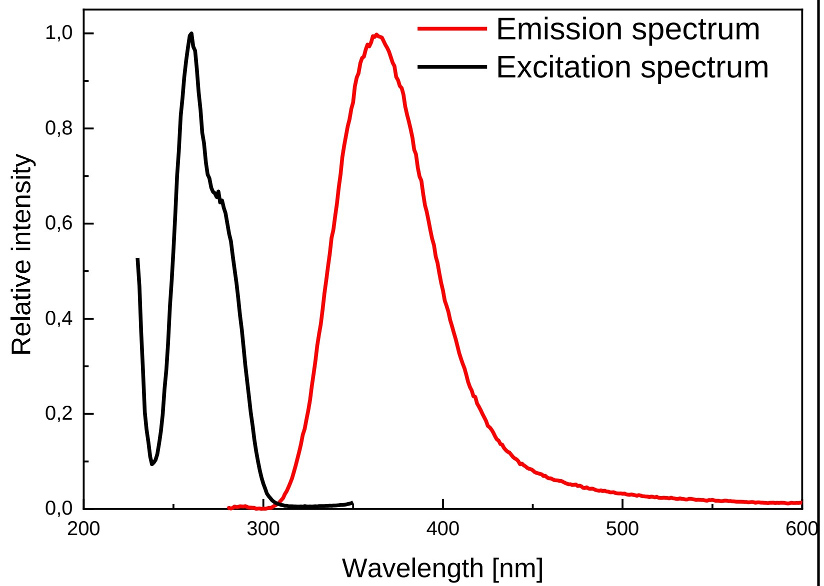

8.11 Luminescence of Ions with s^2-Configuration

Example: Pb^{2+} **Luminescence process: $[Xe]4f^{14}5d^{10}6s^2 \rightarrow [Xe]4f^{14}5d^{10}6s^16p^1$**

$BaSi_2O_5$:Pb

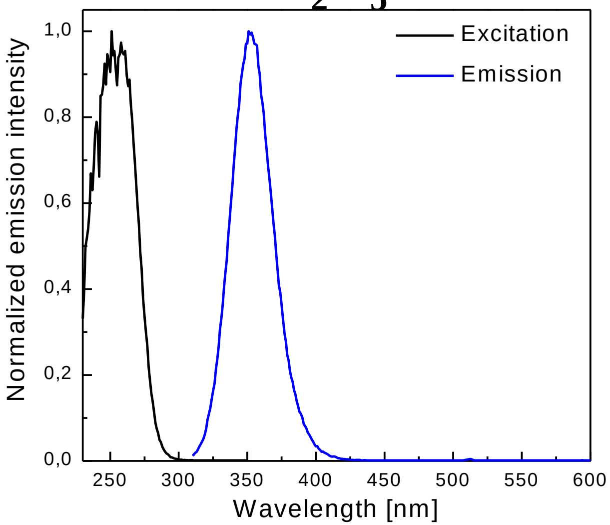

$Sr_2MgSi_2O_7$:Pb

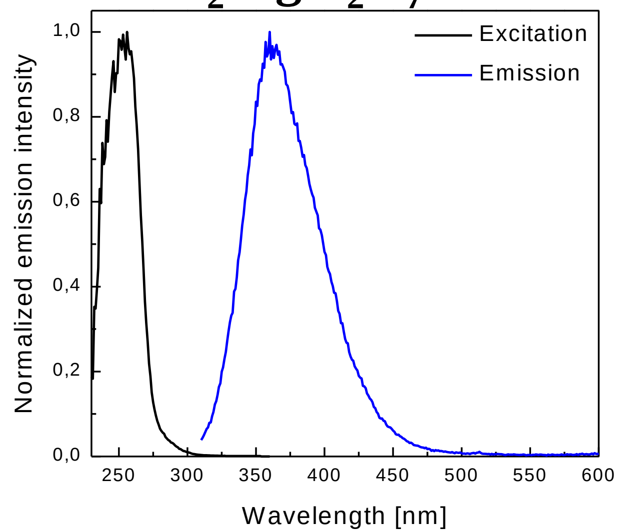

$SrLaBO_4$:Pb

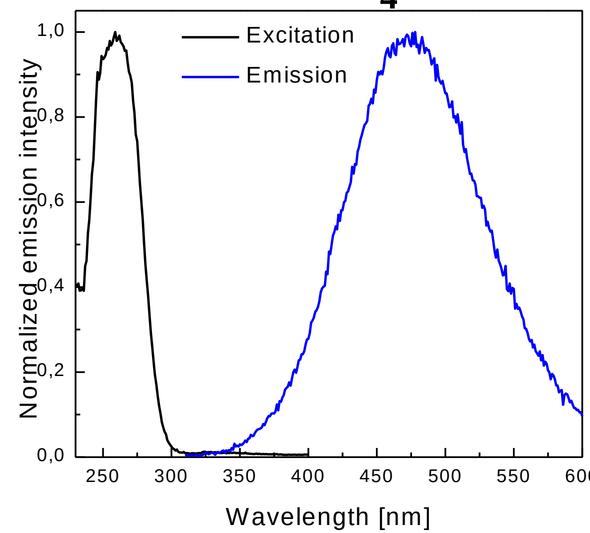

Phosphor	Mineral type	Stokes shift [cm^{-1}]	Half width [cm^{-1}]	QY [%]
$BaSi_2O_5$:Pb	Sanbornite	10600	2700	90
$Sr_2MgSi_2O_7$:Pb	Akermanite	12000	4300	75
$SrLaBO_4$:Pb	-	17700	5300	65

8.12 Luminescence of Rare Earth Ions

Lanthanides originates from the Greek word “λανθανειν”, which means “to lie hidden”
Instead of “to lie hidden” λανθανειν,
a better name would be “to be outstanding”
επιφανης – epifanides (A. Meijerink, PGS 2011)

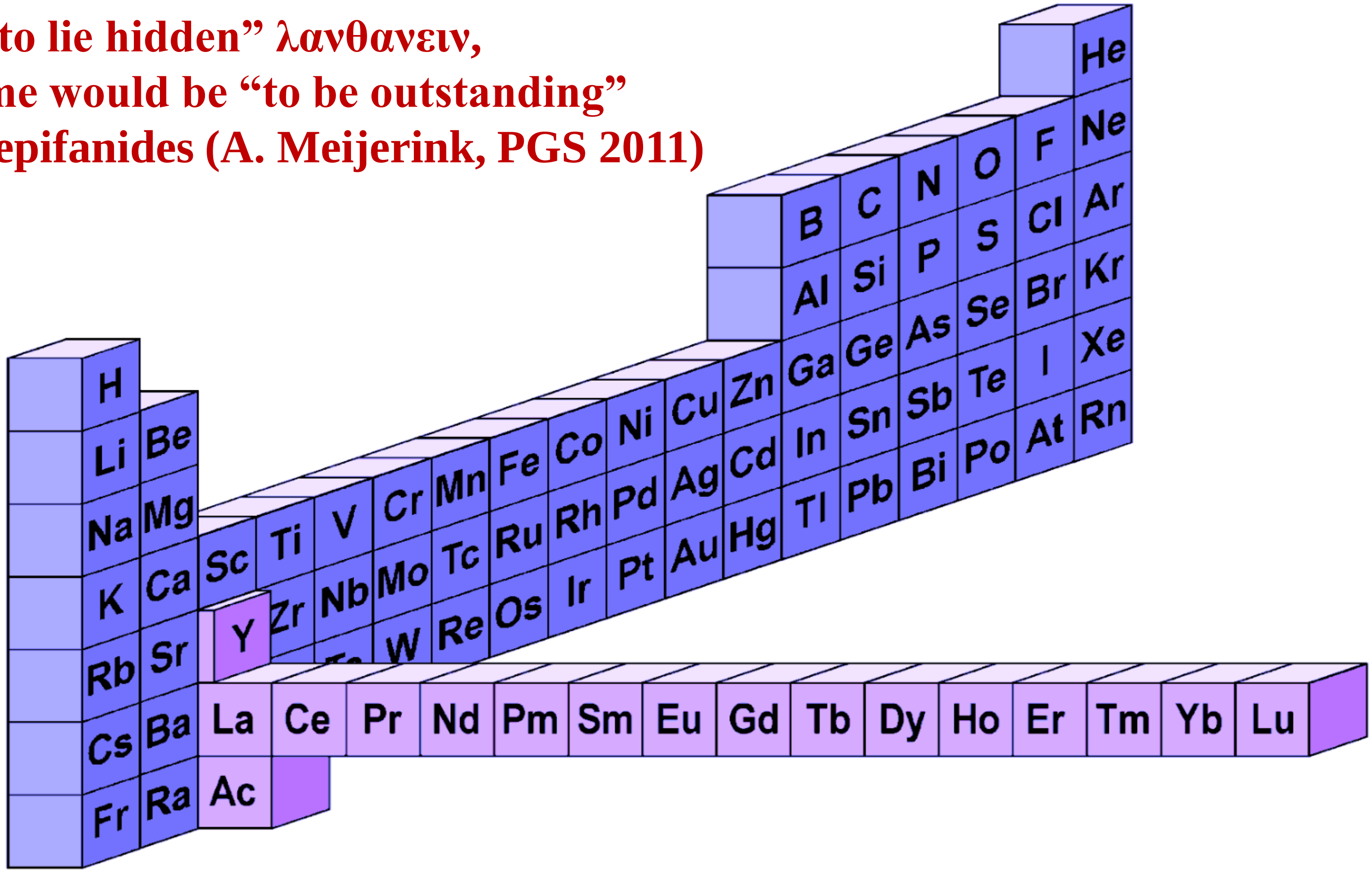

8.12 Luminescence of Rare Earth Ions

Properties of electronic orbitals: s, p, d, f

Shape and orientation

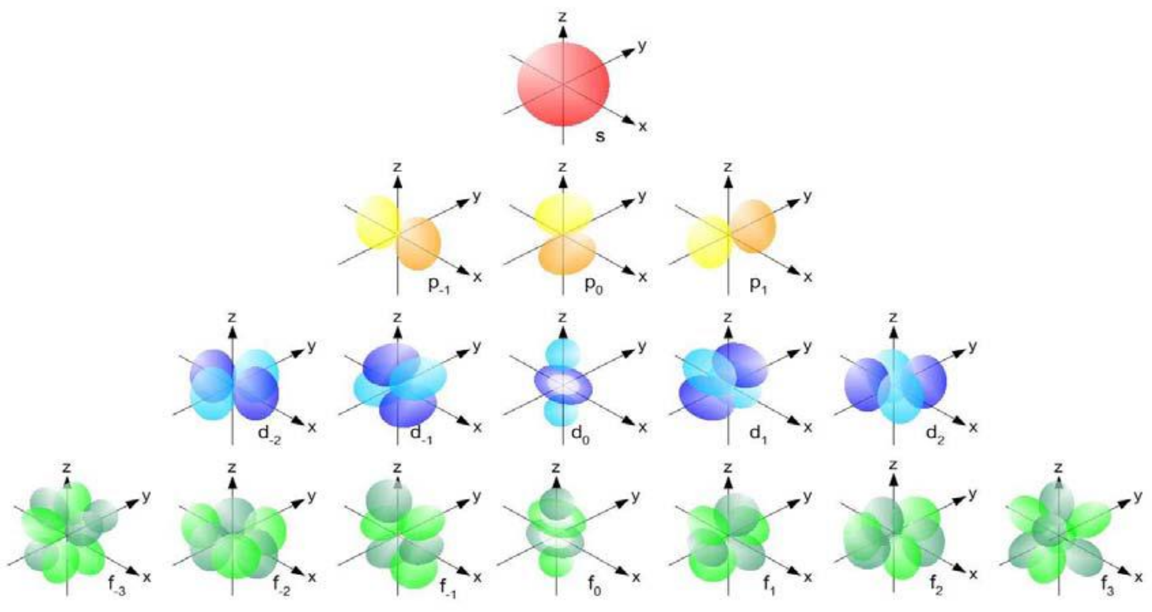

Orbital	Parity	l	m_l
s	g	0	0
p	u	1	-1, 0, 1
d	g	2	-2, ..., 2
f	u	3	-3, ..., 3

8.12 Luminescence of Rare Earth Ions

Electron configuration of rare earth metals and ions

Metals

[Xe]	La	Ce	Pr	Nd	Pm	Sm	Eu	Gd	Tb	Dy	Ho	Er	Tm	Yb	Lu
6s	2	2	2	2	2	2	2	2	2	2	2	2	2	2	2
5d	1	0	0	0	0	0	0	1	0	0	0	0	0	0	1
4f	0	2	3	4	5	6	7	7	9	10	11	12	13	14	14

Ions

[Xe]	La^{3+}	Ce^{3+}	Pr^{3+}	Nd^{3+}	Pm^{3+}	Sm^{3+}	Eu^{3+}	Gd^{3+}	Tb^{3+}	Dy^{3+}	Ho^{3+}	Er^{3+}	Tm^{3+}	Yb^{3+}	Lu^{3+}
	Ce^{4+}	Pr^{4+}	Nd^{4+}				Sm^{2+}	Eu^{2+}						Tm^{2+}	Yb^{2+}
4f	0	1	2	3	4	5	6	7	8	9	10	11	12	13	14

Example

Gd^{3+}/Eu^{2+}

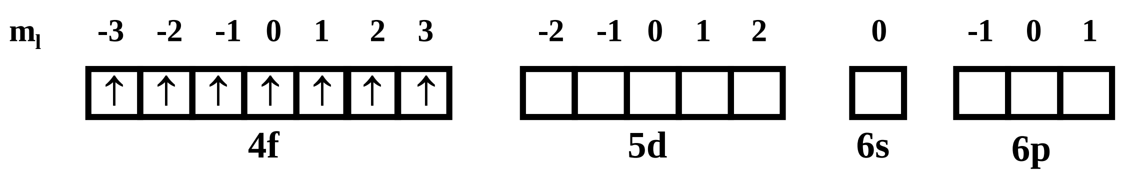

Spectroscopic terms

$^{2S+1}L_J$

$S = \Sigma s = 7/2$ → $2S+1 = 8$ → strongly paramagnetic ions

$L = |\Sigma l| = 0$ → „S“ → LS-Term symbol ^8S

8.12 Luminescence of Rare Earth Ions

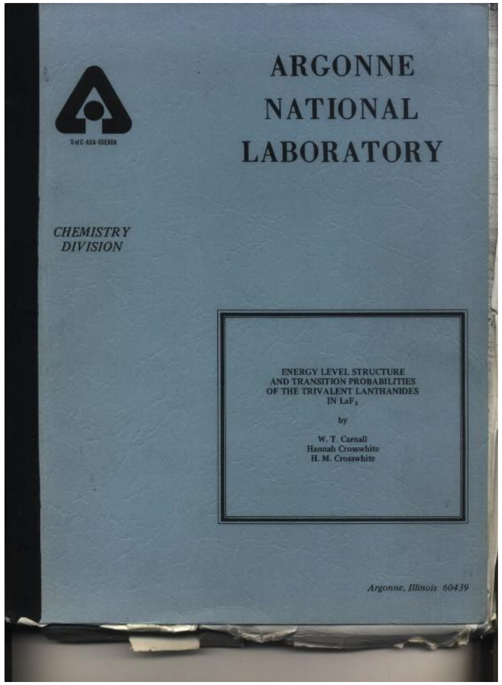

History of distangling the energy level structure

1908 Becquerel

Sharp lines in optical spectra of lanthanide ions

1937 Van Vleck

The Puzzle of Rare-Earth Spectra in Solids

1960s Judd, Wybourne, Dieke, Carnall

Theory for energy level structure and transition probabilities of 4f-4f transitions

1977 Carnall, Crosswhite & Crosswhite: ANL Report on energy levels in LaF_3

Problem: Complicated Hamiltonian (“total energy operator”).....

$H = H_0 + H_C + H_{SO} + H_{CF} + H_Z$ with $H_0 = -\hbar^2/2m \cdot \nabla^2 + V_0$ (single particle in 3D pot.)

8.12 Luminescence of Rare Earth Ions

Energy level structure of [Xe]$4f^n$ ions

Partly filled 4f-shell results in multiple electronic microstates = 14!/((14-n)!*n!)

Example: Tb^{3+} [Xe]$4f^8$ → 8 electrons in 7 f-orbitals → 3003 different arrangements

Free ion energy levels due to:

1. Electrostatic interactions (comparable to $3d^n$ ions): H_C splitting ~ 10000 cm^{-1}
2. Spin-orbit coupling (larger than for $3d^n$ ions): H_{SO} splitting ~ 1000 cm^{-1}
3. Crystal field splitting (smaller than for $3d^n$ ions): H_{CF} splitting ~ 100 cm^{-1}

Ground state m_l = -3 -2 -1 0 1 2 3 S = 6/2, L = 3 (F), J = 6 → $^7F_6$

-3	-2	-1	0	1	2	3
↑	↑	↑	↑	↑	↑	↑↓

4f

1st excited state m_l = -3 -2 -1 0 1 2 3 S = 4/2, L = 2 (D), J = 4 → $^5D_4$

-3	-2	-1	0	1	2	3
↑	↑	↑	↑	↑↓		↑↓

4f

8.12 Luminescence of Rare Earth Ions

1. Electrostatic interactions (H_C)

Shielding due to inner electrons described by the so-called Slater parameters (comparable to Racah parameter A, B, and C)

$$F^{(k)} = \frac{e^2}{4\pi\varepsilon_0}\int_0^\infty\int_0^\infty \frac{r_<^k}{r_>^{k+1}}\left[R'_{4f}(r_i)R'_{4f}(r_j)\right]^2 r_i^2 r_j^2 \,\mathrm{d}r_i\,\mathrm{d}r_j$$

Electrostatic interaction increases with effective charge on the activator ion (ion charge density)

Therefore splitting between different terms depends on

- **Oxidation state**
- **Nucleus charge**
- **Charge flow back from ligands (polarizibility of surrounding anions)**

8.12 Luminescence of Rare Earth Ions

2. Spin-orbit coupling (H_{SO})

Spin-orbit coupling constant ζ increases throughout the lanthanide series, i.e. from ζ(Ce) = 650 cm^{-1} to ζ(Yb) = 2930 cm^{-1}

Further splitting of *LS* terms into *J*-levels by energy, assuming weak spin-orbit coupling:

→ Complete term symbol:

$^{2S+1}L_J$ with $|L-S| < J < L+S$

For Tb^{3+}	**Ground state:**	**$^7F_{6,5,4,3,2,1,0}$**
	Excited state:	**$^5D_{4,3,2,1,0}$**

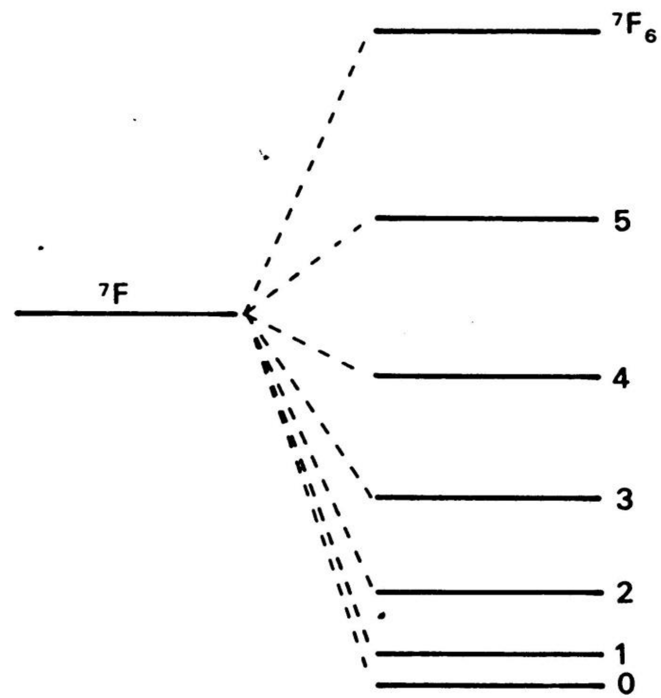

8.12 Luminescence of Rare Earth Ions

3. Crystal field splitting (H_{CF})

Further splitting of *J* multiplets into a maximum of 2*J*+1 levels
Crystal field splitting ~ 100 cm^{-1} = sensitive function of site symmetry

$Lu_3Al_5O_{12}:Nd^{3+}$
$^4F_{3/2} - {}^4I_{11/2}$
$\Delta E = 203\ cm^{-1}$
six levels without external magnetic field

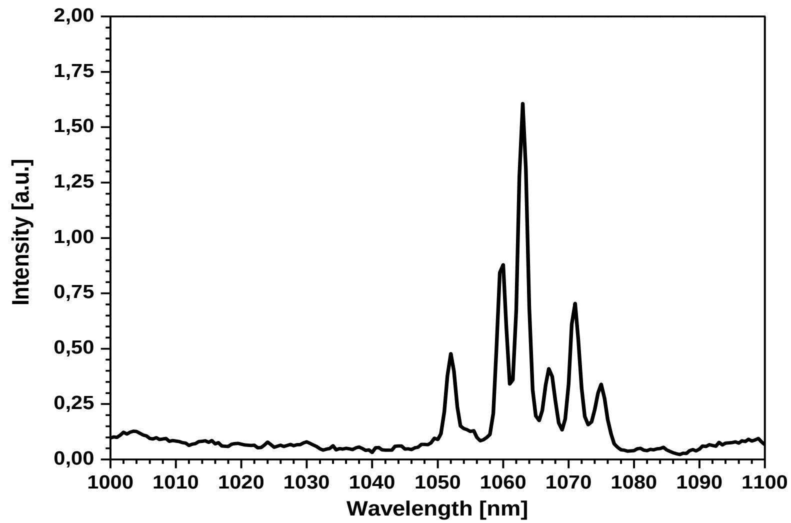

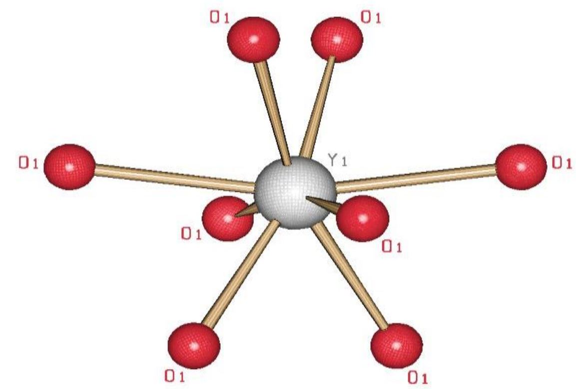

Dodecahedral coordination

Extra fitting parameters B^k_q to graphically fit experimentally observed levels:

$$\mathcal{H}_c^{O_h} = B_0^4\left[C_0^{(4)} + \sqrt{\frac{5}{14}}\left(C_{-4}^{(4)} + C_4^{(4)}\right)\right] + B_0^6\left[C_0^{(6)} - \sqrt{\frac{7}{2}}\left(C_{-4}^{(6)} + C_4^{(6)}\right)\right]$$

8.12 Luminescence of Rare Earth Ions

In summary: RE ions exhibit a large number of energy levels $^{2S+1}L_J$

The number of microstates are

$$\text{Number}\,\# = \frac{n!}{e!h!}$$

n = number of positions
e = number of electrons
h = number of holes

	Ce (Yb)	Pr (Tm)	Nd (Er)	Pm (Ho)	Sm (Dy)	Eu (Tb)	Gd
n	1	2	3	4	5	6	7
SL	1	7	17	47	73	119	119
SLJ	2	13	41	107	198	295	327
SLJM	14	91	364	1001	2002	3003	3432

Early experimental and theoretical work on $LaCl_3:Ln^{3+}$ and $LaF_3:Ln^{3+}$ by Dieke and Carnall (experiments) and Judd, Crosswhite and Wybourne (theory): "Dieke diagram" and the "Blue book"

8.12 Luminescence of Rare Earth Ions

Dieke diagram (1968): Energy levels of trivalent RE ions in LaF_3

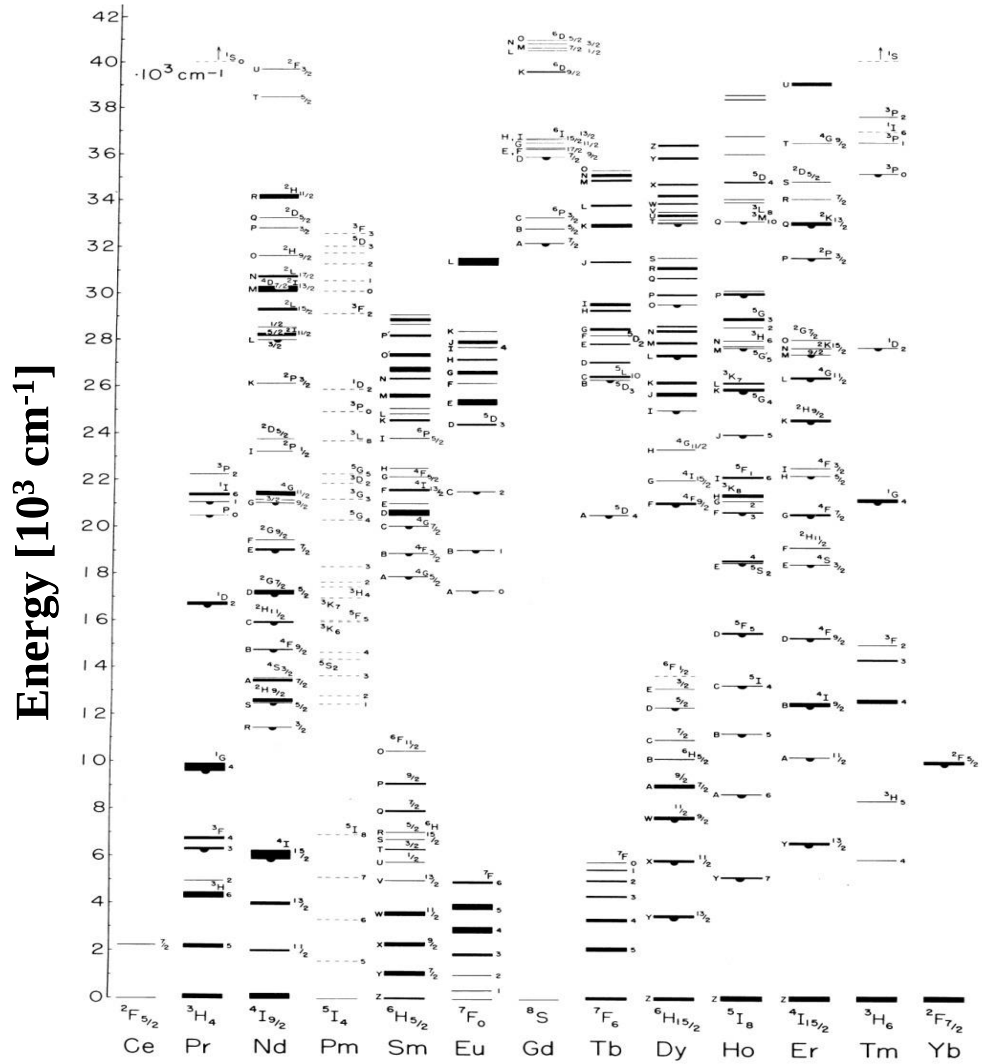

Lit.: W.T. Carnall, G.L. Goodman, K. Rajnak, and R.S Rana, J. Chem. Phys. 90 (1989) 3443

8.12 Luminescence of Rare Earth Ions

Extended Dieke diagram (2005): Energy levels of trivalent RE ions up to the VUV

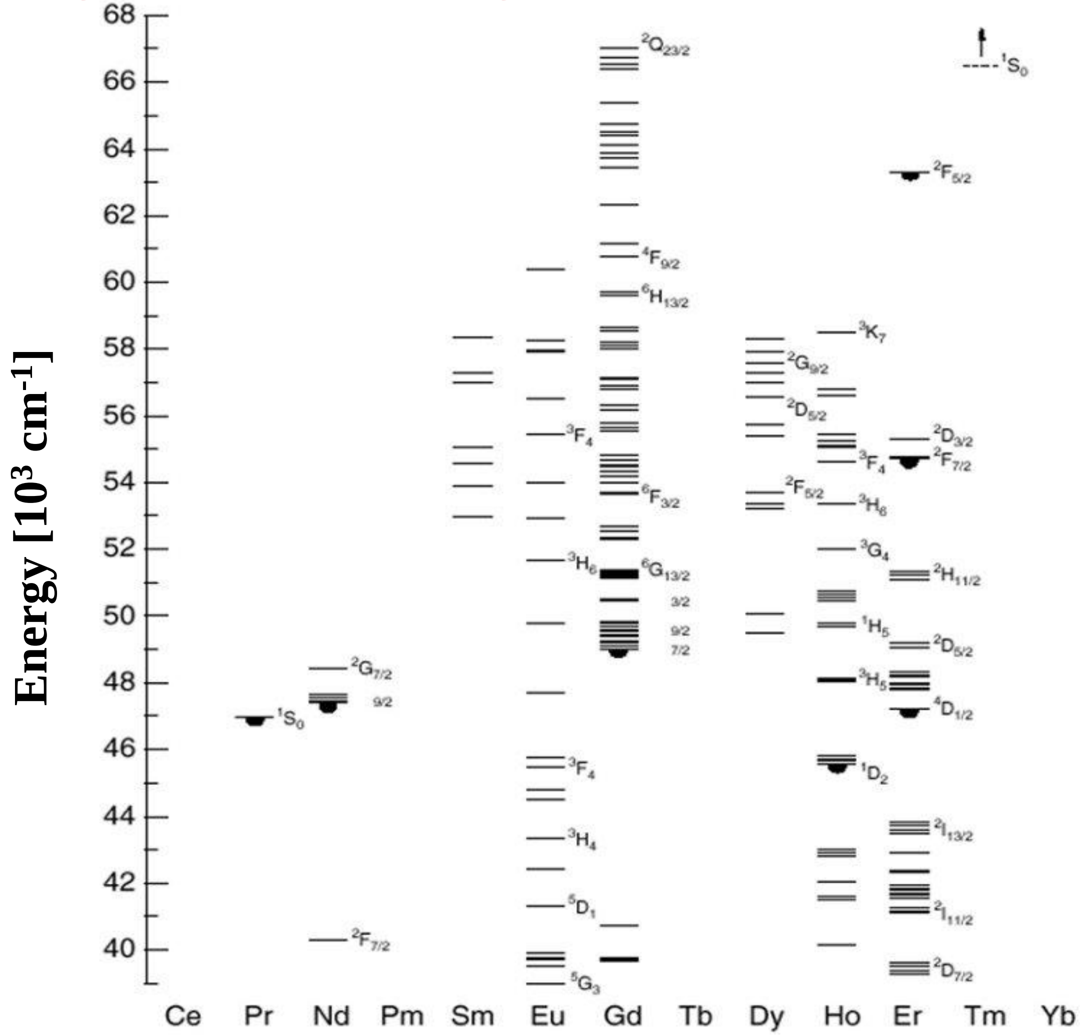

Lit.: P.S. Peijzel, A. Meijerink, R.T. Wegh et al, J. Solid State Chem. 178 (2005) 448

8.12 Luminescence of Rare Earth Ions

Complete energy level diagram

Ce^{3+}	~	Yb^{3+}
Pr^{3+}	~	Tm^{3+}
Nd^{3+}	~	Er^{3+}
Pm^{3+}	~	Ho^{3+}
Sm^{3+}	~	Dy^{3+}
Eu^{3+}	~	Tb^{3+}
Gd^{3+}		

Energy level splitting increases from Ce^{3+} to Yb^{3+} due to increasing nucleus charge

Increasing spin-orbit coupling E_{SO} (ξ)

Free ion	Configuration	ξ [cm^{-1}]
Ce^{3+}	[Xe]$4f^1$	650
Yb^{3+}	[Xe]$4f^{13}$	-2930

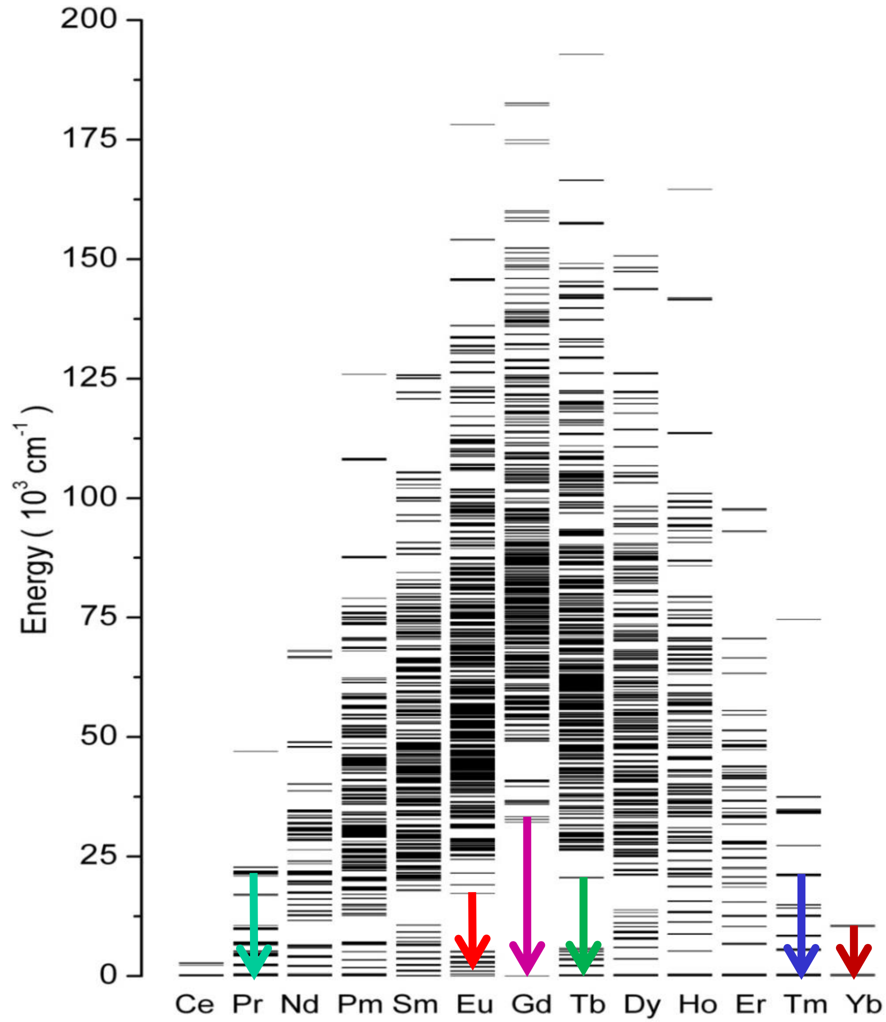

Ln^{3+} Ion

8.12 Luminescence of Rare Earth Ions

Charakteristische optische Eigenschaften

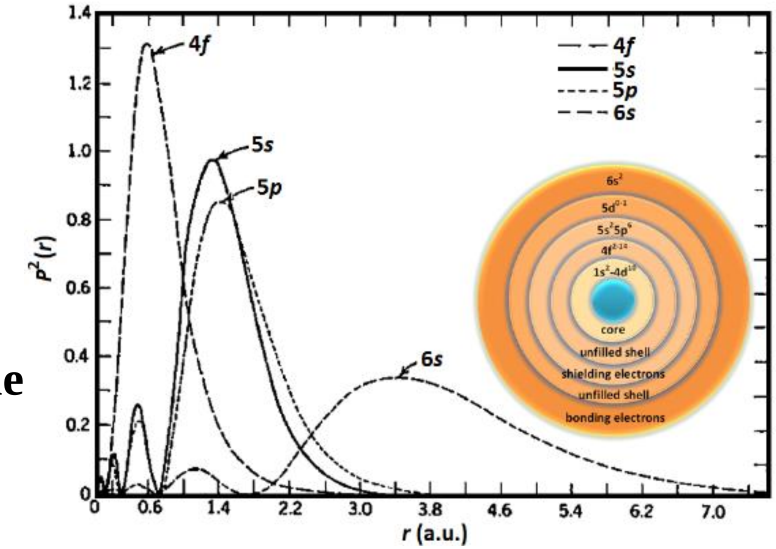

Quelle: V.A.G. Rivera

Intrakonfigurations 4f - 4f Übergänge:

1) Sharp lines (atomic like), Stokes shift ~ 0 cm^{-1}

2) Little influence of environment on energy level scheme

3) Parity forbidden transitions (~ ms life time, f ~ 10^{-5})

Origin: Shielding of 4f^n electrons by filled 5s and 5p shells → vry little shift of excited state parabola and strong zero-phonon (ZP) lines

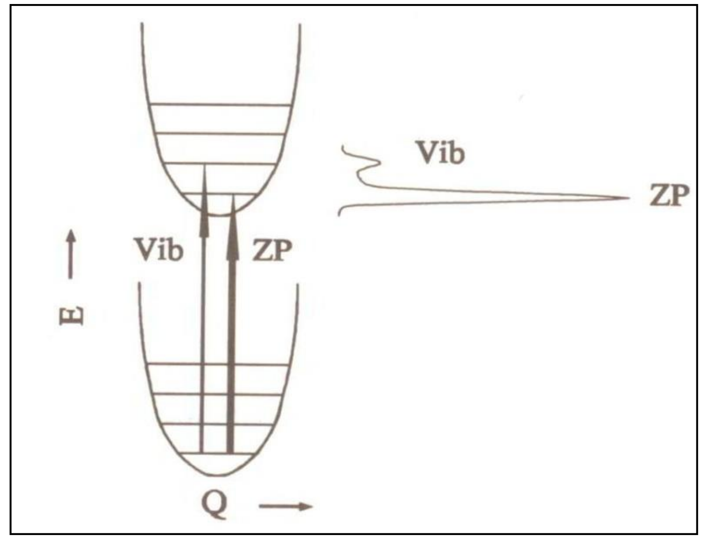

Beispiel:

Gd^{3+} in $Y_3Al_5O_{12}$

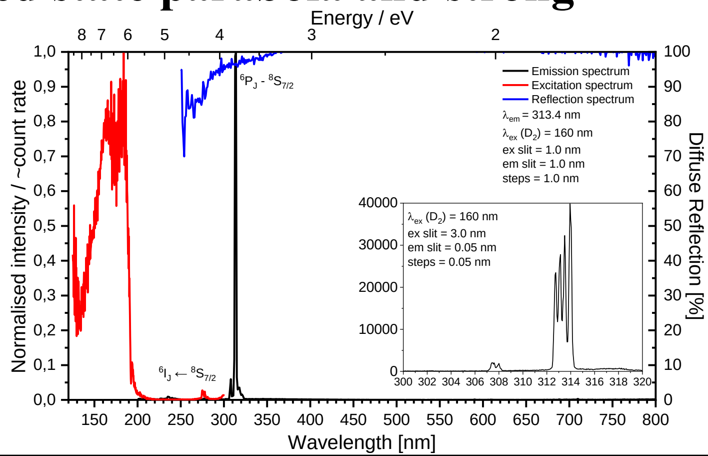

8.12 Luminescence of Rare Earth Ions

Typical emission spectrum of Tb^{3+} (Example: $Lu_3Al_5O_{12}$:Tb)

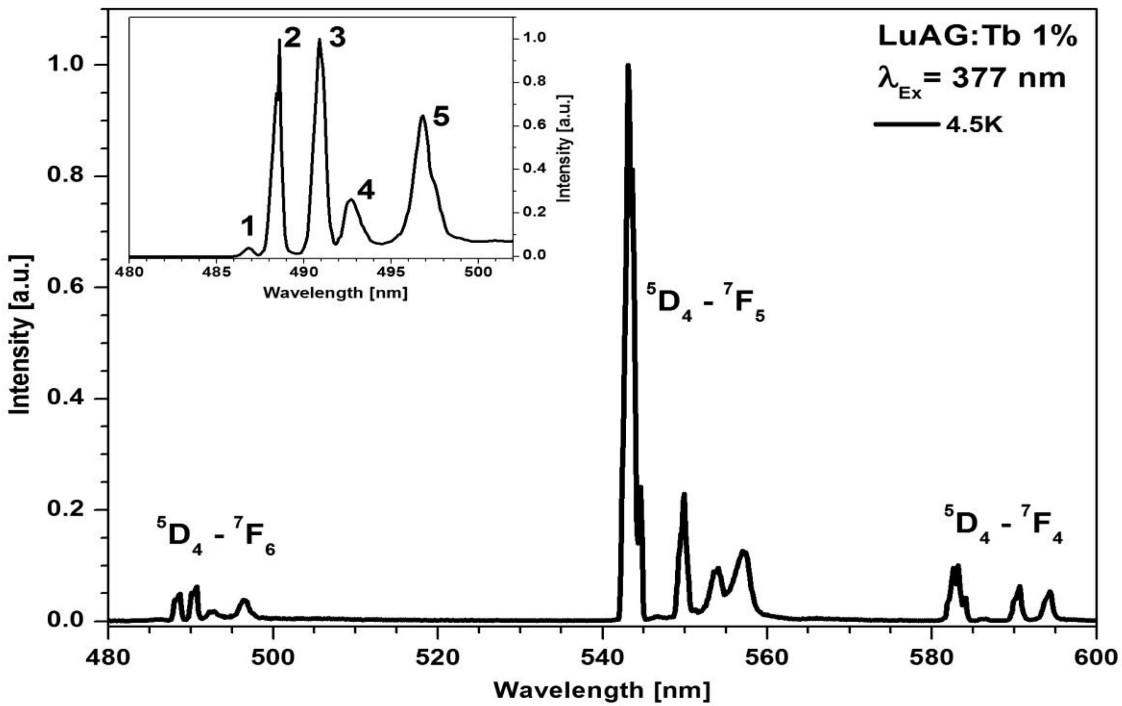

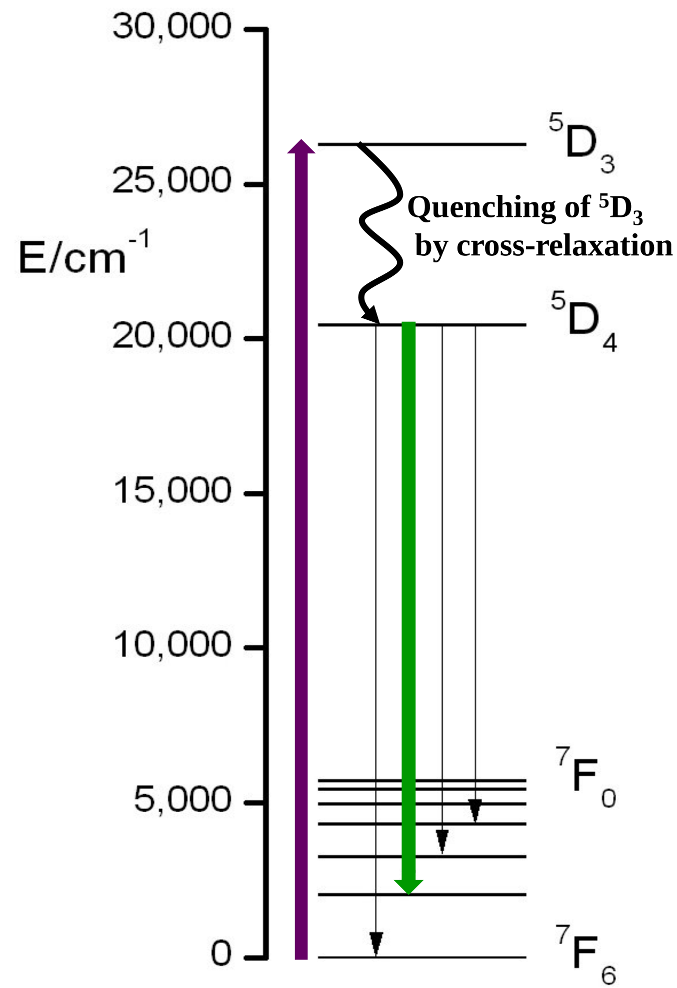

<u>Characteristic luminescence of lanthanides</u>

- Sharp emission lines
- Almost independent of chemical environment,
  e. g. green-yellow emission of Tb^{3+} phosphors
- High quantum yield (> 90%), due to small Stokes shift

8.12 Luminescence of Rare Earth Ions

Example: Eu^{3+} - Typical excitation and emission spectra (Example: Y_2SiO_5:Eu)

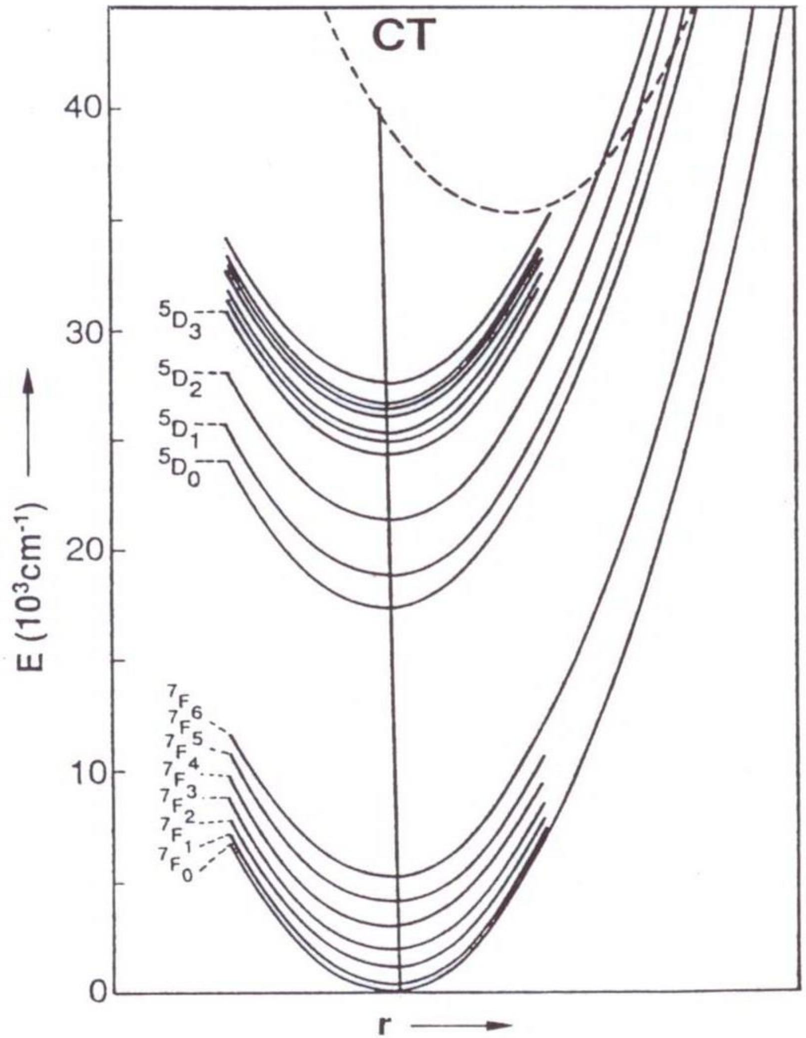

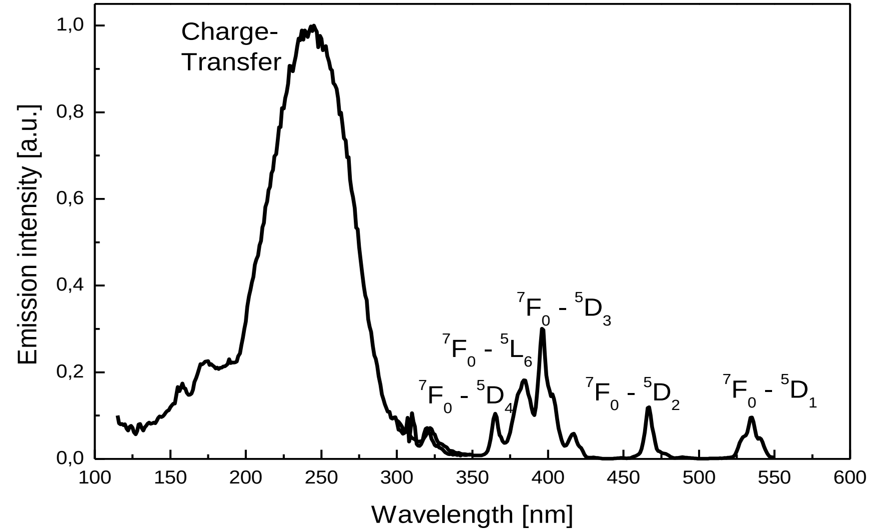

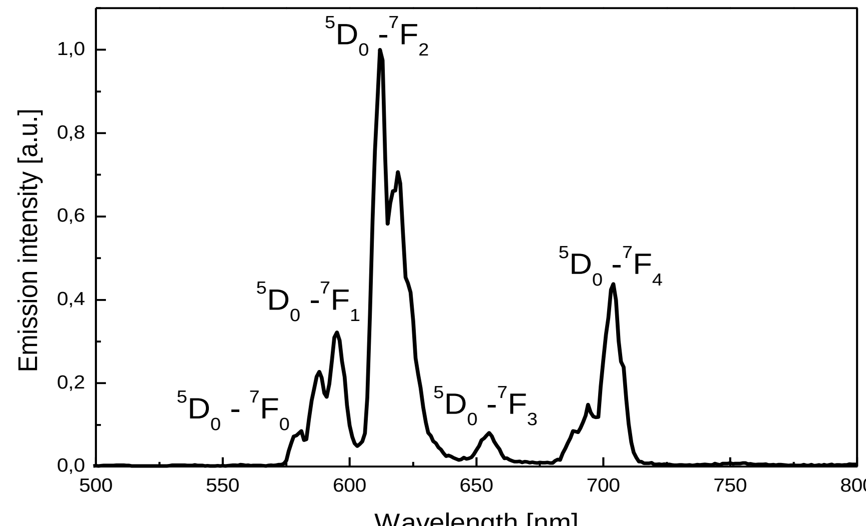

8.12 Luminescence of Rare Earth Ions

Emission spectra and colour points of Eu^{3+} activated phosphors

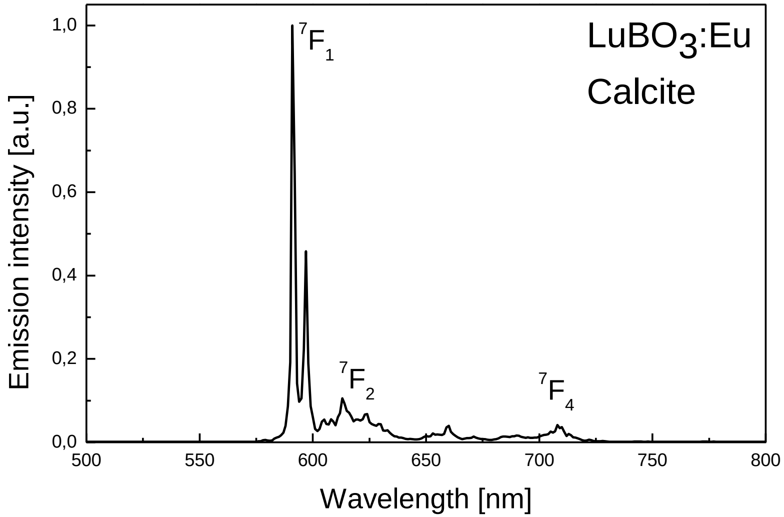

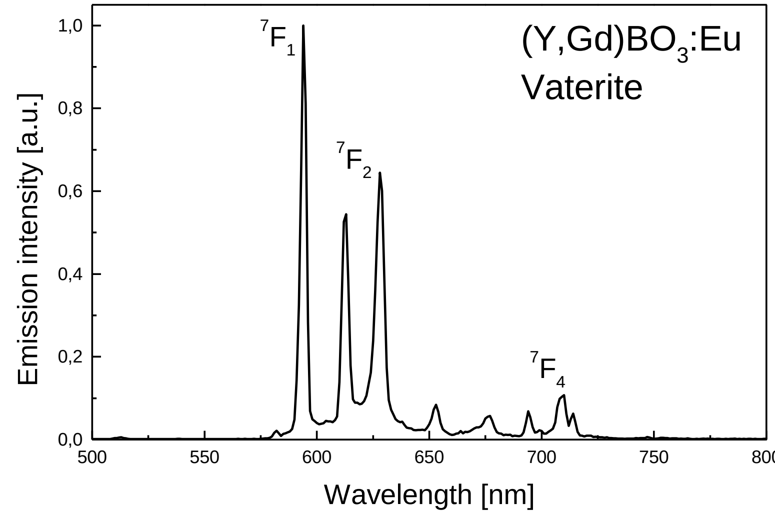

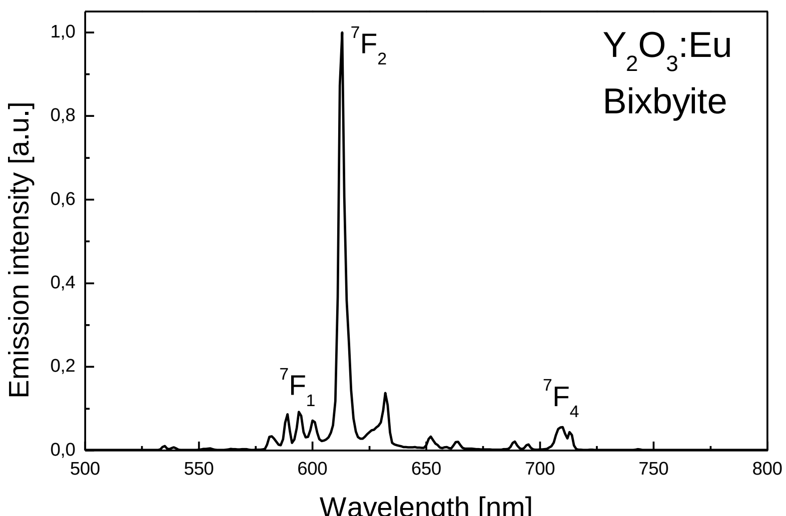

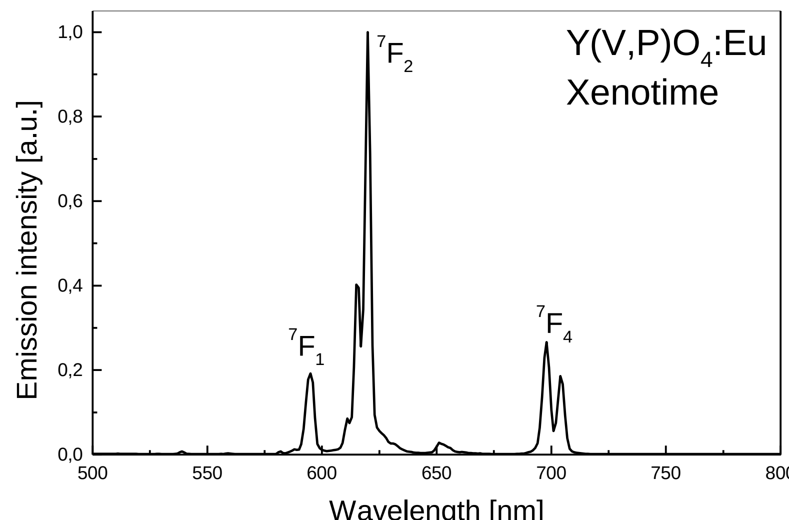

8.12 Luminescence of Rare Earth Ions

Emission spectra and colour points of Eu^{3+} activated phosphors

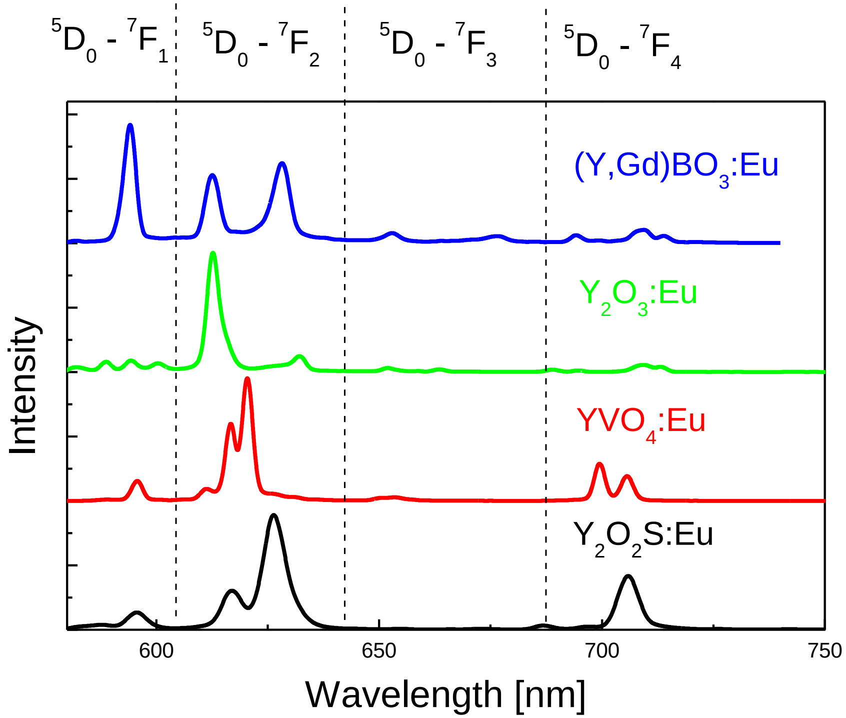

Phosphor	CIE1931 values x	y	Applications
(Y,Gd)BO_3:Eu	0.640	0.360	PDP
Y_2O_3:Eu	0.641	0.344	CFL, PL, TL
YVO_4:Eu	0.645	0.343	Hg-HP-Lamps
Y_2O_2S:Eu	0.650	0.342	CRT, markers

Colour saturation: Y_2O_2S:Eu > YVO_4:Eu > Y_2O_3:Eu > (Y,Gd)BO_3:Eu

8.12 Luminescence of Rare Earth Ions

Emission spectra and colour points of Eu^{3+} activated phosphors

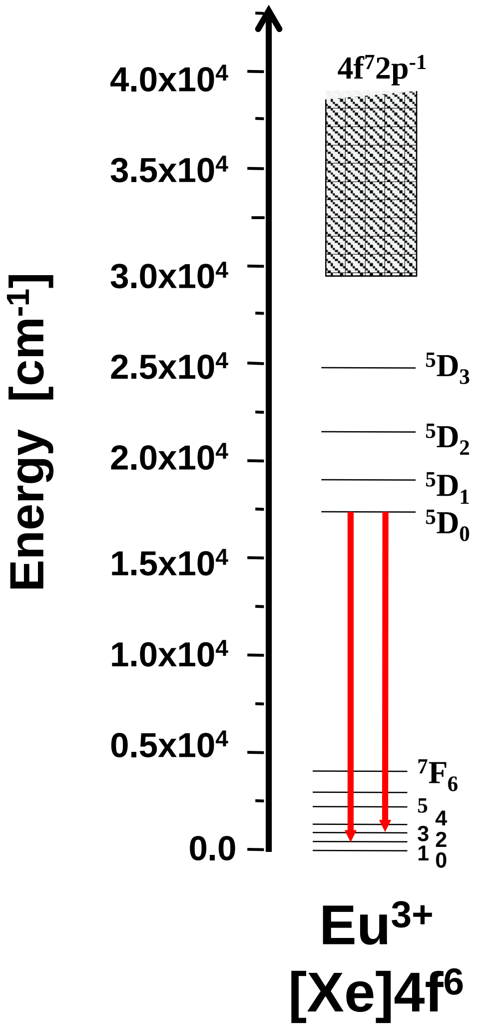

Observed emission spectrum due to
$^5D_0 \rightarrow {}^7F_J$ transitions (lines)

a) Inversion symmetry (S_6, D_{3d})
Magnetic dipole transitions, e.g. $^5D_0$ - $^7F_1$
$\Delta J = 0, \pm 1$ ($J = 0 \rightarrow J = 0$ forbidden)
$MeBO_3$:Eu (Calcite, Vaterite)
$\tau \sim 8 - 16$ ms

b) No inversion symmetry
Electric dipole transitions $^5D_0$ -$^7F_{2,4}$
$\Delta J \leq 6$ ($J_i = 0 \rightarrow J_f = 2, 4, 6$)
Y_2O_3:Eu (Bixbyite), $Y(V,P)O_4$:Eu (Xenotime)
$\tau \sim 2 - 5$ ms

8.12 Luminescence of Rare Earth Ions

Simplified energy level diagram of selected Ln^{3+} ions

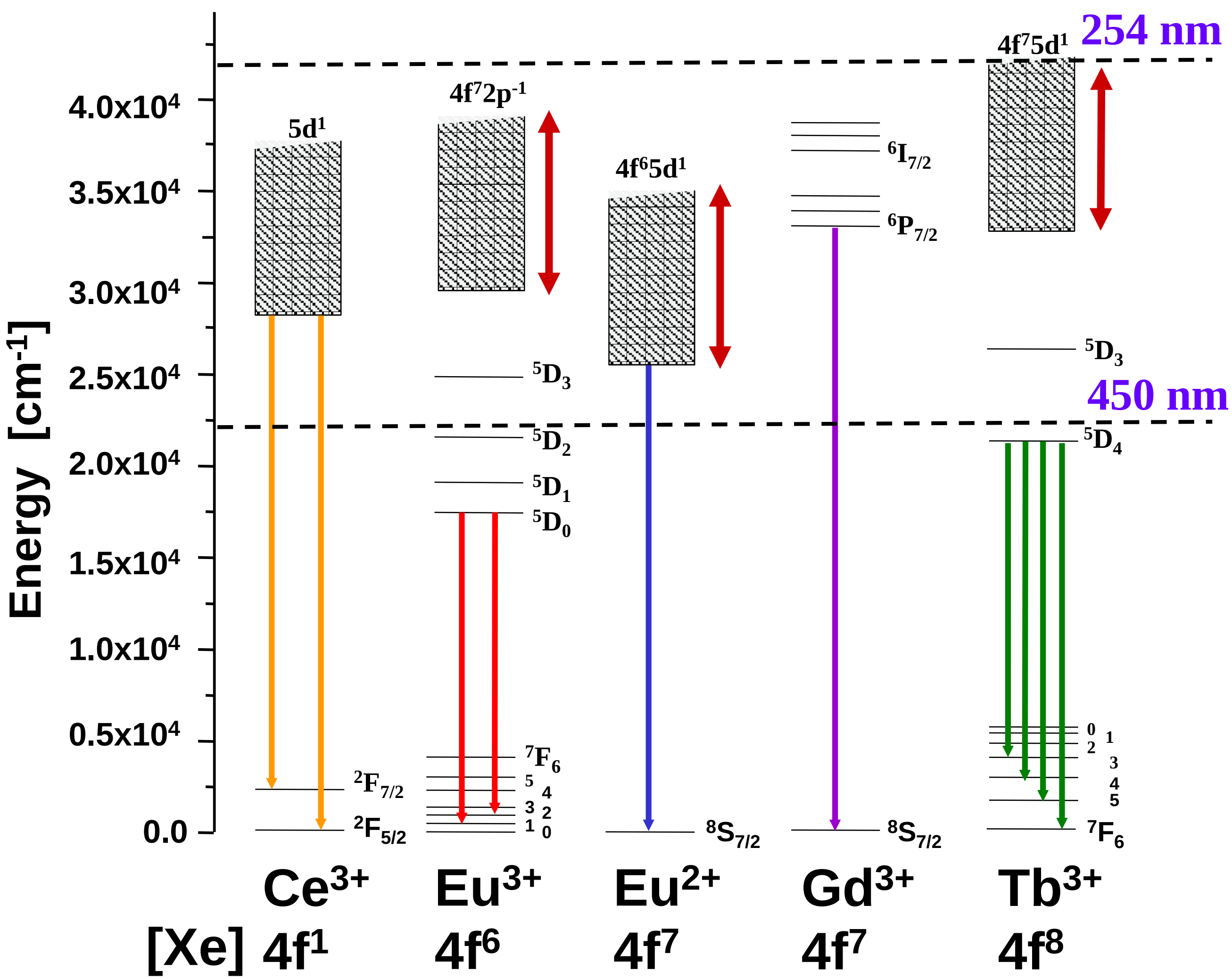

Intraconfigurational transitions

(4f-4f → lines)

- Pr^{3+}
- Nd^{3+}
- $Sm^{2+/3+}$
- Eu^{3+} (Eu^{2+} in fluorides)
- Gd^{3+}
- Tb^{3+}
- Dy^{3+}
- Ho^{3+}
- Er^{3+}
- Tm^{3+}
- Yb^{3+}

Interconfigurational transitions

(4f-5d and CT → bands)

- Ce^{3+}
- Pr^{3+}
- Nd^{3+}
- Eu^{2+}
- Yb^{2+}

8.12 Luminescence of Rare Earth Ions

Excitation and emission spectra of Eu^{3+} and Eu^{2+} activated phosphors

$Y_2O_3:Eu^{3+}$

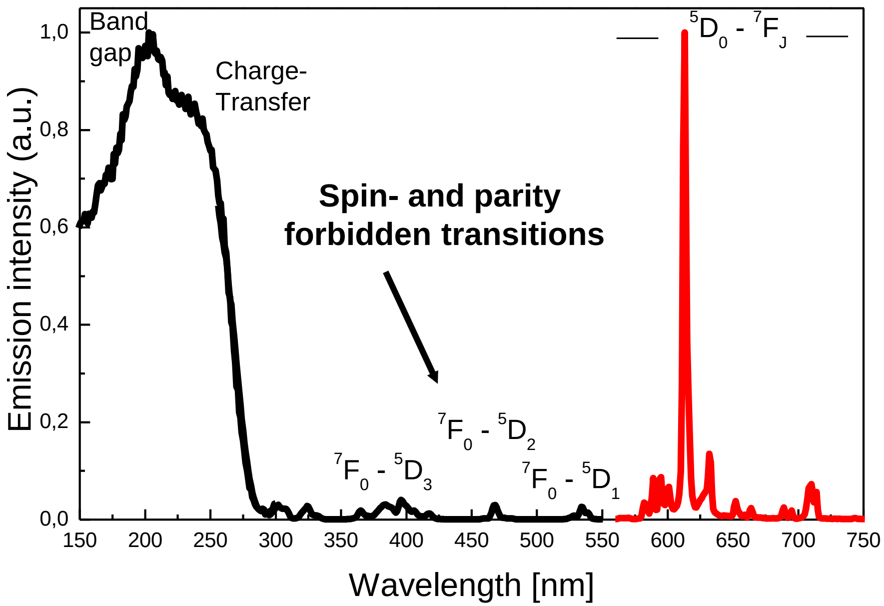

$BaMgAl_{10}O_{17}:Eu^{2+}$

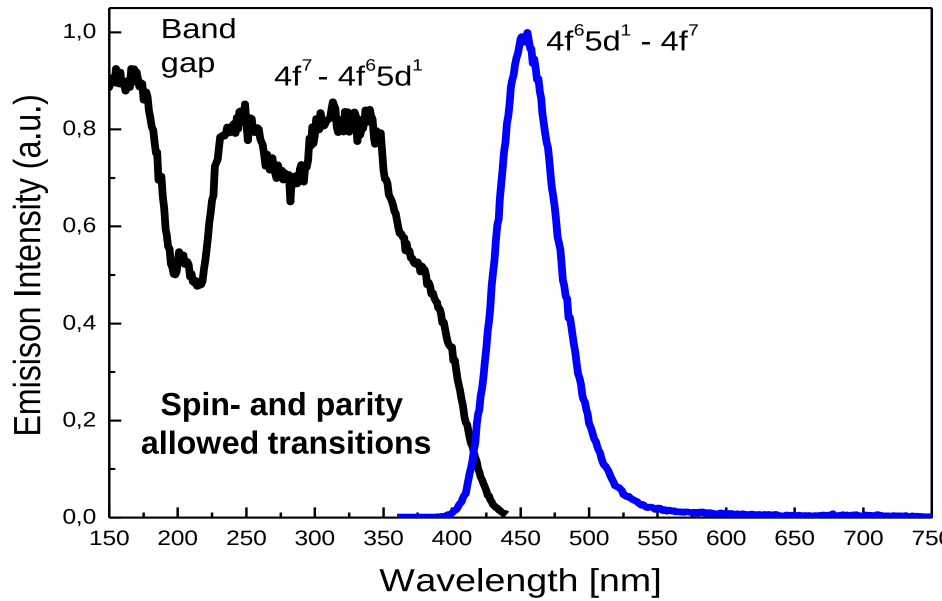

$Eu^{3+} \rightarrow (Eu^{3+})^{**}$	CT	$Eu^{2+} \rightarrow (Eu^{2+})^{**}$	4f-5d
$(Eu^{3+})^{**} \rightarrow (Eu^{3+})^{*}$	Relaxation	$(Eu^{2+})^{**} \rightarrow (Eu^{2+})^{*}$	Relaxation
$(Eu^{3+})^{*} \rightarrow Eu^{3+}$	4f-4f	$(Eu^{2+})^{*} \rightarrow Eu^{2+}$	5d-4f

Strong CT absorption band (broad)
Weak 4f-4f absorption lines (narrow)

Strong 4f-5d absorption bands (broad)

8.12 Luminescence of Rare Earth Ions

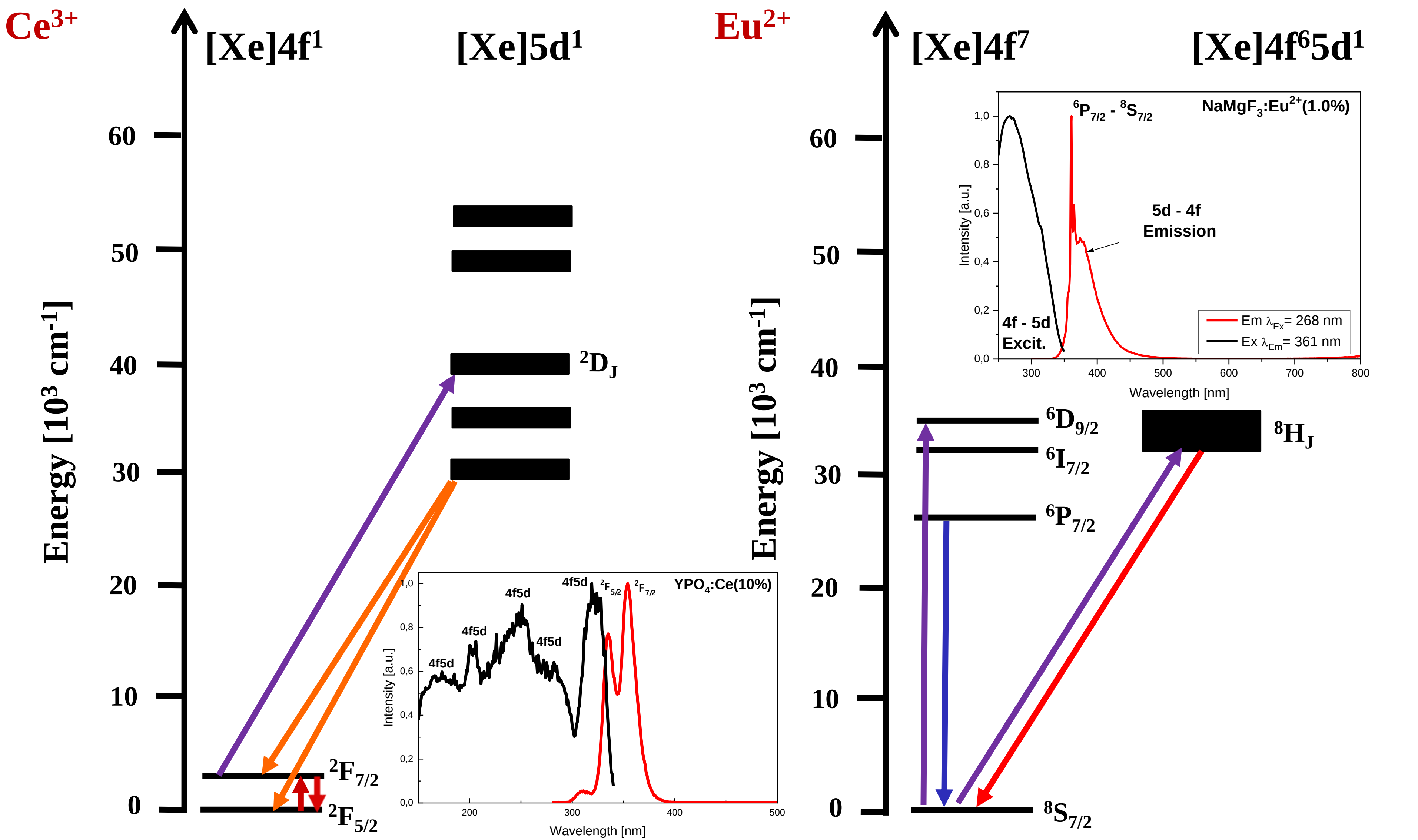

8.12 Luminescence of Rare Earth Ions

Energy gap between states of the $[Xe]4f^n$ and $[Xe]4f^{n-1}5d^1$ configurations

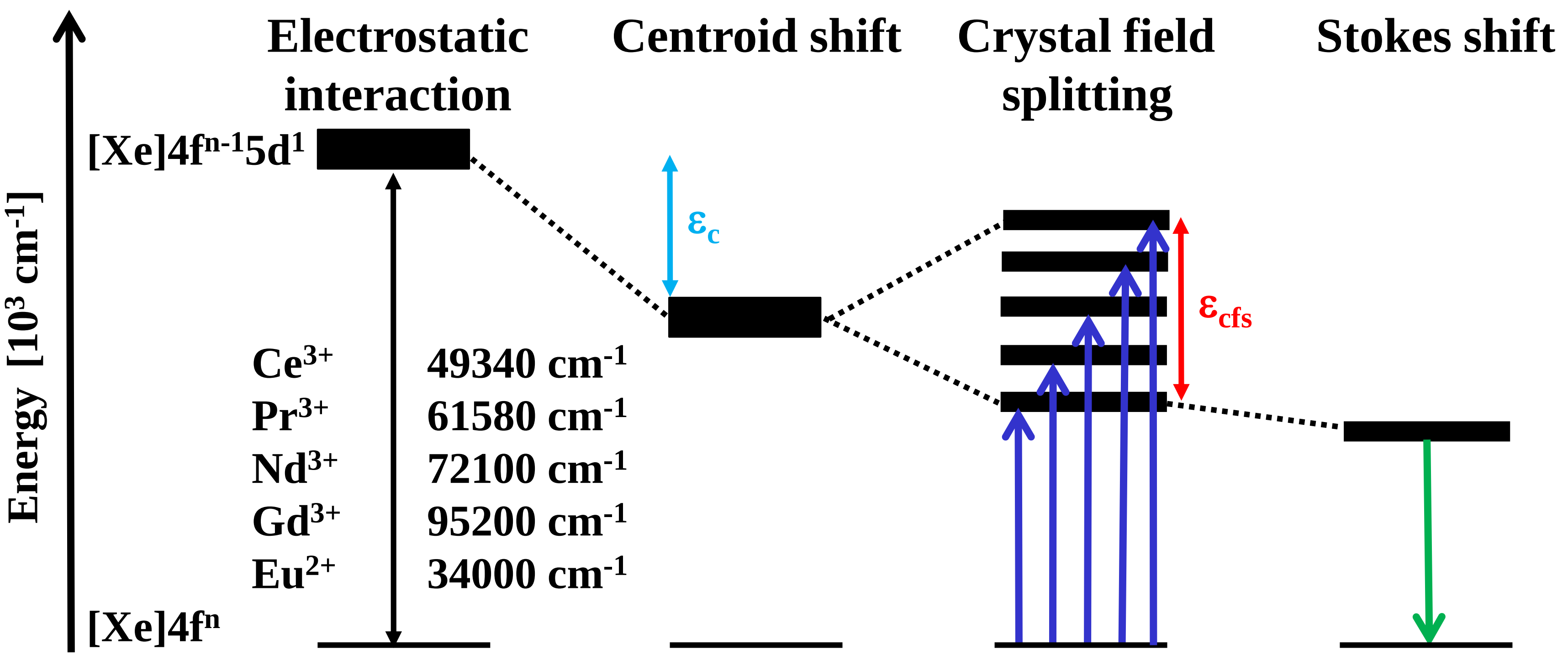

ε_c: Centroid energy proportional to the spectroscopic polarizability α_{sp} (3000 – 20000 cm^{-1})

ε_{cfs}: Crystal field splitting (< 50000 cm^{-1})

8.12 Luminescence of Rare Earth Ions

Centroid shift ε_c ~ electron density between activator and ligands ~ charge flow back

Polarizability of the anions ~ negative charge density (alkalinity!)

- **selenides > sulfides > nitrides > oxides > fluorides**

Charge density of the surrounding anions

- **Type of network former:**

oxides	aluminates	silicates	borates	phosphates	sulfates
O^{2-}	AlO_4^{5-}	SiO_4^{4-}	BO_3^{3-}	PO_4^{3-}	SO_4^{2-}

- **Degree of connectivity of the network former**

nesosilicates	sorosilicates	cyclosilicates	phyllosilicates	tectosilicates
$[SiO_4]^{4-}$	$[Si_2O_7]^{6-}$	$[Si_3O_9]^{6-}$	$[Si_4O_{10}]^{4-}$	$[(Si_2Al_2)O_8]^{2-}$
garnet	akermanite	benitoite	montmorillonite	quartz
zircon	thortveitite	beryl	talc	feldspar
olivine	hemimorphite	emerald	kaolinite	zeolites

8.12 Luminescence of Rare Earth Ions

Covalent character of ionic bonds ~ $\varepsilon_c \Rightarrow$ example: Y^{3+} - O^{2-}

Host lattice	Cation	Type of network former	
YPO_4	Y^{3+}	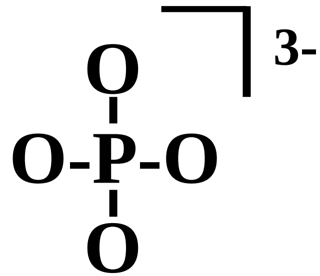 tetrahedral PO_4^{3-}	Low charge density $3/4^-$ per oxygen
$Y_3Al_5O_{12}$	Y^{3+}	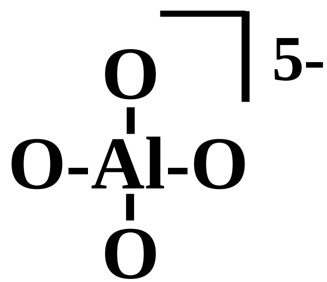 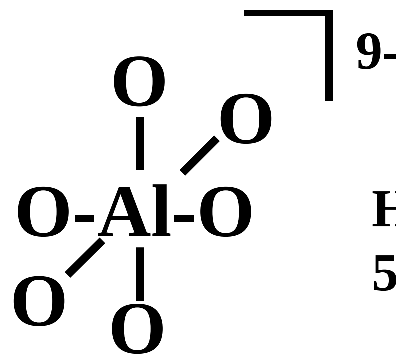 tetrahedral AlO_4^{5-} + octahedral AlO_6^{9-}	High charge density $5/4^-$ or $9/4^-$ per oxygen

P^{5+} attracts more charge density from the O^{2-} anions than Al^{3+} does

8.12 Luminescence of Rare Earth Ions

Negative charge density on the anions ~ $\varepsilon_c \Rightarrow$ example: Y^{3+} - O^{2-}

YPO_4

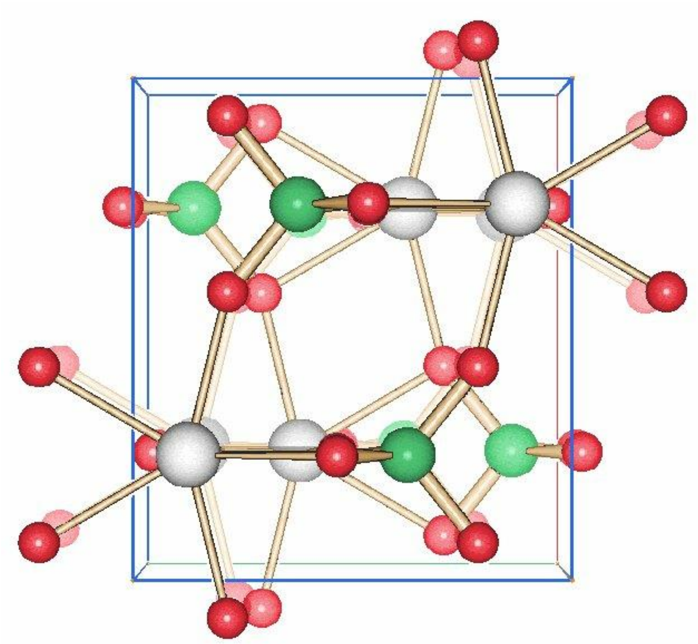

4 x O(1)	7.248
4 x O(2)	7.193

Low charge density on oxygen

$Y_3Al_5O_{12}$

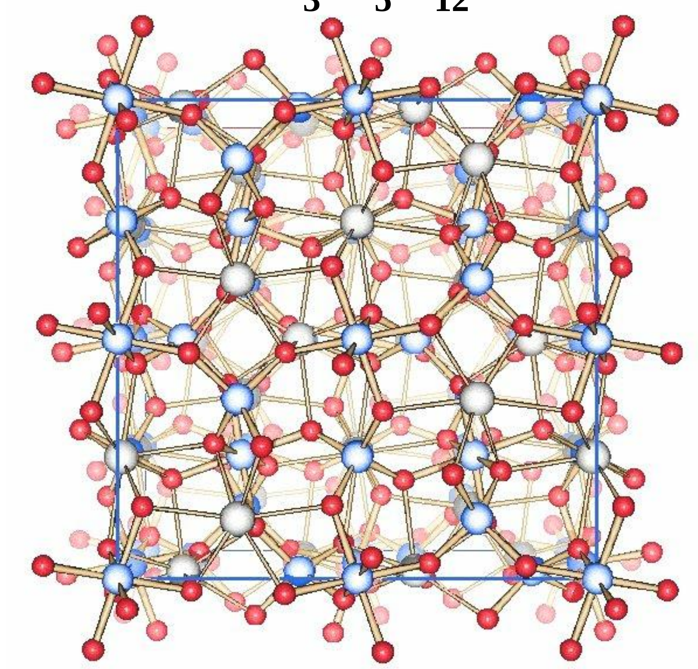

4 x O(1)	7.528
4 x O(2)	7.504

High charge density on oxygen

8.12 Luminescence of Rare Earth Ions

Crystal field splitting ε_{cfs}

Crystal field theory $\Rightarrow$ ionic interaction between metals and point charges (ligands)

Energy splitting of the d-orbitals depends on:

- **Anionic charge / anionic radius (spectrochemical series of solid state compounds)**

  $I^- < Br^- < Cl^- < S^{2-} < F^- < O^{2-} < N^{3-} < C^{4-}$

- **Symmetry (coordination number and symmetry)**

  square-planar > octahedral > cubic, dodecahedral, square-antiprismatic > tetrahedral > spherical

- **Metal to ligand distance (strong dependence from temperature)!**

  $\varepsilon_{cfs} = 5Ze^2r^4/3R^5$

R:	Metal (central atom) – ligands (anions) distance
Z:	Valence of the ligands (anions)
e:	Electron charge
r:	Distance of electron in d orbital from the nucleus of M

8.12 Luminescence of Rare Earth Ions

Crystal field splitting ε_{cfs}

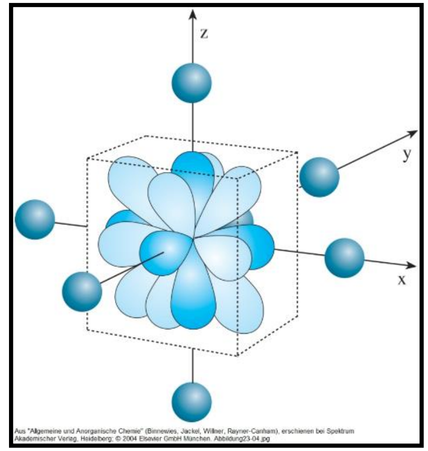

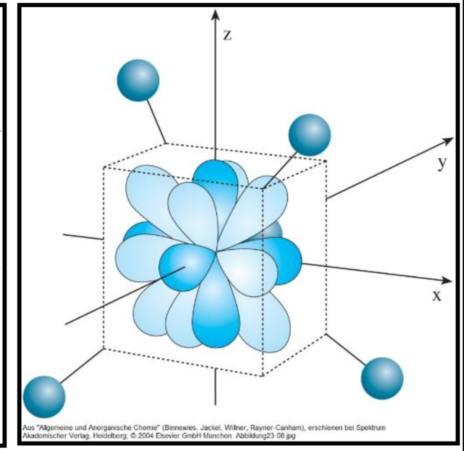

- **Atomic number of the metal cation**
  $\varepsilon_{cfs}(3d) : \varepsilon_{cfs}(4d) : \varepsilon_{cfs}(5d) = 1 : 1.45 : 1.7$

- **Charge of the metal cation**
  $\varepsilon_{cfs}(M^{2+}) : \varepsilon_{cfs}(M^{3+}) : \varepsilon_{cfs}(M^{4+}) = 1 : 1.6 : 1.9$

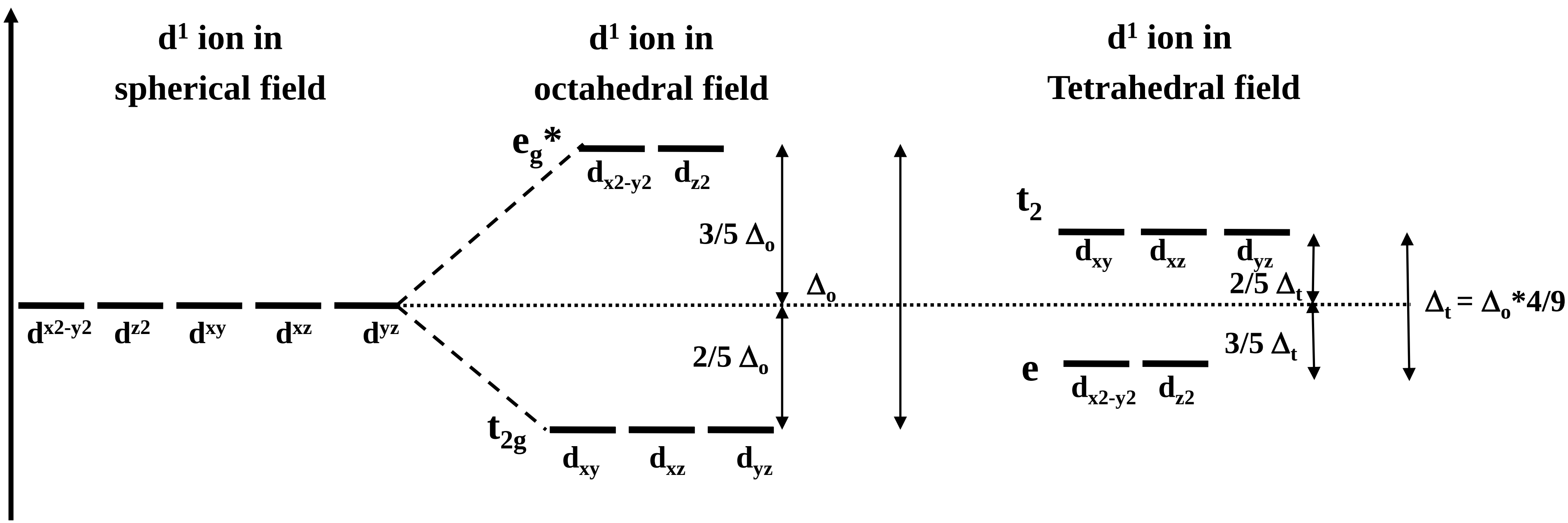

8.12 Luminescence of Rare Earth Ions

Luminescence of YPO_4:Ce

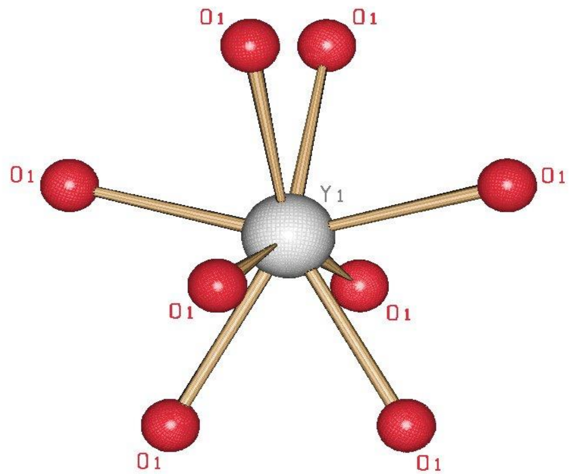

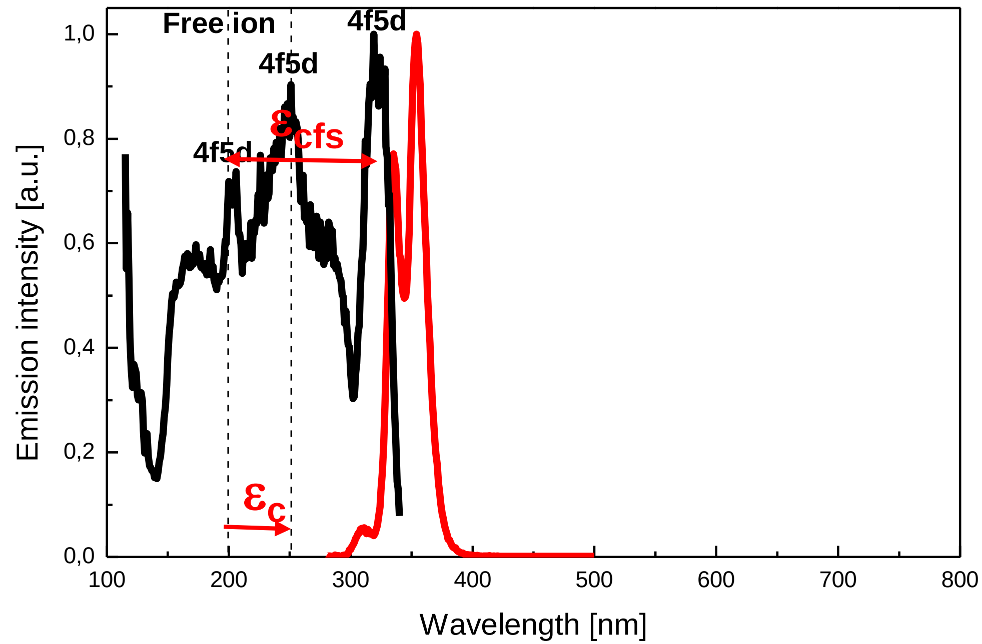

Distorted dodecahedral

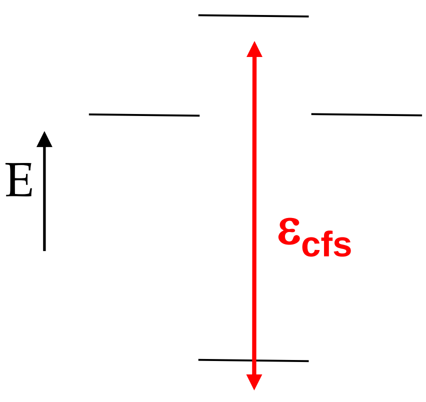

Y-O distances

4x 2.24 Å
4x 2.24 Å

Crystal field splitting ~ 18000 cm^{-1}
Centroid shift ~ 9600 cm^{-1}
(P. Dorenbos, Phys. Rev. B, 64, 2001, 1251)
⇒ Large 4f-5d energy gap
⇒ Emission bands at 335 and 355 nm

8.12 Luminescence of Rare Earth Ions

Luminescence of $Y_3Al_5O_{12}$:Ce

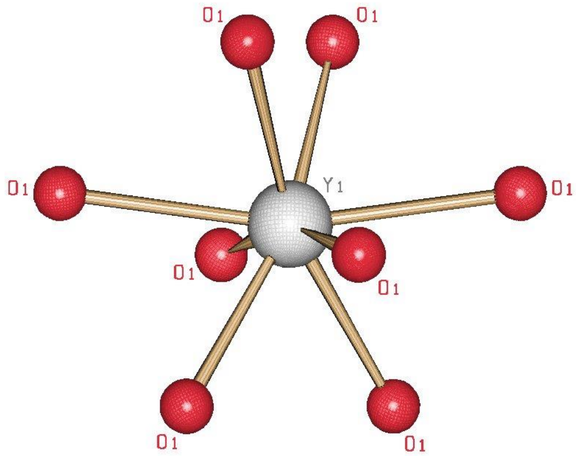

Distorted dodecahedral

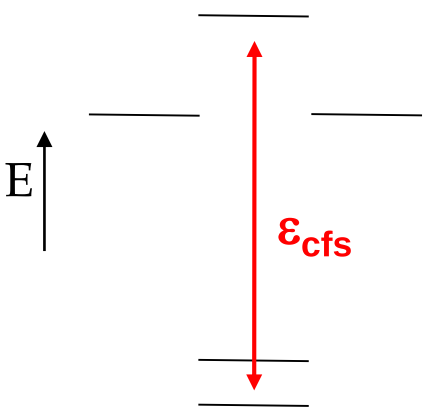

Y-O distances

4x 2.30 Å
4x 2.44 Å

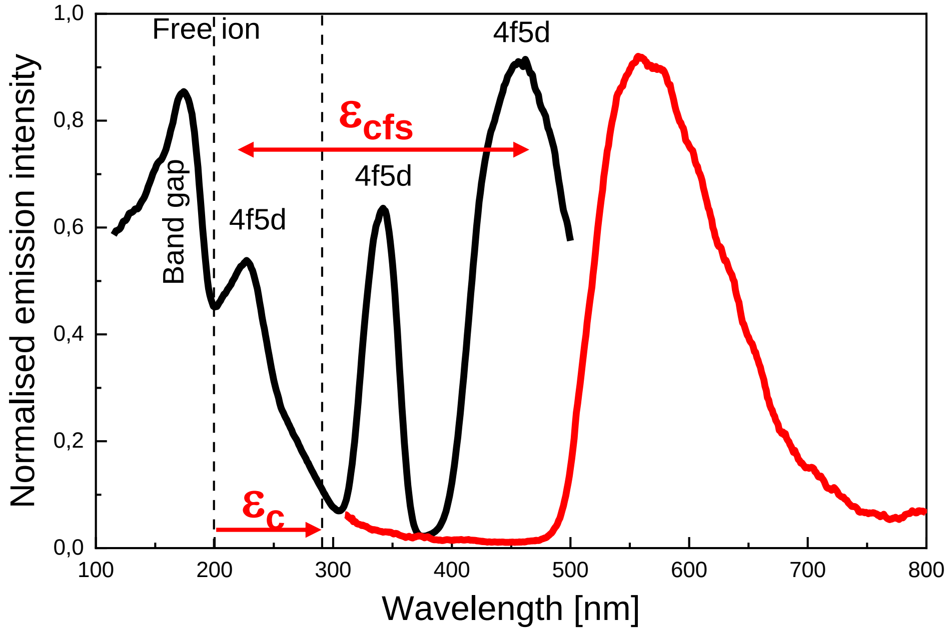

Crystal field splitting ~ 27000 cm^{-1}
Centroid shift ~ 14700 cm^{-1}
(P. Dorenbos, Phys. Rev. B, 65, 2002, 2351)
⇒ Small 4f-5d energy gap
⇒ Emission bands at 560 nm

8.12 Luminescence of Rare Earth Ions

Excitation and emission spectra of Pr^{3+} activated phosphors

YF_3:Pr

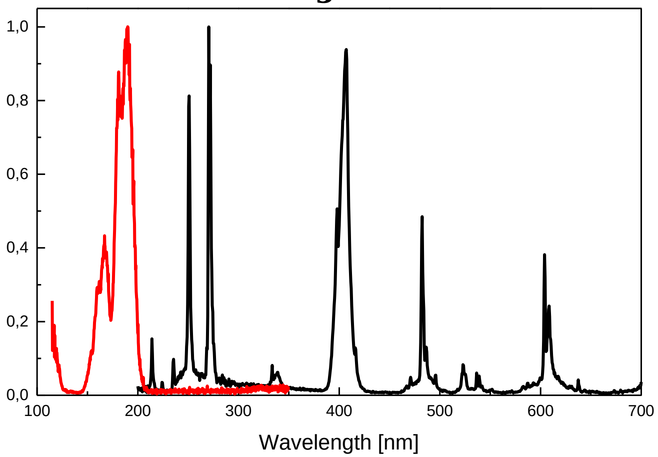

4f²-4f² line emission

YPO_4:Pr

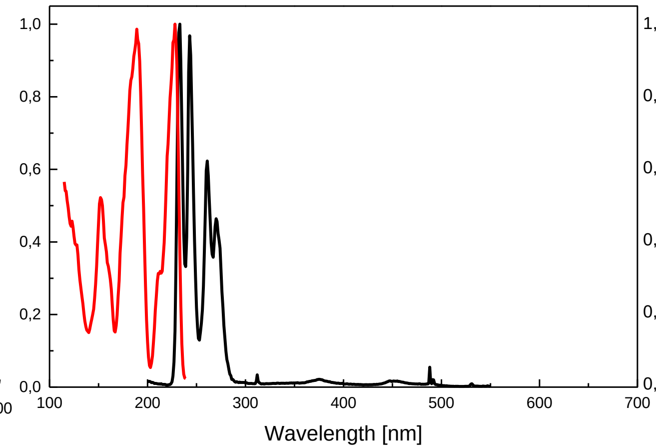

4f¹5d¹-4f² band emission

Y_2O_3:Pr

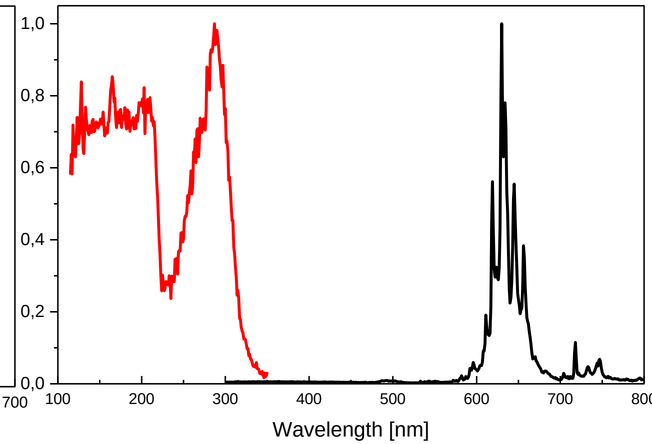

4f²-4f² line emission

The nature of the luminescence spectrum of Pr^{3+}
is strongly determined by the host material!

Fundamentals of Pr^{3+} luminescence

Pr^{3+} ground state configuration

[Xe]$4f^2$ → 13 SLJ-States and 91 microstates (SLJM)

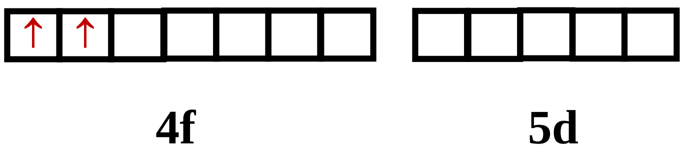

Pr^{3+} excited state configuration

[Xe]$4f^15d^1$ → 2 SLJ-States and 4 microstates

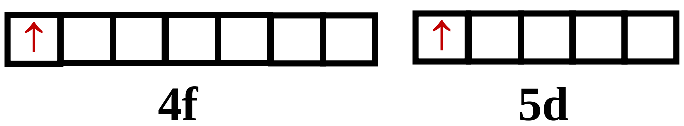

⇒ **[Xe]$4f^2$ – [Xe]$4f^2$ intraconfigurational transitions**

⇒ **[Xe]$4f^2$ – [Xe]$4f^15d^1$ interconfigurational transitions**

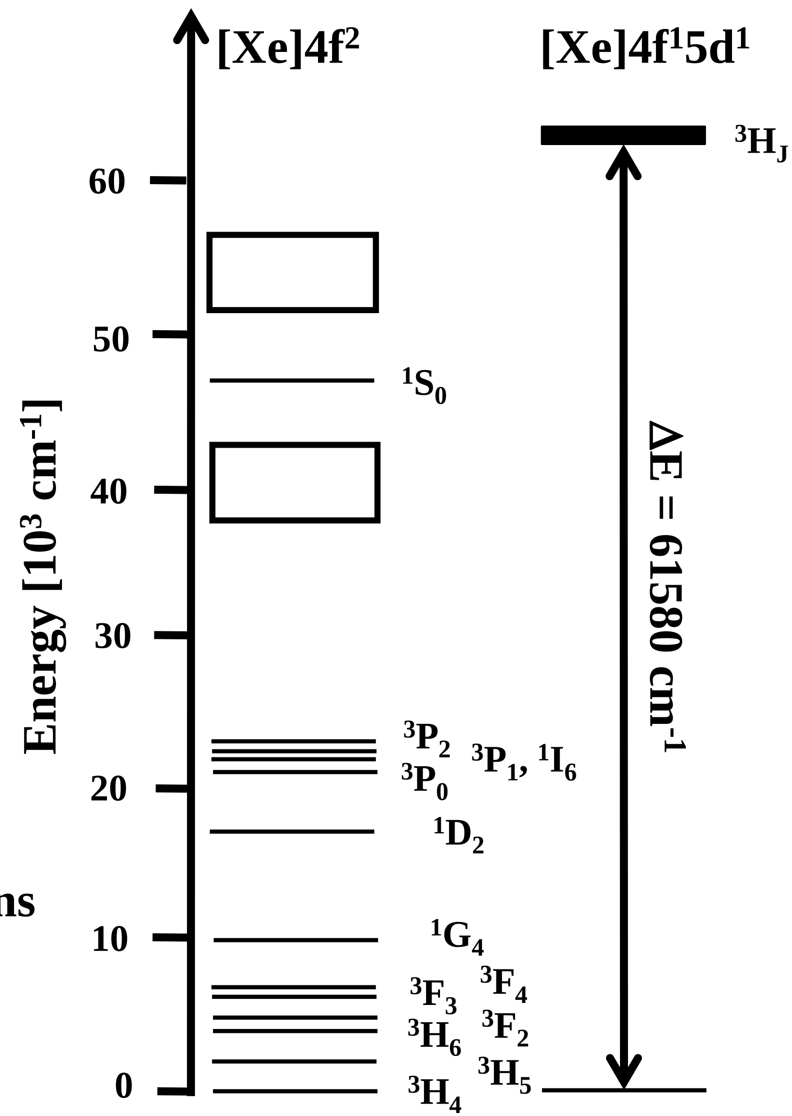

8.12 Luminescence of Rare Earth Ions

Fundamentals of Pr^{3+} luminescence

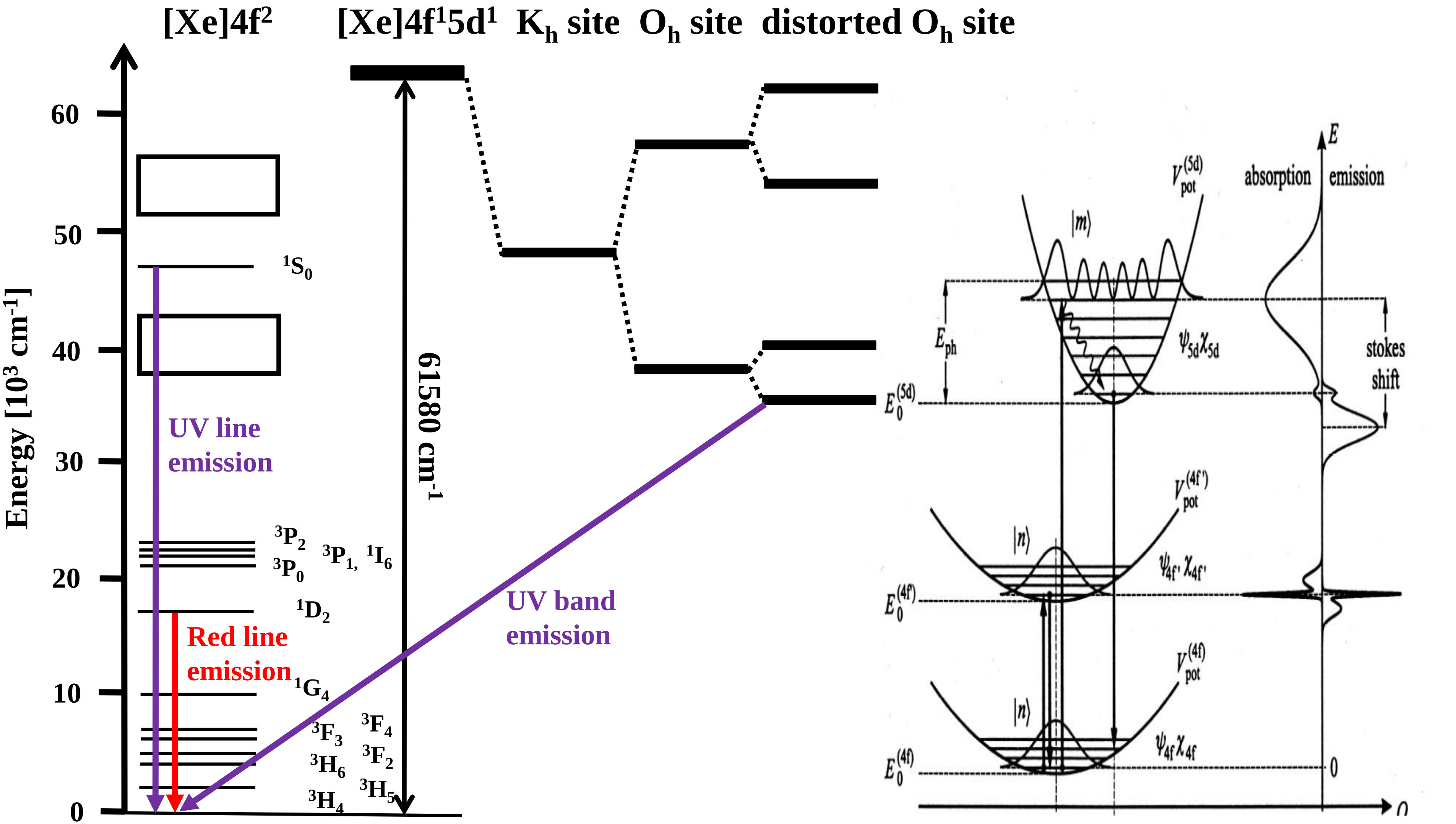

8.12 Luminescence of Rare Earth Ions

Emission spectra of Pr^{3+} phosphors

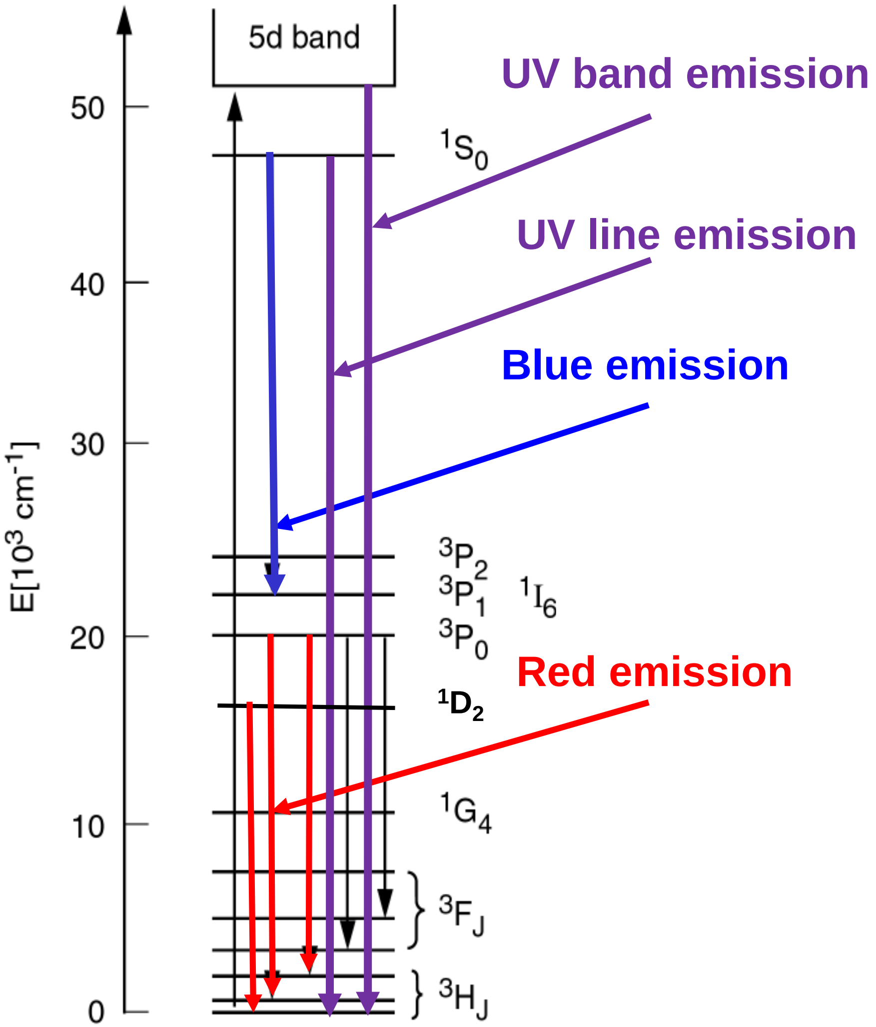

$^1S_0$ – $^{2S+1}L_J$ line emission

YF_3:Pr
$NaYF_4$:Pr
$SrAl_{12}O_{19}$:Pr
$LaMgB_5O_{10}$:Pr
LaB_3O_6:Pr

} 213, 236 252, 271 407 nm

$^1S_0$ – $^{2S+1}L_J$ lines and $4f^15d^1$ – $4f^2$ band emission

KY_3F_{10}:Pr	240, 250, 271 nm

$4f^15d^1$ – $4f^2$ band emission

$LiYF_4$:Pr	218 nm
YPO_4:Pr	232 nm
KYF_4:Pr	235 nm
$YAlO_3$:Pr	245 nm
YBO_3:Pr	263 nm
$Lu_2Si_2O_7$:Pr	273 nm
$Lu_3Al_5O_{12}$:Pr	310 nm
$Y_3Al_5O_{12}$:Pr	320 nm + line emission

$^1D_2$ – ^3H_J line emission

Y_2O_3:Pr	615 nm
$CaTIO_3$:Pr,Na	615 nm

Energy of the lowest crystal field component of [Xe]$4f^15d^1$ config.

8.12 Luminescence of Rare Earth Ions

Luminescence of YF_3:Pr

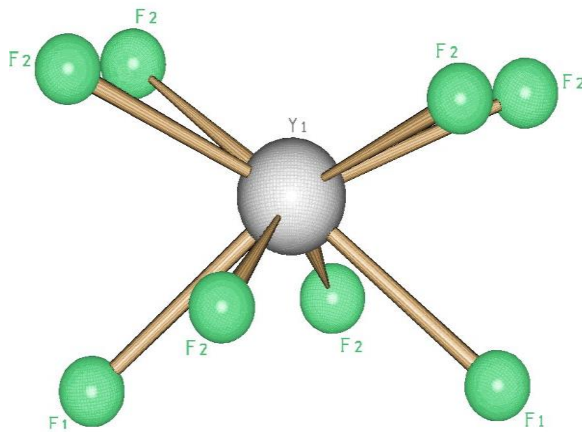

Distorted square-antiprismatic

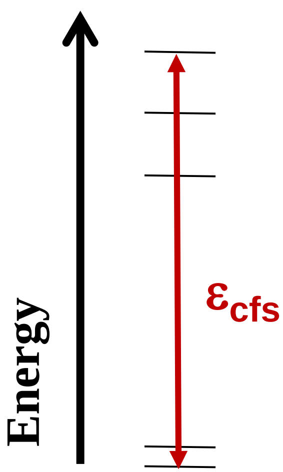

Y-F distances
4x 2.28 Å
2x 2.30 Å
2x 2.31 Å

CF splitting
~ 8000 cm^{-1}
Centroid shift
~ 5600 cm^{-1}

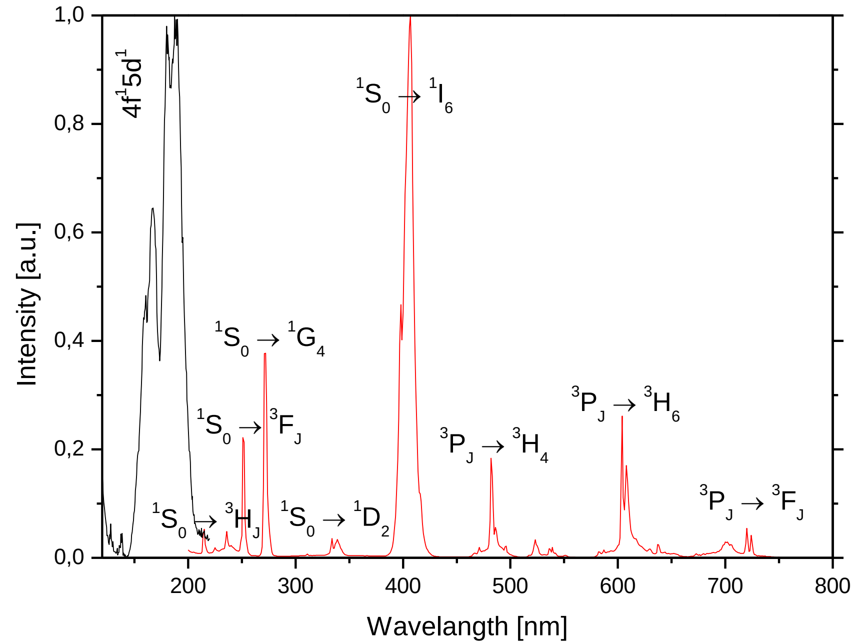

CFS + centroid shift reduces energy of lowest crystal field component of the [Xe]$4f^15d^1$ configuration by ~ 10000 cm^{-1}

⇒ **$E(4f^15d^1) > E(^1S_0)$**

⇒ **$^1S_0 - {}^{2S+1}L_J$ line emission**

8.12 Luminescence of Rare Earth Ions

Luminescence of YPO_4:Pr

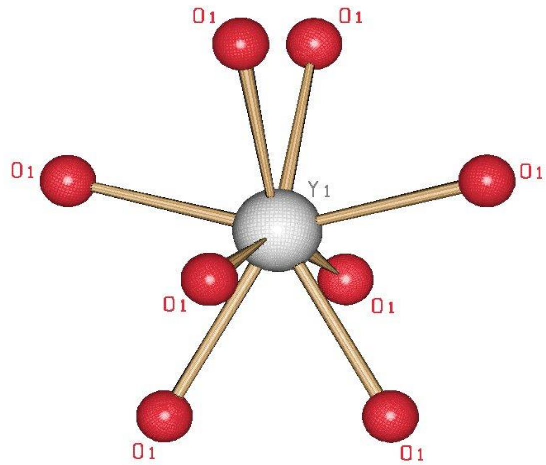

Distorted dodecahedral

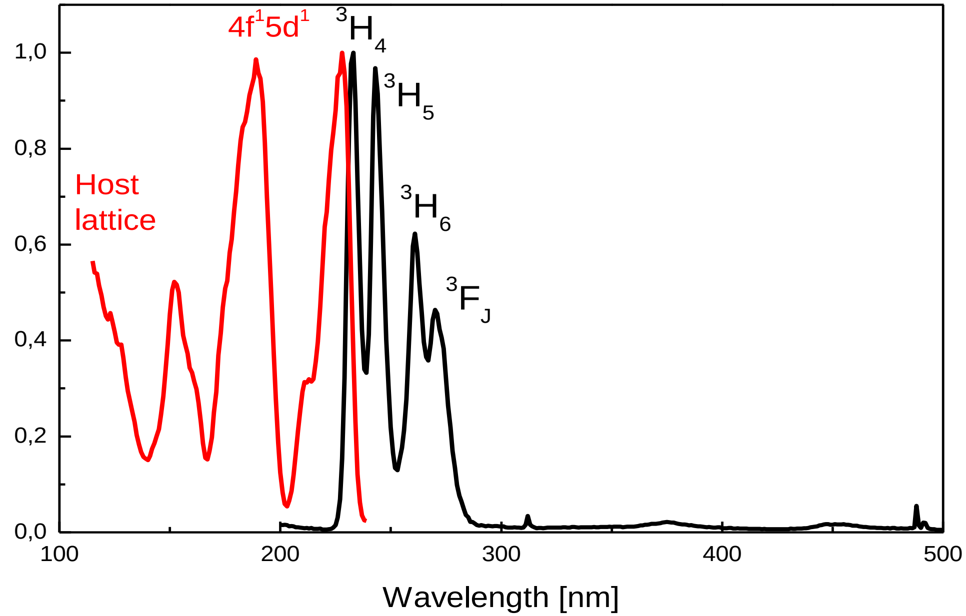

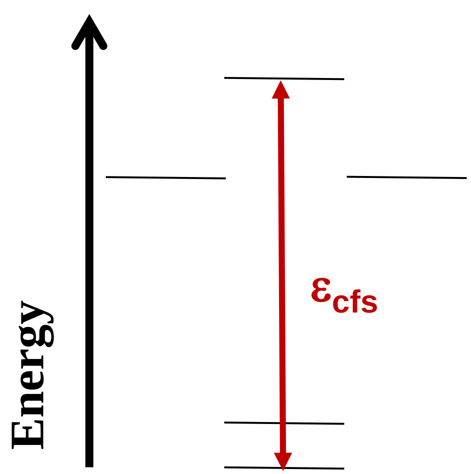

Y-O distances
4x 2.24 Å
4x 2.24 Å

CF splitting
~ 12000 cm^{-1}
Centroid shift
~ 9600 cm^{-1}

CFS + centroid shift reduces energy of lowest crystal field component of the [Xe]$4f^15d^1$ configuration by ~ 16000 cm^{-1}

⇒ $E(4f^15d^1) < E(^1S_0)$
⇒ [Xe]$4f^15d^1$ - [Xe]$4f^2$ band emission

8.12 Luminescence of Rare Earth Ions

Luminescence of $Y_3Al_5O_{12}$:Pr

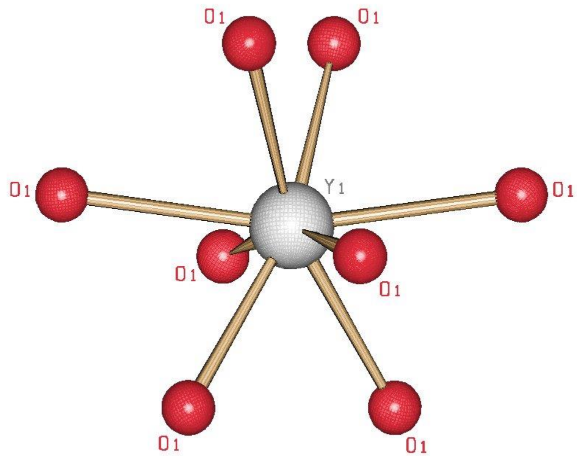

Distorted dodecahedral

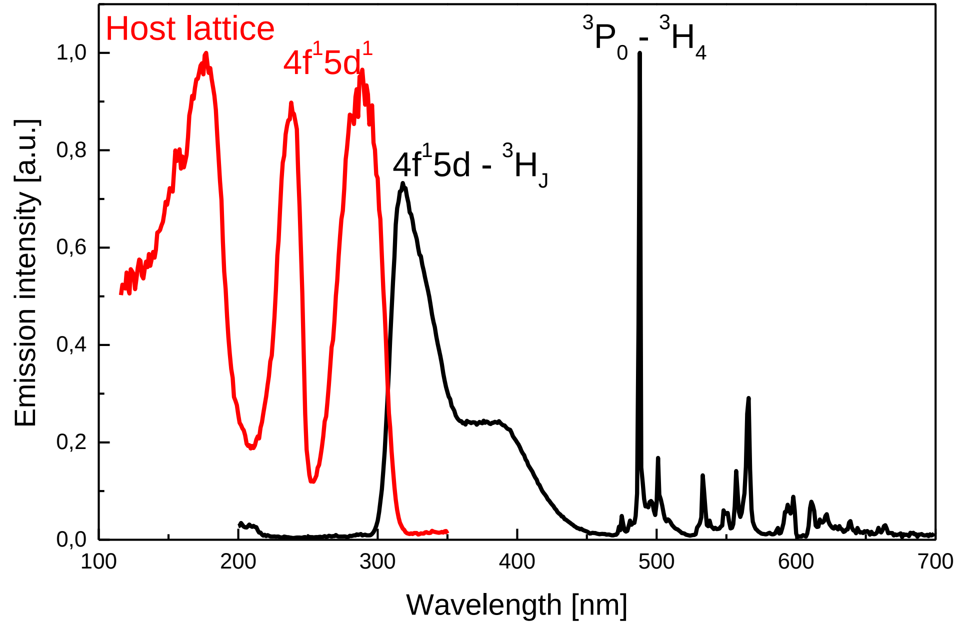

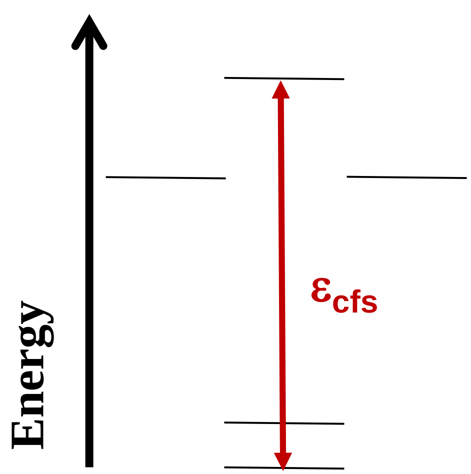

Y-O distances
4x 2.30 Å
4x 2.44 Å

CF splitting
~ 22500 cm^{-1}
Centroid shift
~ 14700 cm^{-1}

CFS + centroid shift reduces energy of lowest crystal field component of the [Xe]$4f^15d^1$ configuration by ~ 26000 cm^{-1}

⇒ E($4f^15d^1$) << E($^1S_0$)
⇒ UV band emission (320 nm) and visible line emission (> 450 nm)

8.12 Luminescence of Rare Earth Ions

Luminescence of Pr^{3+} doped Fluorides

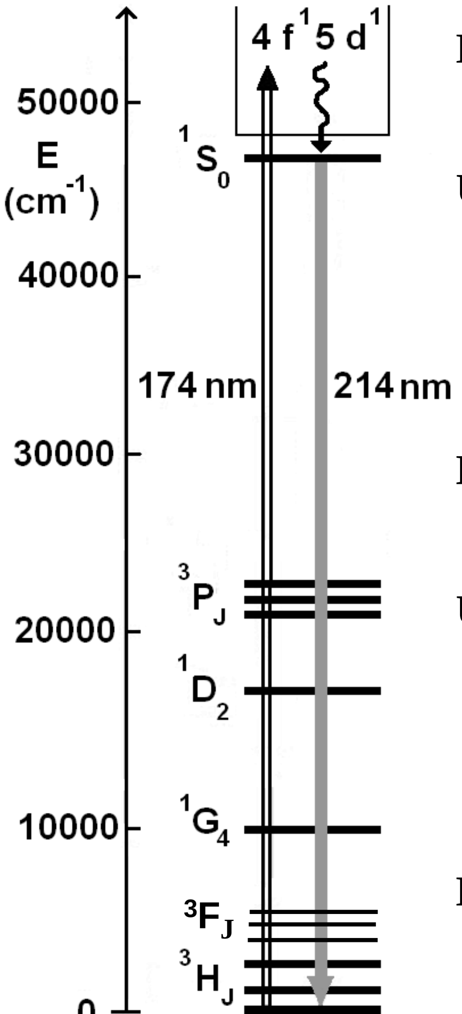

$NaYF_4:Pr^{3+}$ CN 9 (2 sites)

UV Lines 214 nm + Vis

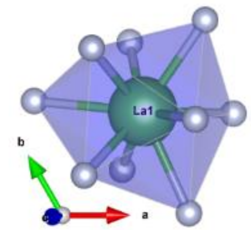

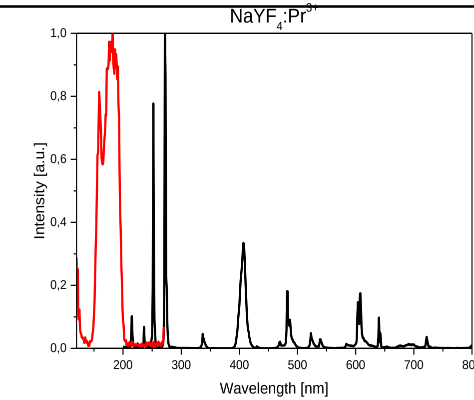

$LiYF_4:Pr^{3+}$ CN 8 (1 site)

UV Bands 218 nm + Vis

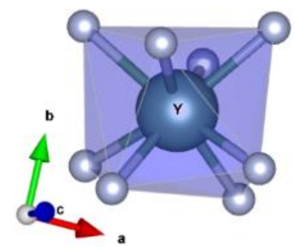

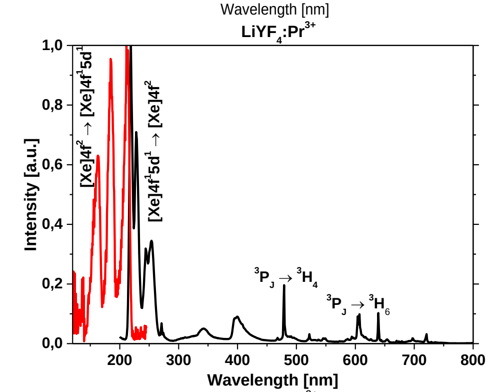

$KYF_4:Pr^{3+}$ CN 7 (6 sites)

UV Bands 232 nm

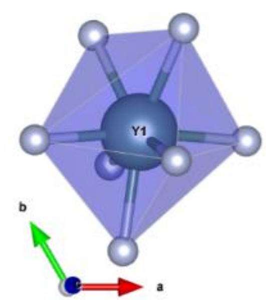

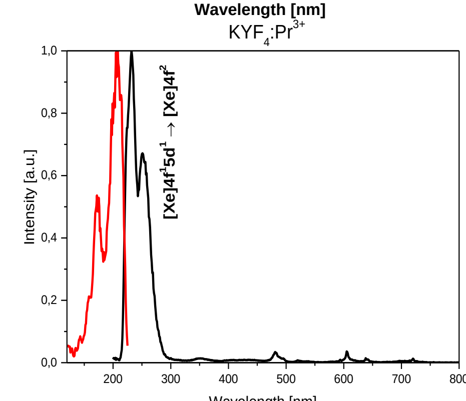

8.13 Down-Conversion

First examples (1974)

Lit.: *Sommerdijk et al., J. Lumin. 8 (1974) 288 (Philips)*

Sommerdijk et al., J. Lumin. 8 (1974) 341 (Philips)

Piper et al., J. Lumin. 8 (1974) 344 (GE)

YF_3:Pr(0.1%) and $NaYF_4$:Pr(0.1%)

$^1S_0$ - $^3P_1$, $^1I_6$ transitions @ 407 nm

$^3P_0$ - ^3H_J, $^3F_2$ transitions in the red

Internal QY = 166% (total) @ 214 nm excitation

Drawbacks of fluorides: Low stability in a Hg discharge causes blackening and fluorides have environmental & safety issues

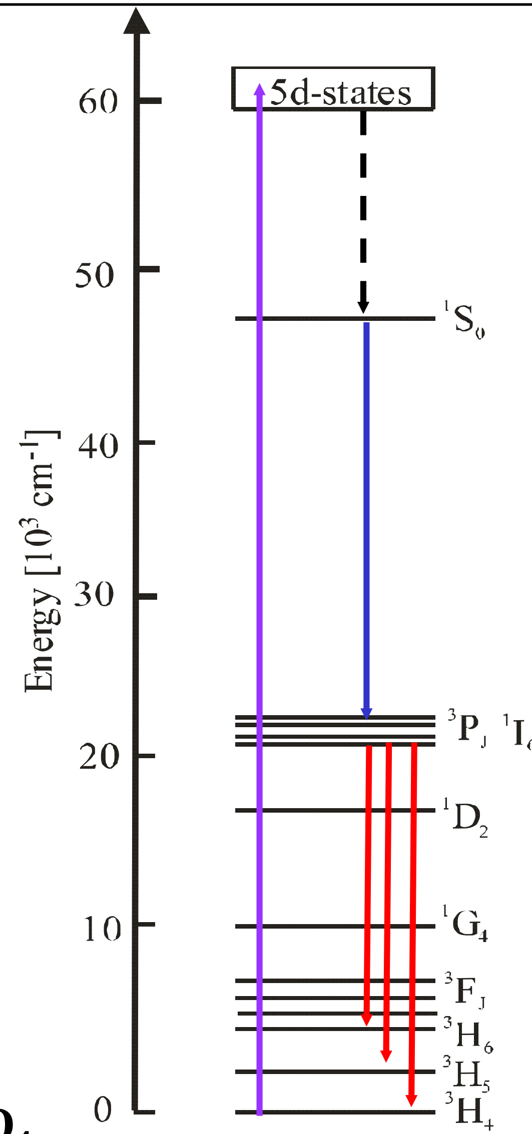

Oxidic materials with photon cascade emission (PCE)

Lit.: *A.M. Srivastava, D.A. Doughty, W.W. Beers (GE)*

Pr^{3+} on cation host sites with high CN (> 8)

$SrAl_{12}O_{19}$:Pr,Mg

Other examples: $LaMgB_5O_{10}$:Pr, LaB_3O_6:Pr, SrB_4O_7, $BaSO_4$, $CaSO_4$

8.13 Down-Conversion

Example: $LiGdF_4:Eu$

Energy level diagram

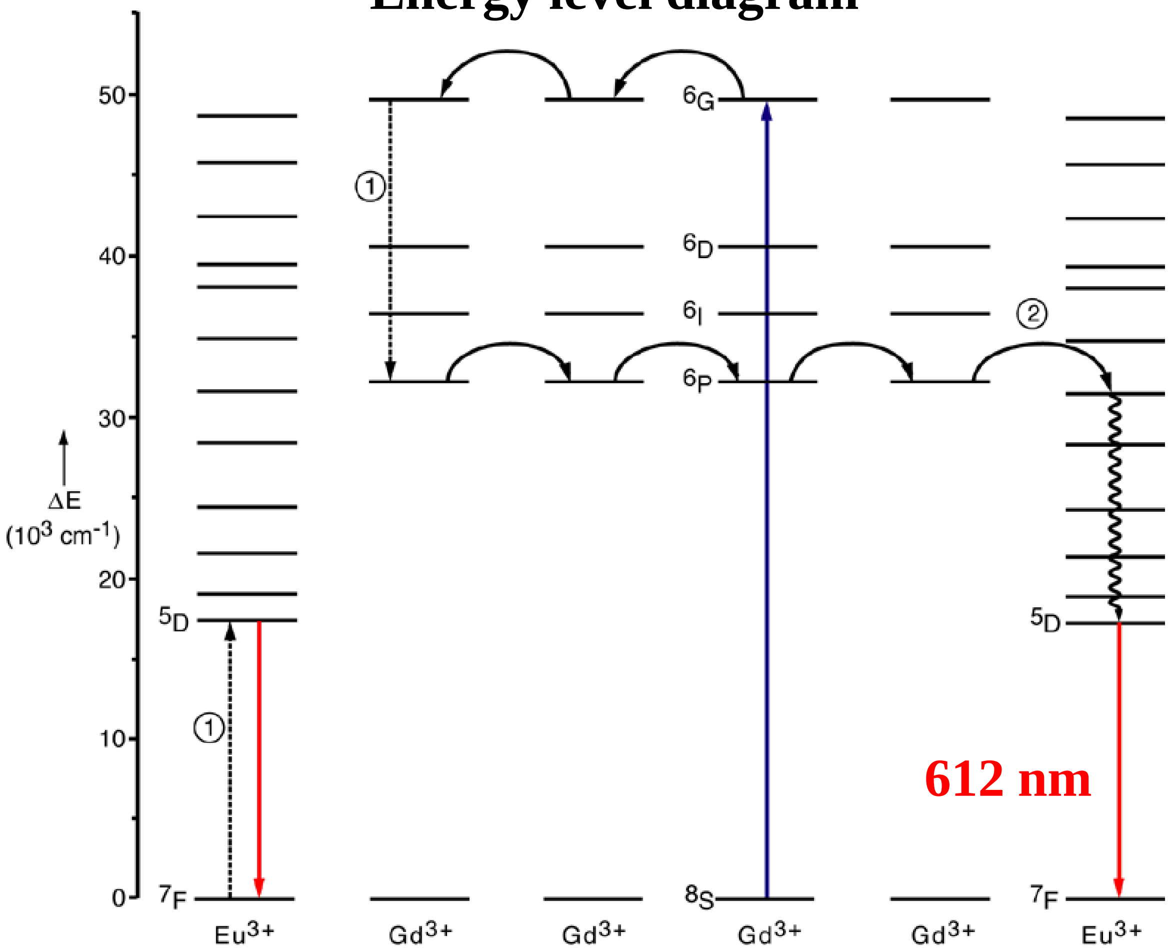

$$Gd \xrightarrow{202\ nm} Gd^{**}$$

$$Gd^{**} + Eu \xrightarrow{CR} Eu^{*} + Gd^{*}$$

$$Eu^{*} \longrightarrow Eu + h\nu$$

$$Gd^{*} + Eu \xrightarrow{ET} Gd + Eu^{*}$$

$$Eu^{*} \longrightarrow Eu + h\nu$$

$$QY_A = 195\%$$

8.13 Down-Conversion

Example: $LiGdF_4$:Er,Tb

Energy level diagram

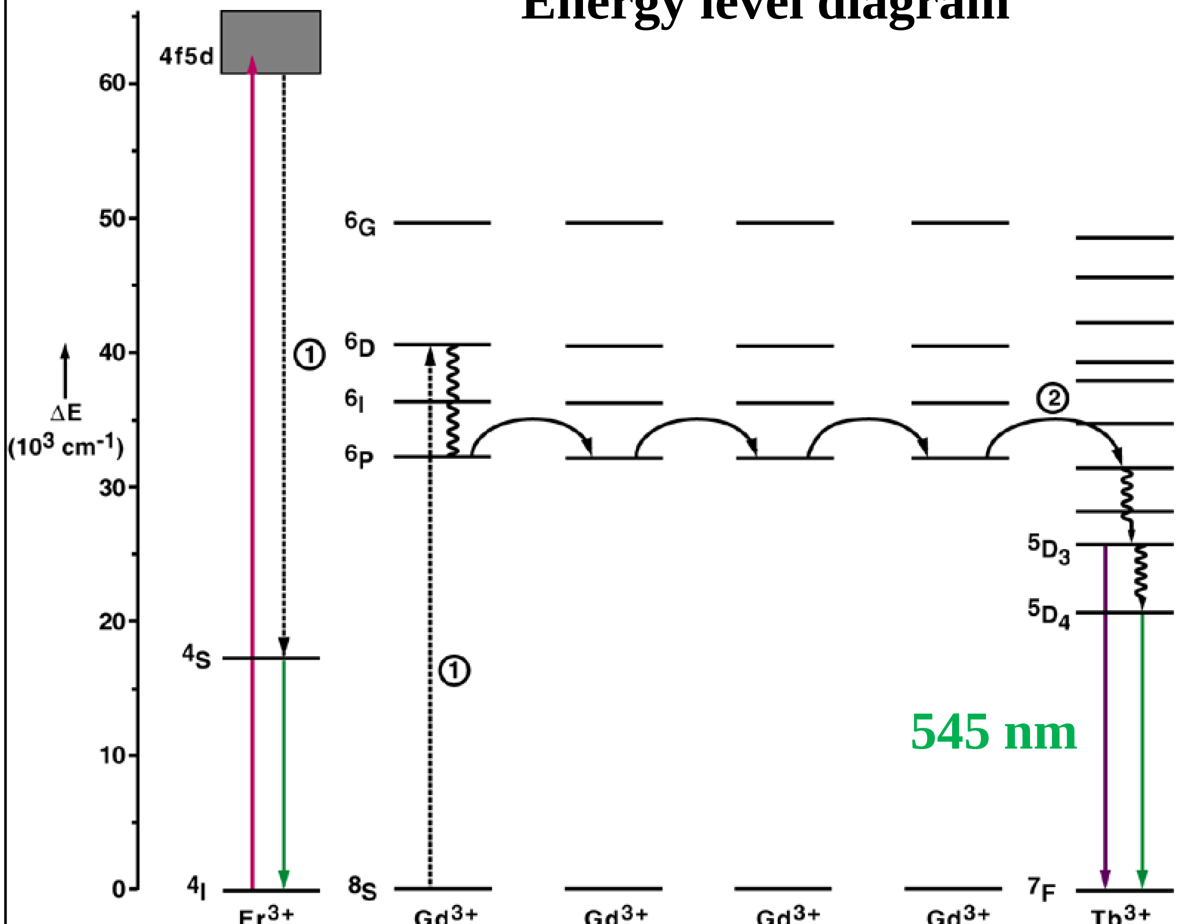

Er —(> 210 nm)→ Er**

Er** + Gd —(CR)→ Er* + Gd*

Er* → Er + hν

Gd* + Tb —(ET)→ Gd + Tb*

Tb* → Tb + hν

$QY_A = 130\%$

8.14 Up-Conversion

Mechanisms (inorganic materials)

Type	Example	Efficiency [cm^2W^{-1}]
a) Anti-Stokes-Raman	Si crystal	~10^{-13}
b) 2-Photon excitation	$CaF_2:Eu^{2+}$	~10^{-12}
c) Second Harmonic Gener. (SHG)	KH_2PO_4, $KNbO_3$, ß-BaB_2O_4	~10^{-11}
d) Cooperative photoluminescence	$YbPO_4:Yb^{3+}$	~10^{-8}
e) Cooperative sensitization	$YF_3:Yb^{3+},Tb^{3+}$	~10^{-6}
f) Excited State Absorption (ESA)	$SrF_2:Er^{3+}$	~10^{-5}
g) Energy Transfer Up-conv. (ETU)	$YF_3:Er^{3+}$	~10^{-3}
h) Sensitized ETU	$NaYF_4:Yb^{3+},Er^{3+}$	~10^{-1}

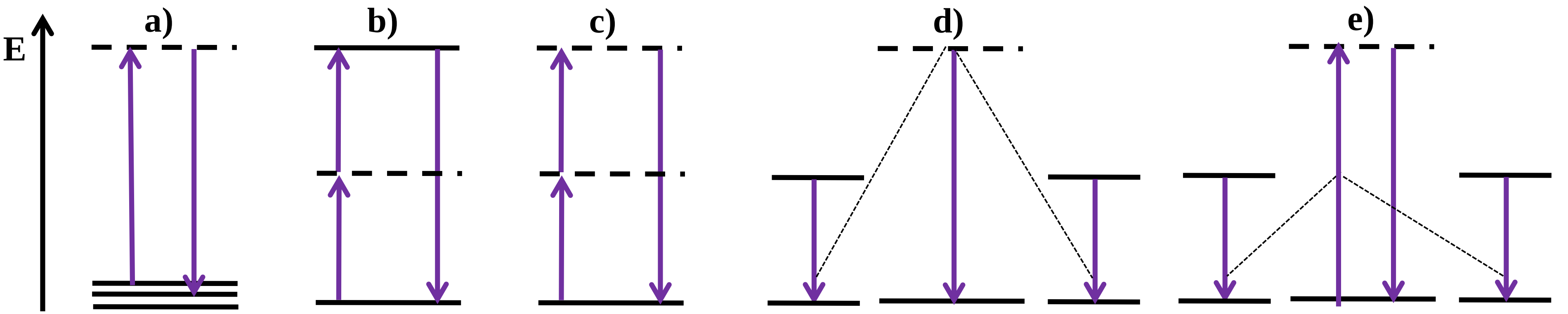

8.14 Up-Conversion

Mechanisms (inorganic materials)

f) Excited State Absorption (ESA)
Subsequent absorption of
2 Photons: Ground state absorption and then ESA
Single RE ion involved

g) Energy transfer Up-conversion (ETU)
Ground state absorption and energy transfer Up-conversion
Two identical RE ions involvied

h) Sensitized energy transfer up-conversion (sensitized ETU)
Involves a sensitizer, which absorbs energy and an activator, which can show ETU
Two non-identical RE ions involved

Example

$SrF_2:Er^{3+}$

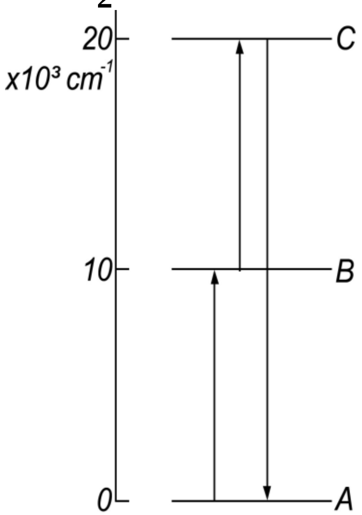

Example

$YF_3:Er^{3+}$

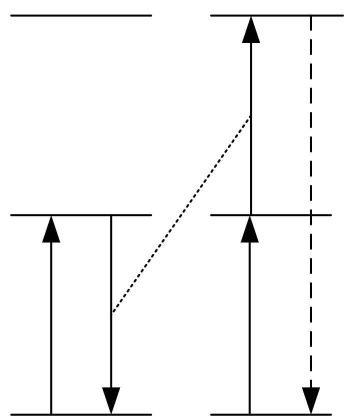

Examples

$YF_3:Yb,Tm$

$YF_3:Yb,Er$

$NaYF_4:Yb,Er$

$BaY_2F_8:Yb,Er$

$YOCl:Yb,Er$

(20-35% Yb^{3+}
1-5% Er^{3+} or Tm^{3+})

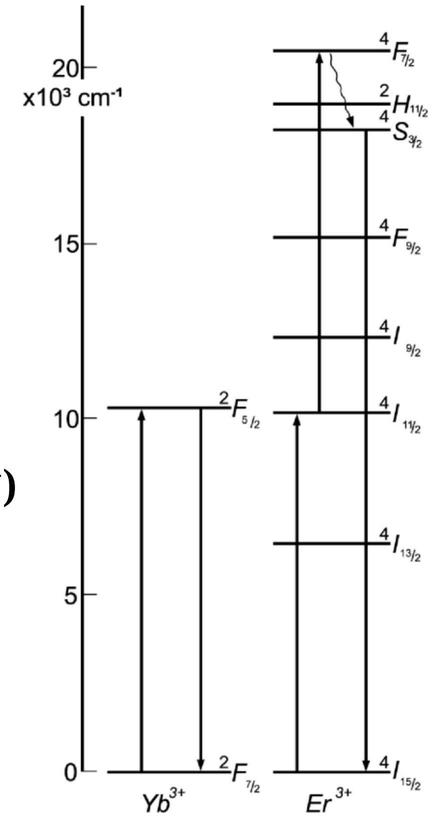

Conversion of IR radiation into the visible range
(in frequency multipliers, laser diodes, night vision goggles)

8.14 Up-Conversion

RE^{3+} activated NIR-to-visible up-converters

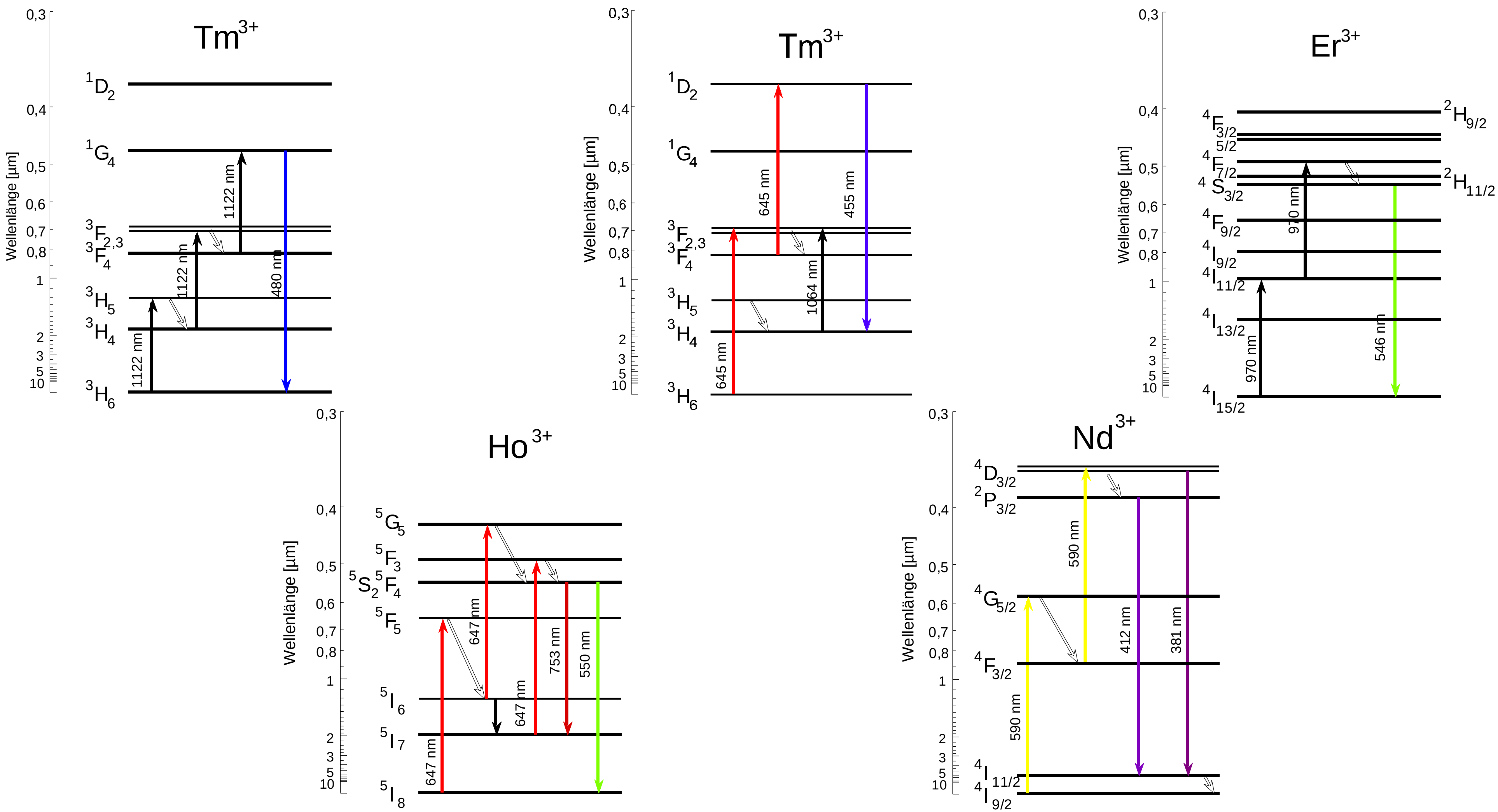

8.14 Up-Conversion

Yb^{3+} as a sensitizer for Er^{3+} and Pr^{3+} up-converters

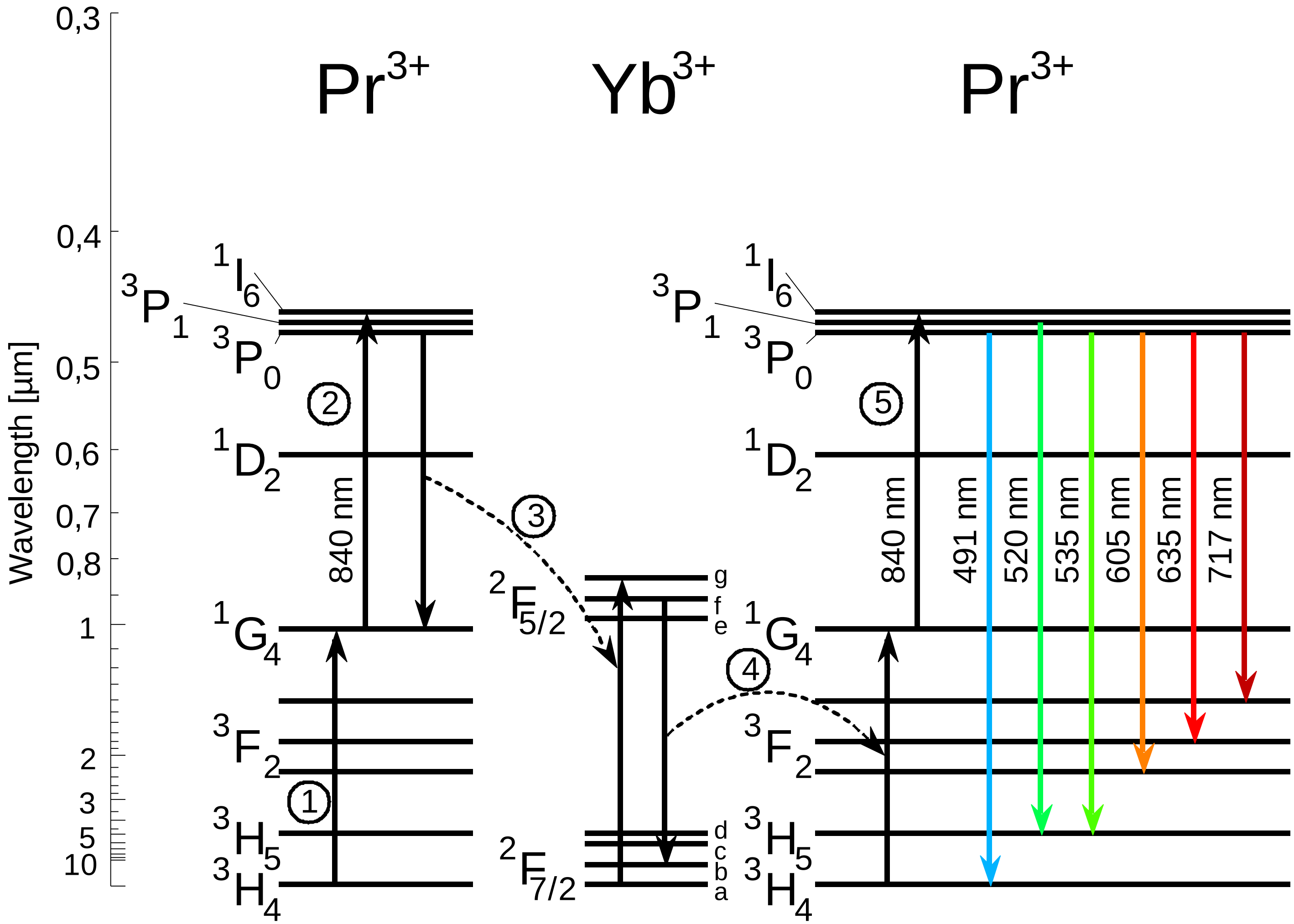

8.14 Up-Conversion

Pr^{3+} activated visible-to-UV up-converters

Example: ETU by 445 nm laser diode + Y_2SiO_5:Pr,Li ceramic, Georgia, Atlanta

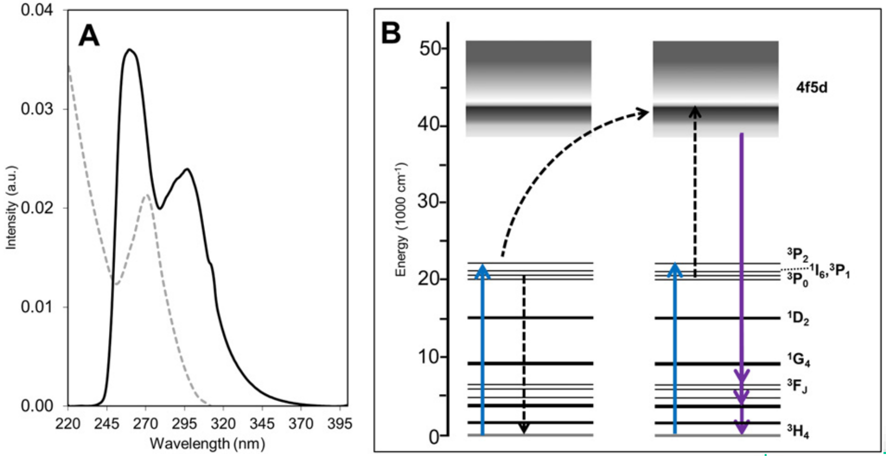

Literature

1. E.L. Cates, A.P. Wilkinson, J.-H. Kim, J. Luminescence 160 (2015) 202

2. E.L. Cates, J.-H. Kim, J. Photochemistry & Photobiology, B: Biology 153 (2015) 405

ABSTRACT: The objective of this study was to develop visible-to-ultraviolet C (UVC) upconversion ceramic materials, which inactivate surface-borne microbes through frequency amplification of ambient visible light. Ceramics were formed by high-temperature sintering of compacted yttrium silicate powders doped with Pr^{3+} and Li^{+}. In comparison to previously reported upconversion surface coatings, the ceramics were significantly more durable and had greater upconversion efficiency under both laser and low-power visible light excitation. The antimicrobial activity of the surfaces under diffuse fluorescent light was assessed by measuring the inactivation of *Bacillus subtilis* spores, the rate of which was nearly 4 times higher for ceramic materials compared to the previously reported films. Enhanced UVC emissions were attributed to increased material thickness as well as increased crystallite size in the ceramics. These results represent significant advancement of upconversion surfaces for sustainable, light-activated disinfection applications.

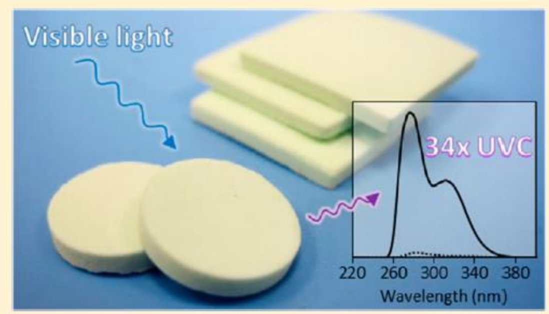

8.15 Afterglow

Cause: Storage of electrons / holes onto certain sites in the lattice (vacancies, impurities)

Shallow traps: Release of electrons from traps is done by ambient thermal energy
Deep traps: Release of electrons from traps is done by stimulation (PSL or TSL)

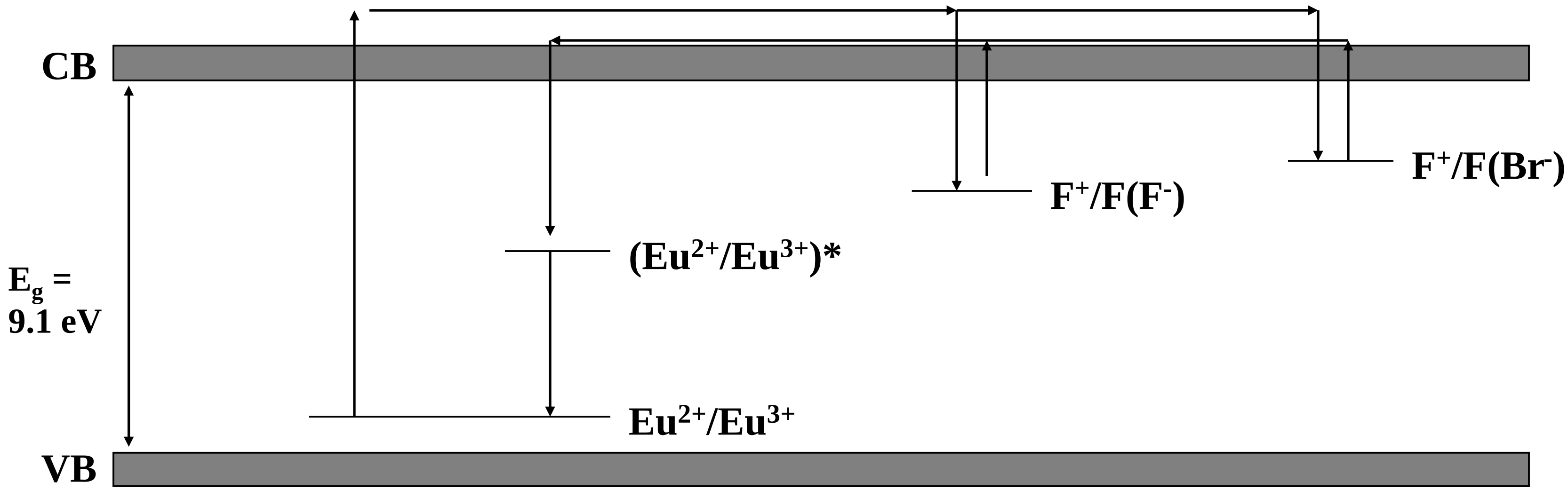

Example: Ba(F,Br):Eu Storage phosphor for imaging plates (detection of x-rays)

Literature: Y. Iwabuchi et al., J. Appl. Phys. 33 (1994) 178

8.15 Afterglow

Deep traps: Storage phosphors - Example: Cs_2NaYF_6:Ce & Cs_2NaYF_6:Pr (elpasolite)

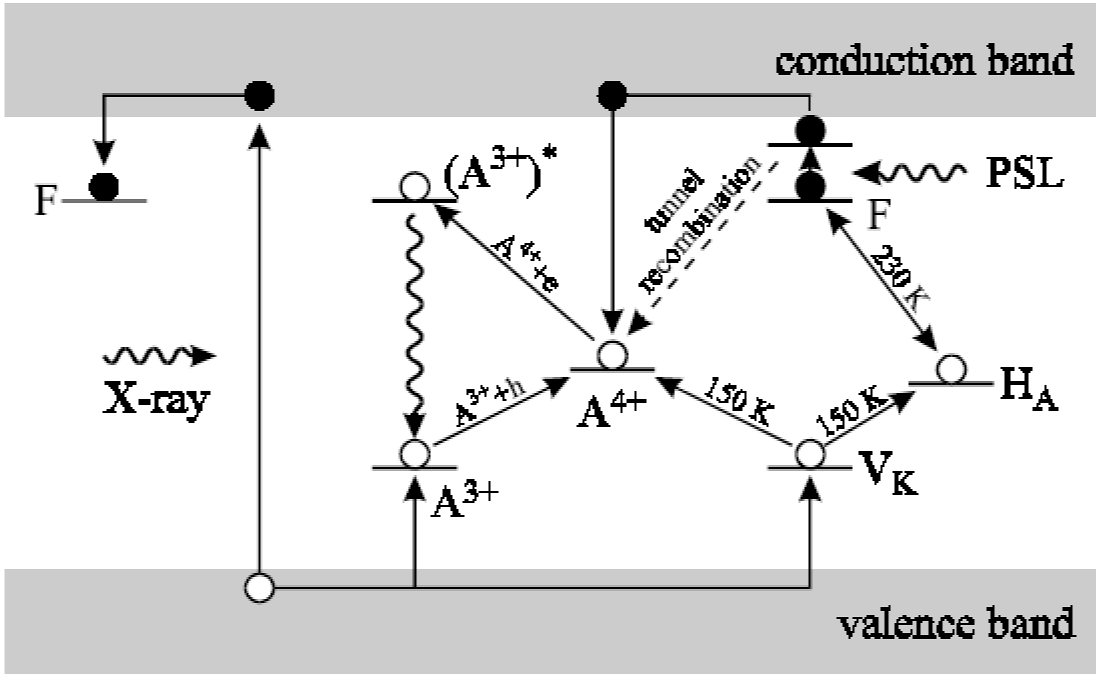

A = Ce, Pr

Literature: Th. Pawlik and J.-M. Spaeth, J. Appl. Phys. 82 (9), 4236 (1997)

8.15 Afterglow

Deep traps: Storage phosphors - Application

Mechanism

1. **Charging of the material, e.g. by high energy particles, x-rays, or UV radiation**
2. **Stimulation of energy release to induce luminescence**
   - **Thermally stimulated luminescence (TSL: T >> 300 K)**
   - **Photostimulated luminescence (PSL: Laser activation)**

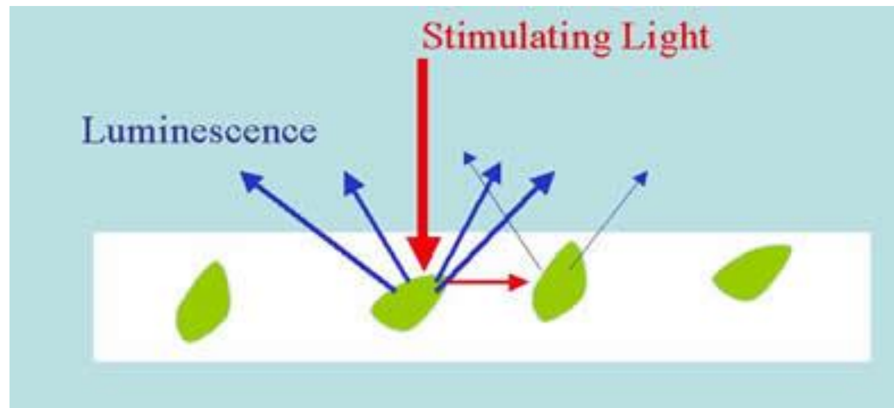

In a storage phosphor radiation energy is stored inside the material by traps and the light of interest is not produced until the material is activated, either by thermal or optical stimulation. Thus information on the radiation can be obtained at a time later than the actual interaction.

8.15 Afterglow

Deep traps: Storage phosphors – Overview

Established storage materials

• $Ba(F,Br):Eu^{2+}$	PSL	
• $RbBr:Tl^{+}$	PSL	
• $SrS:Eu^{2+},Sm^{3+}$	PSL	
• $Ba_3(PO_4)_2:Eu^{2+}$	PSL	
• $Ba_2B_5O_9Br:Eu^{2+}$	PSL	
• $Ba_7Cl_2F_{12}:Eu^{2+}$	PSL	
• $Ba_{12}Cl_5F_{19}:Eu^{2+}$	PSL	
• $Y_2SiO_5:Ce^{3+}$	PSL	
• $Ba_5SiO_4Br_6:Eu^{2+},Nb^{3+}$	PSL and TSL (150 °C)	
• $Sr_5(PO_4)_3Cl:Eu^{2+}$	PSL and TSL (157 °C)	
• $Li_6Gd_{0.5}Y_{0.5}(BO_3)_3:Eu^{3+}$	PSL and TSL (177 °C)	also for neutron storage
• $LiSr_4(BO_3)_3:Ce^{3+}$	PSL and TSL (200 °C)	due to neutron capture
• $LiCaAlF_6:Eu^{2+}$	PSL and TSL (240 °C)	by ^{6}Li!
• $LiYSiO_4:Ce^{3+}$	PSL and TSL (260 °C)	

8.15 Afterglow

Shallow traps: Thermal release of charge carriers at ambient temperature

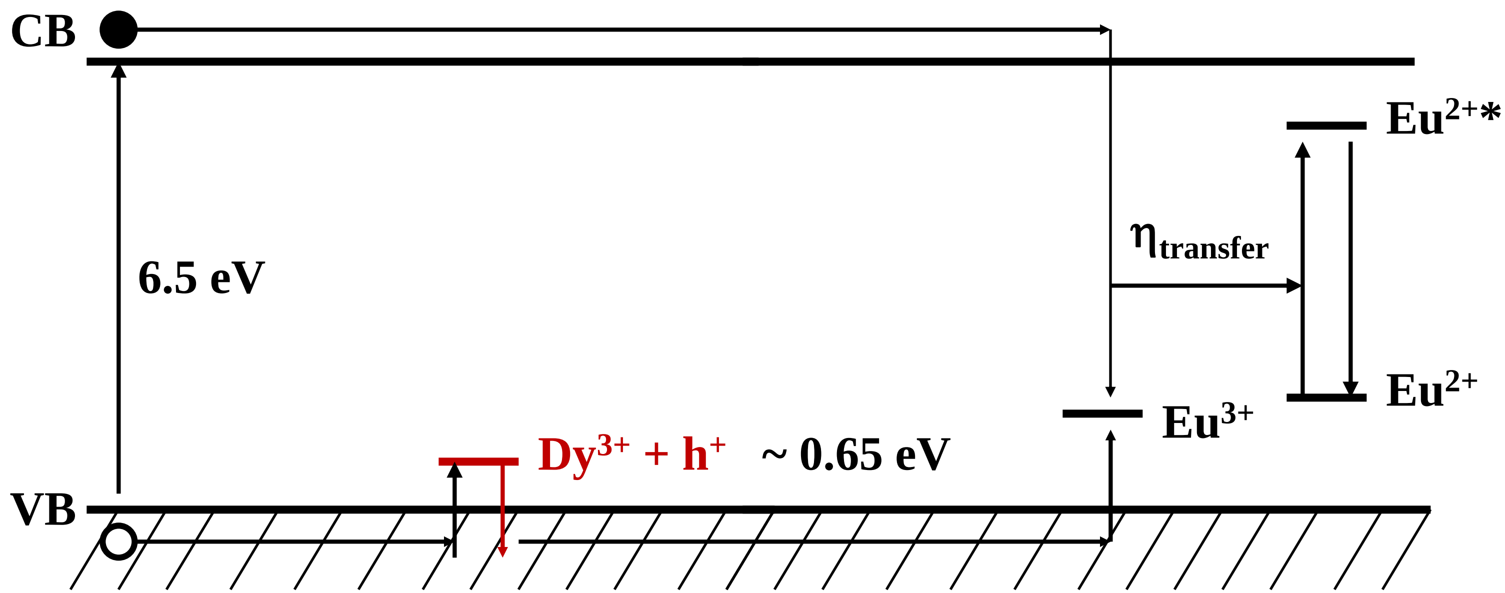

Example

$SrAl_2O_4$:Eu,Dy **Lit.: Nemoto Ltd., JECS 143 (1996) 2670**

8.15 Afterglow

Shallow traps: Afterglow phosphors

Composition	colour	λ_{max} [nm]
$CaAl_2O_4$:Eu,Nd	blue	440 nm
$Sr_2MgSi_2O_7$:Eu,Dy	blue	469 nm
$Sr_4Al_{14}O_{25}$:Eu,Dy	cyan	490 nm
$Mg_2SnO_4:Mn^{2+}$	cyan	499 nm
$SrAl_2O_4$:Eu,Dy	green	520 nm
ZnS:Cu,Co	green	530 nm
Sr_2SiO_4:Eu,Dy	yellow	570 nm
Y_2O_2S:Eu,Ti,Mg	red	620 nm
$CaZnGe_2O_6$:Mn	red	648 nm
CaS:Eu,Tm	red	655 nm
$MgSiO_3$:Eu,Dy,Mn	red	660 nm
$SrSc_2O_4$:Eu	red	685 nm

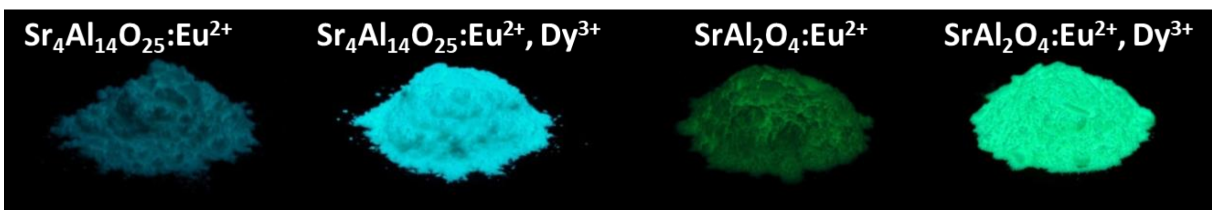

Example: $Sr_4Al_{14}O_{25}:Eu^{2+},Ln^{3+}$

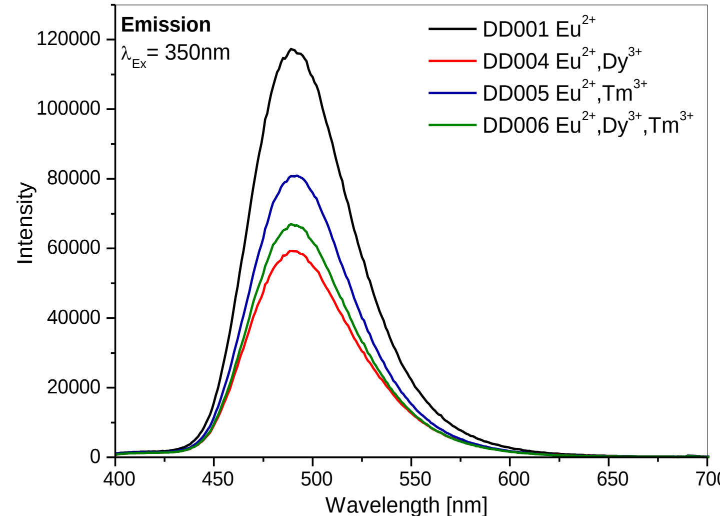

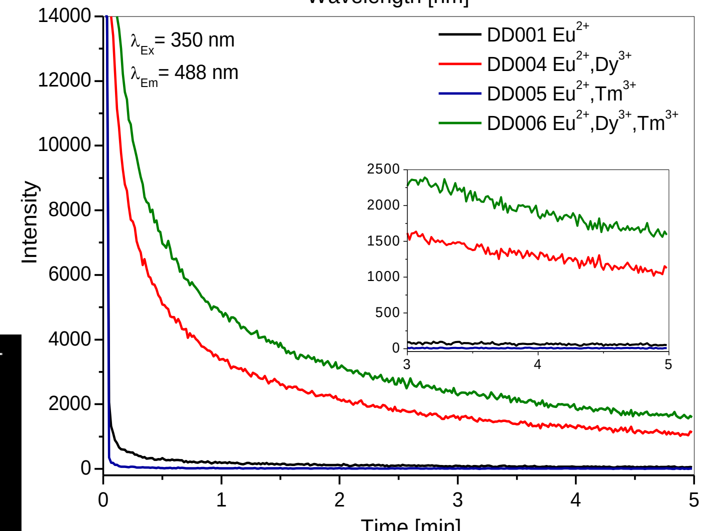

8.15 Afterglow

Shallow traps: Afterglow phosphors applications

- watch dials
- self-sustained night vision materials
- luminous paints, ‘glow in the dark’ toys
- defense surveillance for tagging, tracking and locating the targets of interest
- in-vivo deep-tissue bio-imaging (NIR persistent luminescent phosphors)
- radiation detection or structural damage sensing

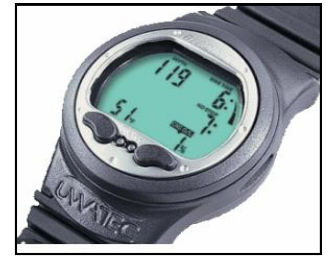

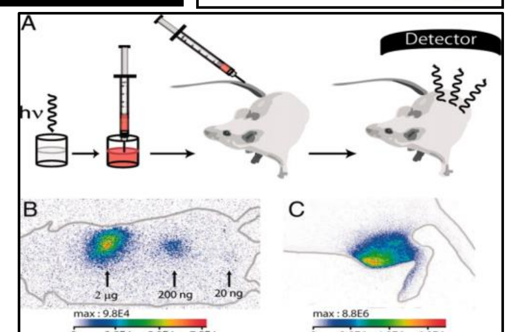

Road N329 in Oss (The Netherlands)